

Please cite the Published Version

Grayson, Amy Kathryn (2018) Elucidating the role of JAK/STAT signalling in polycythaemia vera and essential thrombocythaemia using proteomics. Masters by Research thesis (MSc), Manchester Metropolitan University.

Downloaded from: <https://e-space.mmu.ac.uk/623213/>

Usage rights:  [Creative Commons: Attribution-Noncommercial-No Derivative Works 4.0](https://creativecommons.org/licenses/by-nc-nd/4.0/)

Enquiries:

If you have questions about this document, contact openresearch@mmu.ac.uk. Please include the URL of the record in e-space. If you believe that your, or a third party's rights have been compromised through this document please see our Take Down policy (available from <https://www.mmu.ac.uk/library/using-the-library/policies-and-guidelines>)

Elucidating the role of JAK/STAT
signalling in polycythaemia vera and
essential thrombocythaemia using
proteomics

Amy Kathryn Grayson

A thesis submitted in partial fulfilment of the
requirements of Manchester Metropolitan University
for the degree of Master of Science (by Research)

School of Healthcare Science

Manchester Metropolitan University

2018

Contents

Acknowledgements.....	3
Abstract.....	4
Abbreviations.....	5
1. Introduction.....	8
1.1. Myeloproliferative Neoplasms: An Overview.....	8
1.2. Philadelphia-chromosome negative MPNs.....	9
1.3. The <i>JAK2V617F</i> Mutation.....	10
1.4. JAK2-STAT Signalling.....	12
1.5. Key signalling molecules in the pathogenesis of Ph- MPNs.....	13
1.6. Current therapeutic strategies for Ph- MPNs.....	14
1.7. JAK2 Inhibition by Ruxolitinib.....	18
1.8. Interferon-alpha therapy in MPNs.....	19
1.9. Combination of ruxolitinib and IFN- α in MPN treatment.....	22
1.10. Fludarabine treatment in MPNs.....	23
1.11. Combination of ruxolitinib and fludarabine in MPN treatment.....	25
1.12. Summary.....	25
1.13. Aims and Objectives.....	27
2. Materials and Methods.....	29
2.1. Cell Culture.....	29
2.2. Mass Spectrometry.....	31
2.3. Western Blotting.....	33
2.4. Q-RT-PCR.....	35
2.5. Statistical Analysis.....	38
3. Results.....	39
3.1. The effect of 1 μ M RUX on cellular proliferation and viability.....	39
3.2. The effect of 1 μ M ruxolitinib on global protein expression in ET.....	44
3.3. The effect of 1 μ M ruxolitinib on target gene transcription in ET.....	81
3.4. The effect of 1 μ M ruxolitinib on target protein translation in ET.....	88
3.5. The effect of 1 μ M RUX on STAT1 expression in ET and PV.....	90
3.6. The effect of 1 μ M ruxolitinib and 1 μ g/ml IFN- α on proliferation in ET and PV.....	96
3.7. The effect of 1 μ M ruxolitinib and 5 or 10 μ M fludarabine on proliferation.....	102
4. Discussion.....	109

4.1.	Ruxolitinib significantly decreases proliferation and viability of SET2 and HEL cells	109
4.2.	Ruxolitinib treatment decreases the expression of JAK2 downstream targets.....	112
4.3.	IFN- α and ruxolitinib dual treatment shows little synergy compared to ruxolitinib alone ..	121
4.4.	Combination of fludarabine and ruxolitinib is more effective than ruxolitinib alone	121
5.	Conclusion.....	123
6.	References	127

Acknowledgements

I would like to acknowledge the people who allowed me the opportunity to study my Master's degree at Manchester Metropolitan University and all who made the experience an enjoyable one. I would like to express my gratitude to my supervisors, Dr Ciaren Graham and Dr Nina Dempsey-Hibbert for all their guidance and support during my studies. I would also like to acknowledge Dr Robert Graham at the University of Manchester and thank him for his training and support with the mass spectrometry experiments and use of the equipment at the university.

In addition, I would like to thank the lab technicians, staff and my fellow colleagues within the School of Healthcare Science and the Research Degrees Team for their assistance and motivation throughout my time at Manchester. I would also like to thank Dr Stephen White for his help and advice with revision to my thesis.

Finally, I would like to thank my friends and family for their continued support throughout my studies and for their encouragement upon completion of this thesis. My deepest appreciation goes to all the people named above for their understanding, patience and support during setbacks in my academic and personal life. I am very grateful for the opportunity to have studied at MMU and wish you all the best in your future endeavours.

Abstract

Myeloproliferative neoplasms (MPNs) are hyperproliferative disorders affecting the number of circulating cells within the peripheral blood. Previous research has identified the same *JAK2* point mutation in three different MPNs; polycythaemia vera (PV), essential thrombocythaemia (ET) and myelofibrosis (MF). The *JAK2V617F* mutation is thought to be the driver of malignant transformation however, elucidating the mechanisms in which one mutation can result in three different cancers is still a challenge to researchers. The JAK1/2 inhibitor ruxolitinib has been successfully used to alleviate disease-related symptoms and reduce splenomegaly in MPN patients. Furthermore, it has been suggested that STAT1, a direct downstream target of JAK2 activation, is the genetic modifier involved in the development of the malignant phenotypes, with increased STAT1 activity producing an ET-like phenotype, whereas lower STAT1 activity produces a PV-like phenotype.

This report will investigate the effect of JAK2 inhibition by ruxolitinib on cellular proliferation and expression of downstream JAK/STAT targets in PV and ET representative cell lines (SET2 and HEL respectively). Cells were treated with 1 μ M ruxolitinib and proliferation and cell viability were assessed by growth curve analysis, MTS and Trypan Blue assays. Mass spectrometry was used to identify molecules of significance with respect to JAK2 signalling in ET through differential expression upon ruxolitinib treatment. Following this, Western Blot and Q-RT-PCR was performed on molecules of interest. Ruxolitinib was also investigated as a dual agent alongside IFN- α , a STAT1 activator, and fludarabine, a STAT1 inhibitor, to investigate the specific role of STAT1 in both PV and ET and possible synergistic effects of two treatments currently used with MPN patients.

Results show that ruxolitinib had a similar effect on cell proliferation and viability in both SET2 and HEL cells. Protein and mRNA expression of known JAK2 downstream signalling targets were shown to be downregulated in response to ruxolitinib treatment in SET2 cells and a selection of molecular chaperone genes, transcription factors, cell cycle regulators and genes involved in antigen presentation were affected by ruxolitinib treatment. Treatment of SET2 and HEL cells with a combination of IFN- α and ruxolitinib showed a similar pattern as treatment with ruxolitinib alone with respect to cell proliferation and viability, suggesting this combination may not be the most effective treatment for PV and ET. Combination treatment of fludarabine and ruxolitinib resulted in a much greater decrease in proliferation and viability in both cell lines compared to ruxolitinib treatment alone, proposing a new potential treatment combination for this subset of MPNs.

Abbreviations

ACN – acetonitrile

AML – acute myeloid leukemia

ANOVA – analysis of variance

ATP – adenosine triphosphate

BAT – best available therapy

BCA – bicinchoninic acid

cDNA – complimentary DNA (see DNA for full abbreviation)

CFU-MK – megakaryocyte colony forming unit

CML – chronic myeloid leukemia

DDA – data-dependent acquisition

DIA – data-independent acquisition

DMSO – dimethyl sulfoxide

DNA – deoxyribosenucleic acid

DPBS – Dulbecco's phosphate buffered saline

DTT - dithiothreitol

ECL – enhanced chemiluminescence

EEC – endogenous erythroid colonies

EPO – erythropoietin

EpoR – erythropoietin receptor

ER – endoplasmic reticulum

ET – essential thrombocythaemia

FBS – foetal bovine serum

FLU – fludarabine

GM-CSF – granular macrophage colony stimulating factor

HLA – human leukocyte antigen

HSC – haematopoetic stem cell

HSP – heat shock protein

HU – hydroxyurea

IANH2 – iodoacetamide

IFN -interferon

IMS – industrial methylated spirits

JAK – Janus kinase

LC/MS-MS – liquid chromatography coupled with tandem mass spectrometry

MF – myelofibrosis

MHC – major histocompatibility complex

MPL - myeloproliferative leukemia protein

MPN – myeloproliferative neoplasm

mRNA – messenger RNA (see RNA for full abbreviation)

MS – mass spectrometry

MS1 – first stage of mass analysis in tandem mass spectrometry, where a single precursor ion m/z values are measured

MS2 – second stage of mass analysis in tandem mass spectrometry. Precursor ions identified in MS1 undergo fractionation and create product ions. These product ion m/z values are then measured in MS2

NaCl – sodium chloride

NK – natural killer

PEG – polyethylene glycol

Ph- - Philadelphia-chromosome negative

Ph+ - Philadelphia-chromosome positive

PV – polycythaemia vera

Q-RT-PCR – quantitative reverse-transcription polymerase chain reaction

RNA – ribonucleic acid

RUX – ruxolitinib

SDS – sodium dodecyl sulphate

SO - sodium orthovanadate

SOCS – suppressors of cytokine signals

SP – sodium pyrophosphate

SRM – selective reaction monitoring

STAT – signal transducer and activators of transcription

SWATH-MS – Sequential Window Acquisition of all Theoretical Fragment ions Mass Spectrometry

TCEP - tris(2-carboxyethyl)phosphine

TEAB – triethylammonium bicarbonate

TFA – trifluoroacetic acid

TPO – thrombopoietin

TpoR – thrombopoietin receptor

VC – vehicle control

WHO – World Health Organisation

1. Introduction

1.1. Myeloproliferative Neoplasms: An Overview

Myeloproliferative neoplasms (MPNs) are a group of rare haematopoietic disorders of the bone marrow characterised by the increased number of circulating mature myeloid cells (Vardiman, et al., 2009). All haematopoietic cells differentiate from one type of blood cell, the haematopoietic stem cell (HSC) (Birbrair & Frenette, 2016). These stem cells can undergo asymmetric cell division to produce one stem cell and one differentiated cell of either the lymphoid or myeloid lineage (Orkin, 2000). Figure 1 illustrates the diverse maturation lineages possibly undertaken by HSCs and consequent development of differentiated mature haematopoietic cells.

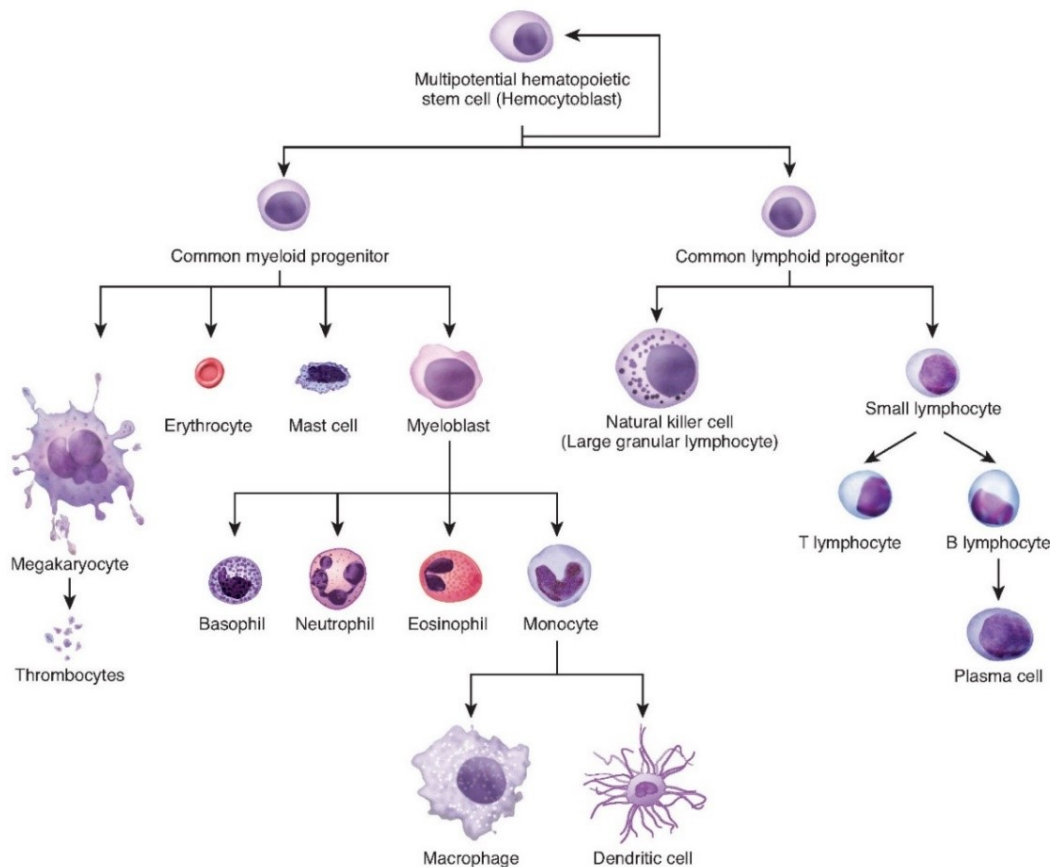


Figure 1: Diagram of the haematopoiesis process showing the differentiation and maturation of a haematopoietic stem cell into the distinct lineages. Haematopoietic stem cells can divide by asymmetric division and produce one stem cell and one cell destined to differentiate into a mature cell of one of the haematopoietic lineages; myeloid or lymphoid progenitors. Further differentiation and maturation of progenitor cells produces a wide range of mature haematopoietic cells with various functions in the innate and adaptive immune response, thrombosis and oxygen transportation. (OpenStax College, 2013).

As the name suggests, MPNs are proliferative disorders of cells within the myeloid lineage. MPNs are sub-divided into two types: classical MPNs and non-classical MPNs, with the latter affecting a smaller population of people. Classical MPNs include chronic myeloid leukaemia (CML), polycythaemia vera (PV), essential thrombocythemia (ET) and myelofibrosis (MF) (Tefferi & Vardiman, 2008). CML is a disorder resulting in the unregulated growth of granulocytes (neutrophils, eosinophils and basophils) within the myeloid lineage and their subsequent accumulation within the bone marrow and peripheral blood. Conversely, both PV and ET are hyperproliferative disorders which affect primarily the red blood cells and platelets respectively, while MF is the development of scar tissue within the bone marrow which inhibits the development and maturation of other haematopoietic cells. MF can be idiopathic (primary MF (PMF)) or develop secondary to PV or ET (secondary MF or post-PV/post-ET MF) (Tefferi & Vardiman, 2008).

1.2. Philadelphia-chromosome negative MPNs

Since the discovery of the Philadelphia chromosome (Ph) in myeloid stem cells of CML patients (Nowell & Hungerford, 1960), classical MPNs have been further subdivided into Ph+ and Ph-. The Philadelphia chromosome is the genetic abnormality relating to the translocation between chromosomes 9 and 22, creating a fusion gene (*BCR-ABL*). This translocation leads to the translation of a mutant tyrosine kinase within myeloid stem cells and constituent activation of proliferative signalling. As such, the development of therapeutic agents has been targeted to the presence of this mutated protein and success in the treatment of CML followed in the form of the small molecule tyrosine kinase inhibitor, Imatinib (Buchdunger, et al., 1996). In contrast, the genetic mutations underpinning the development of the three Ph- MPNs is more complicated than previously understood, as mutations within JAK, CALR and MPL have all been linked to MPN pathogenesis, making it difficult to develop targeted therapeutic strategies for these disorders.

The prevalence of PV within the Europe is estimated at 0.4-2.8 per 100,000 people per year while ET and MF prevalence is estimated at 0.4-1.7 and 0.1-1 per 100,000 people per year respectively (Moulard, et al., 2014). Although these disorders are relatively rare within the population, ET and PV are associated with an increased risk of thrombotic events such as heart attack and stroke, which are a major cause of early morbidity and mortality (Marchioli, et al., 2005) (Barbui, et al., 2011). Quality of life in patients is

drastically decreased due to cytokine-mediated constitutional symptoms including pruritus, headaches and fatigue, coupled with symptoms arising from abnormally high numbers of circulating blood cells such as splenomegaly and cardiovascular disease. In addition, all three MPNs have the potential to progress to acute myeloid leukaemia, due to the underlying nature of the disease or sometimes due to treatments for the initial disease (Chen & Mullally, 2014) (Björkholm, et al., 2011). The risk of transformation to MF or AML, as a result of clonal evolution of the two disorders, is the cause of the majority of deaths associated with MPNs (Marchioli, et al., 2005) and can promote additional symptoms such as anaemia and thrombocytopenia, due to fibrosis suppressing the bone marrow function.

The phenotypic relationship between the three Ph- MPNs was first noted by William Dameshek in a 1951 editorial of *Blood*, where he commented on the existence of pancytosis and elements of bone marrow fibrosis in PV patients, at that time thought to affect the proliferation of erythroid cells only (Dameshek, 1951). Advances in molecular and genetic technology have allowed for the better understanding of MPN pathology as clonal disorders arising from a multipotent myeloid progenitor (Delhommeau, et al., 2007) (Fialkow, et al., 1981). One of the main findings in this field of haematology came in 2005 when four independent research groups identified the same point mutation within the *JAK2* gene in 95% of patients with PV and 50-60% of patients with ET and MF (James, et al., 2005) (Kralovics, et al., 2005) (Levine, et al., 2005) (Baxter, et al., 2005).

1.3. The *JAK2V617F* Mutation

Janus kinases (JAK) are a family of four non-receptor tyrosine kinases, named JAK1-3 and TYK2. These serine-threonine protein kinases transduce extracellular signals following cytokine receptor activation to regulate several haematopoietic processes such as cellular proliferation, differentiation, cell migration and apoptosis (Wilks, et al., 1991) (Ihle, et al., 1995). JAK proteins are comprised of seven homology domains (JH1-7), with the catalytically active domain, JH1, at the C-terminus and a pseudokinase domain, JH2, directly following (Kawamura, et al., 1994), as shown in Figure 2A. With respect to JAK2, the JH2 domain contains an activation loop which binds to the JH1 catalytic domain to negatively regulate the activity of the JAK2 protein (Feng, et al., 1997). Residue V617 is thought to reside within the activation loop of the pseudo kinase domain and translocations at this point may disrupt the interactions between the JH2 loop and the JH1 catalytic domain, which negatively regulate the protein's

kinase activity. The location of residue 617 and interactions of the wild-type JAK2 the JAK2V617F mutant with the JH1 domain are illustrated in Figure 2B and 2C. The V617F mutation leads to constitutively active JAK2 and ligand-independent JAK/STAT signalling (Chen & Mullally, 2014). Constituent activation of downstream signalling pathways including the RAS/MAPK, P-I3K and Akt pathways have also been seen in JAK2V617F-positive cells (James, et al., 2005). As a result, JAK2V617F clones are capable of cytokine-independent growth and hypersensitivity to cytokine signals. It is estimated that 25-30% of PV and MF patients and 2-4% of ET patients are homozygous for JAK2V617F (Baxter, et al., 2005) (James, et al., 2005) (Levine, et al., 2005) (Kralovics, et al., 2005).

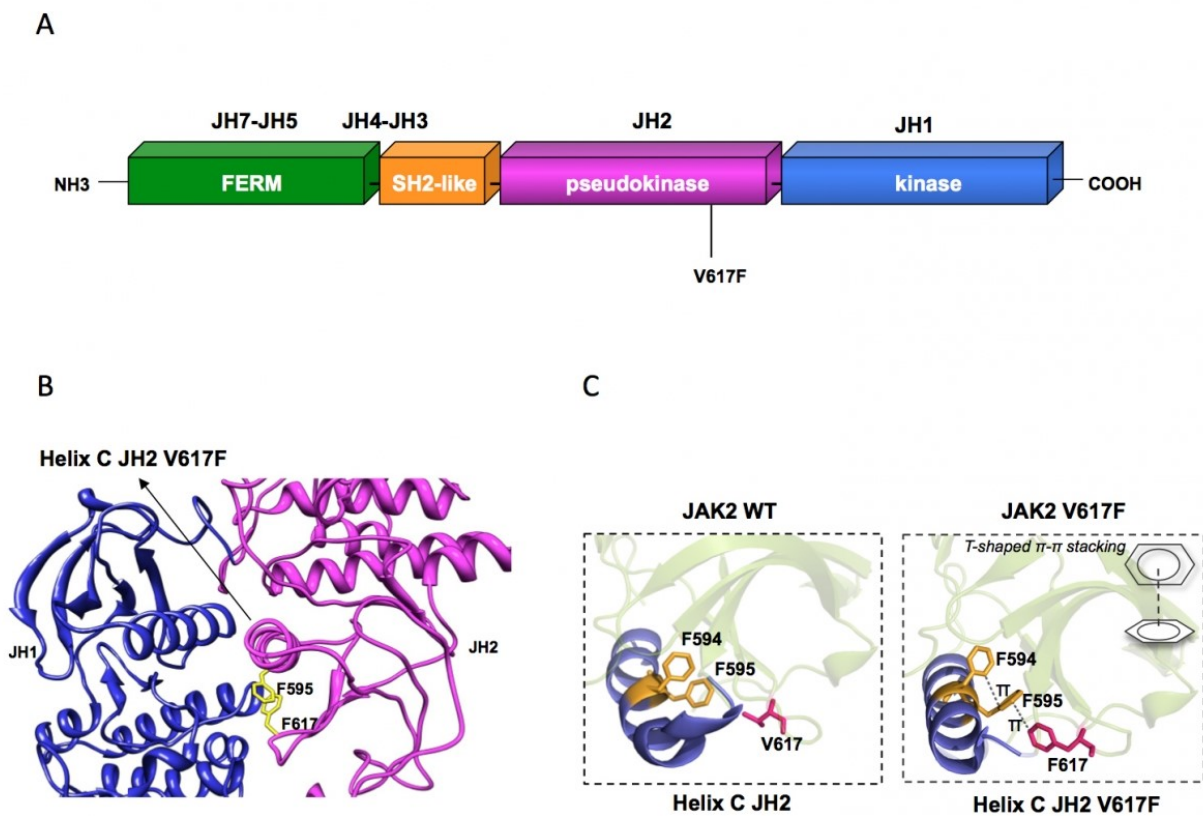


Figure 2: Location of the JAK2V617F mutation in relation to the JAK2 gene domains and protein's tertiary structure. (A) JAK2 contains seven homology domains including the JH1 kinase domain and JH2 pseudokinase domain. (B) Interaction between JH1 and JH2 domains of JAK2 occur to inhibit JH1 activation. (C) The X-ray crystal structures of wild-type JH2 and JH2 V617F solved by the Hubbard laboratory (Constantinescu, 2014)

1.4. JAK2-STAT Signalling

JAK2 mediates extracellular cytokine signals via Type II receptors, including erythropoietin receptor (EpoR), thrombopoietin receptor (TpoR, also known as MPL) and receptors for the granular-macrophage colony stimulating factor receptor (GM-CSF), which form homodimers and heterodimers with other members of the JAK family and possess varying affinities for cytokine and growth factor ligands (Brooks, et al., 2014). The JAK2-STAT signalling pathway is illustrated in the figure below (Figure 3).

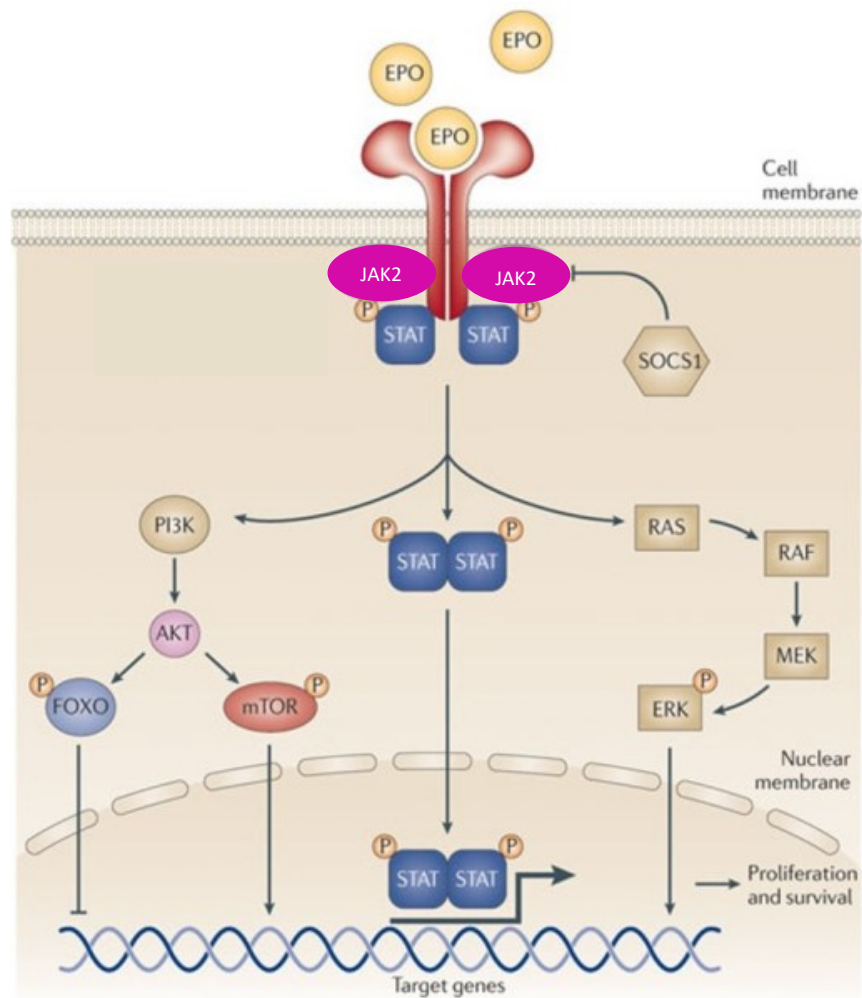


Figure 3: The JAK2/STAT signalling pathway. JAK/STAT signalling pathway illustrating the transduction of extracellular signalling instigated by erythropoietin (EPO). The binding of the EPO ligand to EpoR recruits JAK2 monomers to the intracellular domains of the receptor. JAK2 monomers auto-phosphorylate and recruit STAT proteins which are then phosphorylated by the active JAK2. STAT proteins activate several other intracellular signalling pathways, including MAPK/ERK and P-I3K pathways. STAT proteins also translocate to the nucleus to initiate target gene transcription. SOCS proteins are one of many JAK/STAT targets and they function to negatively regulate the activity of JAK proteins. Diagram adapted from (Ostojic, et al., 2012).

Upon ligand binding and subsequent receptor dimerization, the Type II receptors' intracellular domains recruit and bind JAK2 proteins. Two JAK2 monomers auto-phosphorylate one another at receptor-borne tyrosine residues, resulting in the formation of phosphotyrosine-based docking sites for SH2 domain-containing targets, such as signal transducers and activators of transcription (STATs) and members of the MAPK/ERK pathway (Argetsinger, et al., 2004) (Ihle, et al., 1995). In the case of STAT proteins, JAK2 causes tyrosine phosphorylation of STAT monomers, which then homo- or heterodimerise with other STATs and undergo conformational changes that allow nuclear localisation through the Ran nuclear import pathway. STAT dimers then bind to palindromic base sequences within the DNA and consequently initiate target gene transcription (Stark & Darnell, 2012) (Hebenstreit, et al., 2005).

This signalling pathway is negatively controlled by suppressors of cytokine signals (SOCS), proteins whose gene sequences are targeted by STAT proteins, resulting in a negative feedback loop. SOCS proteins bind to active JAK2 monomers and inhibit their catalytic activity (Krebs & Hilton, 2001). SOCS1 and SOCS3 are negative regulators of the JAK2/STAT pathway (Greenhalgh & Hilton, 2001) and work by degrading JAK2 through the E3 ubiquitin ligase ECS complex (Frantsve, et al., 2001) (Ungureanu, et al., 2002). SOCS1 and SOCS3 directly bind to JAK2's catalytic domain to inhibit kinase activity (Ungureanu, et al., 2002) (Nicholson, et al., 1999) whereas SOCS3 can also indirectly affect JAK2 by binding to cytokine receptors such as EpoR (Sasaki, et al., 2000). Since JAK/STAT signalling plays a central role in haematopoiesis, dysregulation of this pathway has been implicated in a wide range of haematological malignancies such as chronic myeloid leukaemia, T-acute lymphoblastic leukaemia and B-cell leukaemia (Tefferi & Vardiman, 2008), with the *JAK2V617F* mutation being identified in AML, other MPNs and myelodysplastic syndromes (James, et al., 2005) (Levine, et al., 2005) (Tono, et al., 2005) (Steensma & Tefferi, 2008) (McLornan, et al., 2006).

1.5. Key signalling molecules in the pathogenesis of Ph- MPNs

Since the *JAK2V617F* mutation accounts for 95% of PV cases, and 50-60% of ET and MF cases, this mutation cannot be assumed as the genetic modifier in the development of these MPNs. It has been discovered that the remaining 5% of PV patients exhibit mutations within exon 12 of *JAK2*, while mutations within *MPL* and *CALR* account for the majority of non-*JAK2* mutant ET and MF cases (Passamonti, et al., 2011) (Rumi, et al., 2014) (Rumi, et al., 2013).

Myeloproliferative leukaemia protein, encoded by the MPL oncogene, is the receptor for thrombopoietin (TPO) which regulates megakaryopoiesis (Kaushansky, 1995). TPO initiates megakaryocyte colony forming unit (CFU-MKs) maturation by activation of three major signalling pathways: MAPK, P-I3K and JAK/STAT (Rojnuckarin, et al., 1999) (Geddis, et al., 2001) (Drachman, et al., 1995). Signalling through MPL has been shown to activate JAK2, STAT1, STAT3 and STAT5 (Sattler, et al., 1995) (Bacon, et al., 1995) (Drachman, et al., 1995). Furthermore, differential expression of *STAT1* has been observed when comparing PV and ET-like phenotypes in mice models of MPNs and as such, increased expression of *STAT1* is associated with an ET phenotype (Chen, et al., 2010). Conversely, STAT5 has been shown to have a key role in the development of PV-like phenotype in mice models and loss of STAT5 expression prevents the development of *JAK2V617F+* MPNs (Yan, et al., 2012). STAT5 phosphorylation is strongly associated with JAK2 activation and signal transduction and research demonstrates that constitutive activation of STAT5 in erythroid progenitors induced the formation of endogenous (EPO-independent) erythroid colonies (EEC), a hallmark of the PV phenotype but also seen in ET patients (Garçon, et al., 2006) (Mondet, et al., 2015).

Calreticulin is a chaperone protein encoded by the CALR gene. The protein functions to prevent the export of misfolded proteins from the endoplasmic reticulum (ER) by binding to their N-glycosylated sites (Michalak, et al., 2009). Active cytokine receptors are highly N-glycosylated (Royer, et al., 2005) (Albu & Constantinescu, 2011) and therefore the association between aberrant MPL and JAK/STAT signalling and CALR mutations in the pathogenesis of Ph-MPNs was discovered (Chachoua, et al., 2016). Mutant CALR has been shown to induce constitutive, ligand-independent activation of the TPO receptor MPL, which leads to the direct dimerization of JAK2 and subsequent JAK2/STAT signalling (Chachoua, et al., 2016). Overall, dysregulation of the JAK2/STAT pathway is thought to be fundamental for the development of Ph-negative MPNs and as such, current therapeutic approaches are moving towards JAK2 inhibition.

1.6. Current therapeutic strategies for Ph- MPNs

At present, the first treatment option for PV patients is phlebotomy, used to decrease the number of circulating blood cells and help alleviate symptoms caused by the increased peripheral blood volume. However, limitations include no change in the molecular pathogenesis of the disease and the inability to

control pruritus or splenomegaly. Failure of phlebotomy to successfully alleviate symptoms usually results in the use of hydroxyurea (HU) therapy, a chemotherapeutic agent used to suppress bone marrow function. Use of HU has been linked to an increased risk of progression to leukaemia but is still effective at controlling haematocrit and normalising white blood cell counts in patients that need cytoreductive therapy (Björkholm, et al., 2011) (Nielsen & Hasselbalch, 2003) (Harrison, et al., 2005) (Cortelazzo, et al., 1995). Figure 4 shows the current treatment algorithm for PV, as of this year.

For ET patients, HU is the first-line therapeutic agent, followed closely by anagrelide, a platelet-modifying drug considered less effective than HU but not associated with risk of leukaemogenesis (Barosi, et al., 2013). Interferon therapy may also be used to treat PV and ET (this topic will be discussed in greater detail in Section 1.8). PV and ET patients who are resistant or intolerant to HU are considered high-risk for the development of complications. High-risk patients also include those over 60 years of age and who have a history of thrombotic events or presence of cardiovascular events. Low dose aspirin is recommended, particularly in this group to reduce risk of thrombotic complications. Figure 5 shows the most recent treatment algorithm for ET.

Current Treatment Algorithm in Polycythemia Vera

↓

Phlebotomy to hematocrit <45% in both male and female patients
+
Once-daily aspirin (40-100 mg)

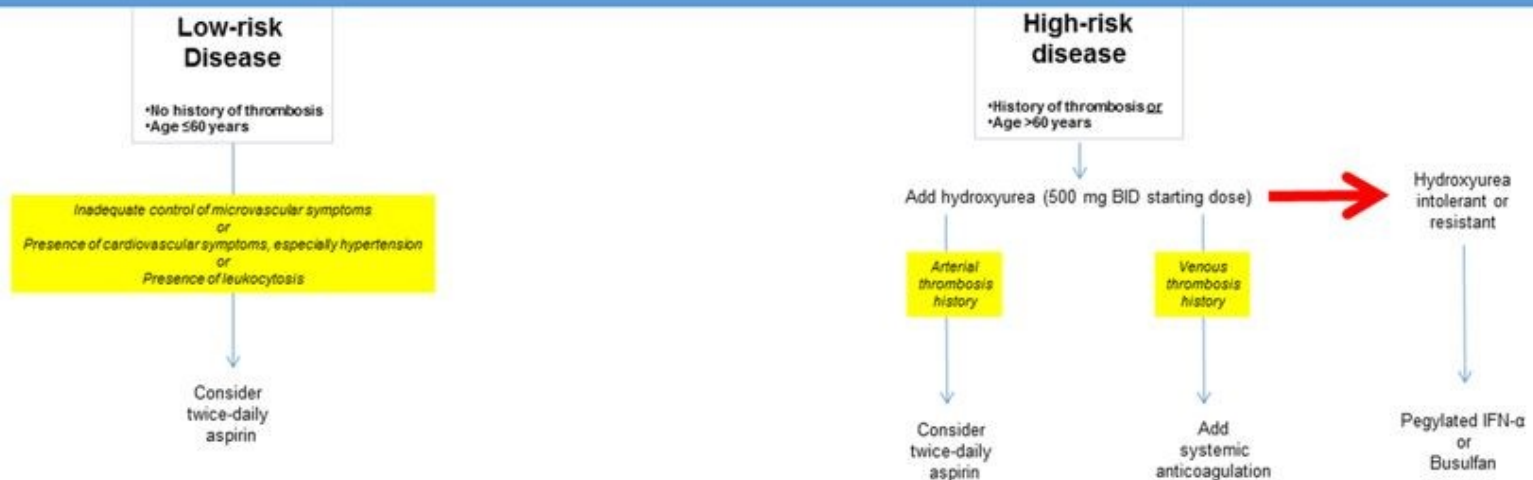
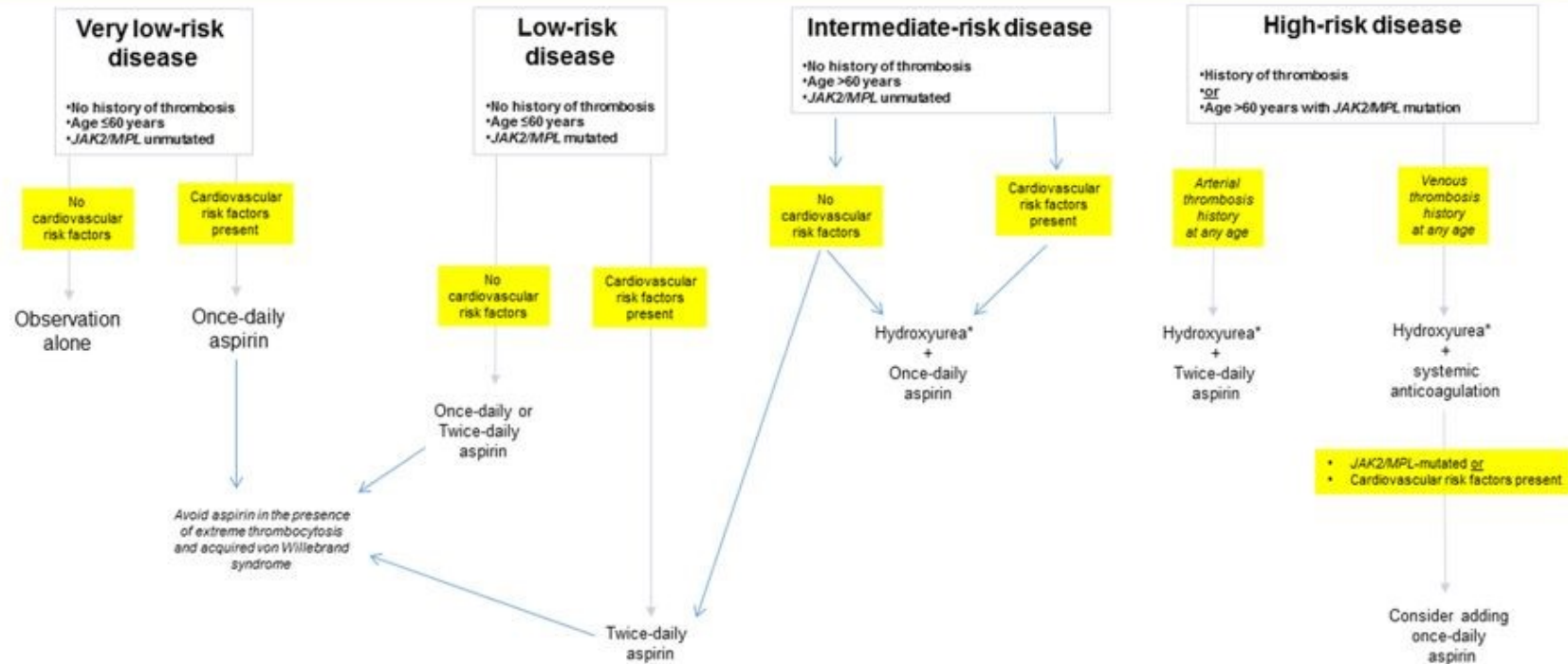


Figure 4: Current treatment algorithm for polycythemia vera. Flow chart containing information on the current treatment of PV upon differentiating patients into high- and low-risk disease based on history of thrombosis and advanced age. (Tefferi, et al., 2018).

Current Treatment Algorithm in Essential Thrombocythemia



*Second-line treatment in hydroxyurea intolerant or refractory patients is pegylated IFN- α or busulfan

Figure 5: Current treatment algorithm for essential thrombocythaemia. Flow chart containing information on the current treatment of PV upon differentiating patients into high-, intermediate-, low- and very low-risk disease based on history of thrombosis, advanced age and presence of JAK2 or MPL mutations (Tefferi, et al., 2018)

1.7. JAK2 Inhibition by Ruxolitinib

Currently, the small molecule JAK1/2 inhibitor ruxolitinib is being used for the treatment of high-risk PV and ET patients with limited success in clinical practice. Ruxolitinib was first approved by the FDA for the treatment of MF based on the two COMFORT studies in which the drug has proven to be significantly more effective in reducing spleen volume by an average of 32% and improving disease-related symptoms by $\geq 50\%$ in 46% of patients compared to a placebo in which symptom improvement was only 5% and placebo-treated patients also experienced weight loss and spleen volume increases by 8.1% (COMFORT-I) (Verstovsek, et al., 2012). In comparison to best available therapy (BAT)(COMFORT-II) (Harrison, et al., 2012), 28% of patients achieved $\geq 35\%$ reduction in spleen volume when treated with ruxolitinib compared to no patients within the BAT group, making ruxolitinib a more effective treatment for MF patients who are not suitable candidates for allogeneic stem cell transplantation (Harrison, et al., 2016). Recently, studies have shifted to investigate the use of ruxolitinib in treating PV and ET patients who have intolerance or resistance to HU (Verstovsek, et al., 2014) (Verstovsek, et al., 2017) (Verstovsek, et al., 2014) (Verstovsek, et al., 2016). These studies show that ruxolitinib successfully reduced splenomegaly and improved disease-related symptoms such as pruritus, bone pain and night sweats. Haematocrit and platelet count was also reduced in each respective disease (Verstovsek, et al., 2014) (Verstovsek, et al., 2014).

Ruxolitinib has also been compared to BAT in HU-resistant or intolerant ET patients in the MAJIC trial (Harrison, et al., 2017). Results demonstrate that ruxolitinib was not superior to BAT with respect to complete or partial haematological response, but was superior with respect to molecular responses, which was only seen in ruxolitinib-treated patients. Ruxolitinib treatment is not currently approved for the treatment of ET and more research is needed to fully support its use as a routine therapy in ET management. With respect to PV, ruxolitinib has been shown to be superior to BAT in reducing splenomegaly, controlling haematocrit and improving disease-related symptoms as shown in the RESPONSE trials (Vannucchi, et al., 2015) (Verstovsek, et al., 2016) (Verstovsek, et al., 2014). As a result, ruxolitinib is now the second-line therapy in PV after failure of HU (resistance or intolerance) (Barosi, et al., 2010) (Barosi, et al., 2009), with its use supported by the RESPONSE studies (Vannucchi, et al., 2015) (Verstovsek, et al., 2016) (Passamonti, et al., 2017).

Despite its clinical success, clonal burden and risk of leukaemic transformation are still unaffected by ruxolitinib treatment (Mesa et al, 2016) and many studies also associate its use with an increased risk of haematological complications such as anaemia, thrombocytopenia, bleeding and increase risk of opportunistic infections (Verstovsek, et al., 2014) (Verstovsek, et al., 2012) (Verstovsek, et al., 2014) (Harrison, et al., 2012) (Harrison, et al., 2016), possibly due to adverse immunosuppressive effects (Schönberg, et al., 2015) (Yajnanarayana, et al., 2015). Complete remission such as that seen in Ph-positive CML patients treated with Imatinib is unlikely to be achieved in Ph-negative MPNs and a much more complex, multi-target approach may have to be administered. Furthermore, drug resistance and reduced sensitivity is also a challenge with prolonged use of JAK2 inhibitors (Koppikar, et al., 2012). If new and improved therapeutic strategies are to be developed for malignancies involving mutated JAK2, it is important that we gain a more comprehensive understanding of the global cellular signalling and the significance of JAK2 signalling in the pathogenesis of MPNs.

1.8. Interferon-alpha therapy in MPNs

Interferons (IFN) are signalling cytokines made and released by host cells in response to the presence of pathogens or tumour cells. Type-I interferons are a class of interferons known to be induced directly by viral infections, in contrast to Type-II IFNs which are synthesised after T- and natural killer (NK) cell antigen recognition (Welsh, et al., 2012). They play a major role in promoting antigen presentation via the upregulation of antigen-presentation genes and consequently induce the activation of T and B cells in response to pathogenic or tumour-associated antigens. IFNs also activate NK cells and macrophages to destroy infected or transformed cells. IFN- α is a Type-I IFN that activates JAK1 and TYK2, therefore recruiting and activating STAT1 and STAT2 (Ivashkiv & Donlin, 2014). IFN- α has been shown to cause elongation of the G2 and S phases of the cell cycle to inhibit the proliferation of malignant cells (Katayama, et al., 2007) (Yin, et al., 2015). IFN- α is also known to cause cell cycle arrest in the G1 phase (Falchi, et al., 2015). Figure 6 shows a selection of anti-tumour mechanisms initiated by IFN- α .

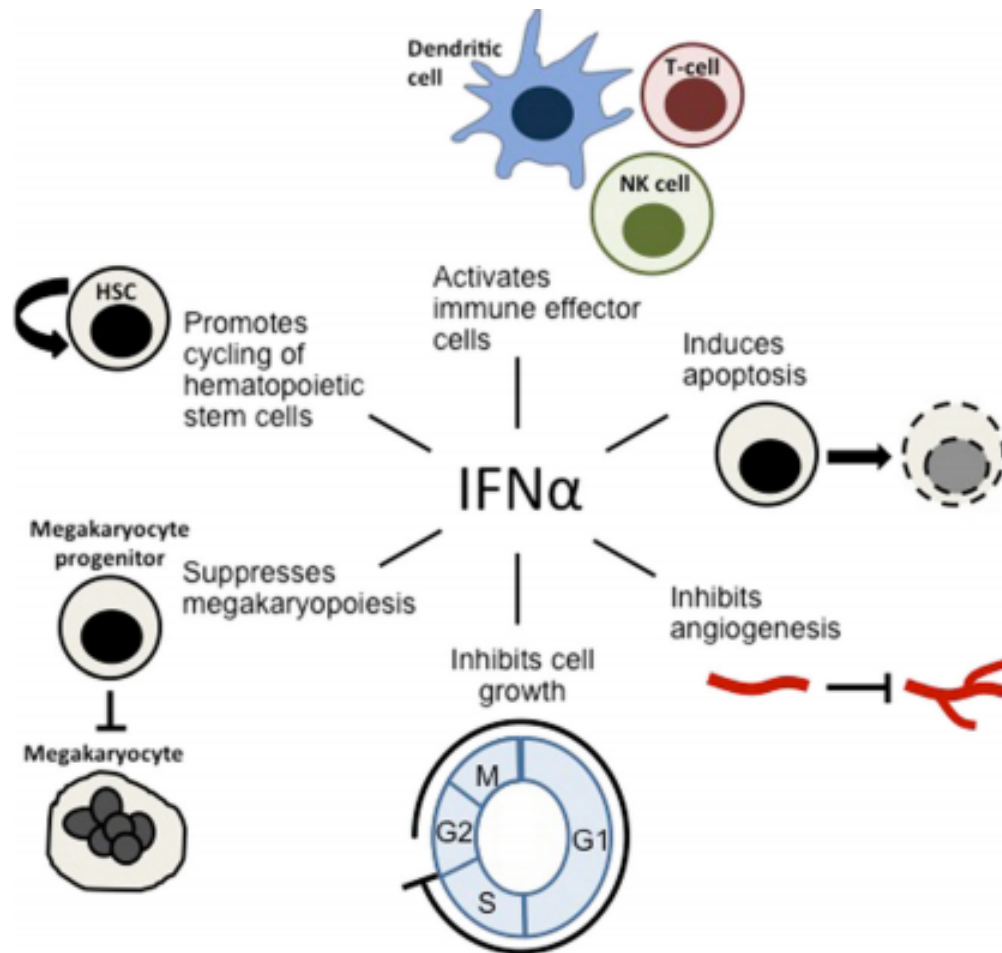


Figure 6: Biological mechanisms of interferon-alpha. *IFN- α is known to affect several biological processes that contribute to its anti-tumour effects in haematological malignancies (Talpez, et al., 2015)*

Interferon alpha-2a (IFN- α) therapy has been used to treat MPNs for more than 30 years (Bellucci, et al., 1988) (Ludwig, et al., 1985) (Cimino, et al., 1993), however reports of high rates of short-term adverse reaction and long-term resistance limited its use to rare cases (Bellucci, et al., 1988) (Kiladjian, et al., 2011) (Kiladjian, et al., 2008) (Geyer & Mesa, 2014) (Hasselbalch, et al., 2011). The use of IFN- α in the treatment of ET was first introduced due to the increasing incidence of ET in young adults, with a slightly higher frequency in females (Landgren, et al., 2008). With younger patients needing to receive treatment for many years, this increases their risk for treatment-related side effects. In addition, pregnancies in women affected by ET may suffer foetal complications due to elevated platelet counts such as recurrent abortions, foetal growth restriction, stillbirth and placental abruption and maternal complications such as bleeding and thrombotic events (Vantroyen & Vanstraelen, 2002). To reduce these complications, the use of antiplatelet drugs or cytoreductive agents is often considered however,

there have been controversies regarding the use of hydroxyurea during pregnancy and suggestions of potential teratogenic effects (abortion, congenital malformations, intrauterine growth restrictions) (Vantroyen & Vanstraelen, 2002).

More recently, the use of IFN- α in treating PV and ET has been reported in multiple studies and phase II trials (Bellucci, et al., 1988) (Kiladjian, et al., 2011) (Stein & Tiu, 2013) (Kiladjian, et al., 2008) (Kiladjian, et al., 2006) (Quintás-Cardama, et al., 2009). Results of the phase II trials have shown IFN- α to be effective in eliminating the risk of thrombotic events, reducing the risk of MF and AML transformation, and inducing complete haematological response in 75-95% and complete molecular response in 15-20% of participants, marked by an inability to detect *JAK2V617F* clones (Quintás-Cardama, et al., 2009) (Quintás-Cardama, et al., 2013) (Stauffer Larsen, et al., 2013) (Mascarenhas, et al., 2014), overcoming known limitations of the JAK2 inhibitor ruxolitinib. IFN- α is the only treatment to date able to induce this level of response in such a significant proportion of patients and is currently used to treat younger patients based on lack of leukemogenicity (Mesa, et al., 2017) (Vannucchi, et al., 2015). IFN- α has also been shown to reduce symptoms and splenomegaly and decrease red blood cell, white blood cell and platelet counts in MPN patients (Falchi, et al., 2015).

In consideration of this evidence, IFN- α therapy is not without its downfalls as its use has been associated with serious side effects such as risk of depression, exacerbation of autoimmune diseases, neuropathy, hypothyroidism, retinitis and myelosuppression (Kiladjian, et al., 2008) (Samuelsson, et al., 2006) (Gowin, et al., 2012). Toxicity was one major limitation to the use of IFN- α as a viable therapy for MPNs, as shown by the phase II trials, and a resulting PEGylated isoform of IFN- α has been synthesised which seems to be better tolerated than the previous isoform due to its increased half-life within the body. Furthermore, PEGylated IFN- α has been approved by regulating agencies for MPN treatment due to its decreased toxicity and has been proven to reduce MPN tumour burden (Kiladjian, et al., 2008) (Quintás-Cardama, et al., 2009) (Them, et al., 2015) (Stauffer Larsen, et al., 2013). In comparison to the current first-line therapy, there was no significant difference in overall response rate in PV and ET patients when comparing PEGylated IFN-2 α and HU (Mascarenhas, et al., 2016).

Due to PEGylated IFN- α 's continued association with myelosuppression and non-haematologic toxicity leading to 15-20% of PV and ET patients discontinuing treatment (Masarova, et al., 2017) (Kiladjian, et al., 2008) (Samuelsson, et al., 2006) (Gowin, et al., 2012), a mono-PEGylated isoform (ropeginterferon alpha-2b) was synthesised. Advantages of this new isoform include the administration to patients decreased to every 2 weeks and that has produced overall response rates of 90% and complete molecular response in 21% of patients in the phase I/II PEGIN-VERA study (Gisslinger, et al., 2015). Phase III trial comparing ropeginterferon- α 2b to HU showed no significant difference in the two therapies in terms of complete haematological response (Gisslinger, et al., 2016) however, it has been shown that MPN patients treated with HU have a higher risk of secondary malignancies compared to those treated with IFN- α (Hansen, et al., 2017).

The exact mechanism of action of IFN- α is currently unknown, however it appears to involve the preferential targeting and depletion of *JAK2V617F* malignant clones via a direct pro-apoptotic mechanism (Kiladjian, et al., 2011) (Chawla-Sarkar, et al., 2003) (Bekisz, et al., 2010) (Gugliotta, et al., 1989). It is known that Type-I interferons such as IFN- α can inhibit the proliferation of cancer cells and increase the cytotoxic activity of NK cells and T-cells (Paul, et al., 2015). As a pleiotropic agent, the efficacy of IFN- α is likely due to a multitude of biological properties including enhancing the immune system (Biron, 2001) (Burchert, et al., 2010) (Burchert, et al., 2015) and direct effects of the drug on malignant stem cells. More recently, the role of inflammation in cancer promotion supports the role of IFN- α in MPN therapy (Hasselbalch, 2013). The presence of additional non-driver mutations may result in the resistance of *JAK2V617F* mutants to IFN- α therapy, as reported previously (e.g. *TET2* mutations), therefore using a combined therapy may be most useful to fully eradicate MPN clones. Despite the toxicity of IFN- α , it has been recently shown that MPN patients treated with HU have a greater risk of secondary malignancies compared to those treated with IFN- α (Hansen, et al., 2017) however it has been speculated that factors such as length of treatment, age and follow up period differences may have influenced the outcomes of this report.

1.9. Combination of ruxolitinib and IFN- α in MPN treatment

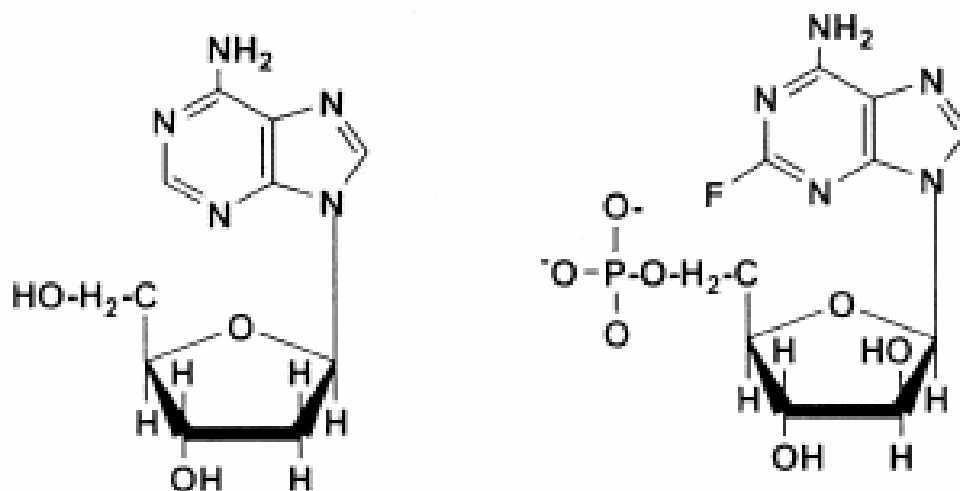
There is limited research investigating the effect of a combinational treatment of ruxolitinib and IFN- α despite a generous amount of evidence suggesting that both have a significant effect on alleviating

disease-related symptoms and improving haematocrit. One case study reported use of the two drugs in combination in a PV patient resistant to HU (Bjørn, et al., 2013). The study explains how the patient achieved complete haematological remission and normalisation of haematocrit within 4 weeks of treatment. 10-month follow up showed the *JAK2V617F* allele burden was reduced from 90% to 28% (Bjørn, et al., 2013) (Bjørn, et al., 2014). Furthermore, the RUXOPeg clinical trial is recruiting patients with primary MF to investigate the effects of PEGylated IFN- α 2a in combination with ruxolitinib in PMF patients (ClinicalTrials.gov Identifier: NCT02742324). In addition, a recent ad-hoc analysis was published comparing ruxolitinib and IFN-2 α therapy in PV patients (Kiladjian, et al., 2018). Results indicated that ruxolitinib was superior to IFN with respect to haematocrit control and tolerance. Patients initially treated with IFN-2 α before crossover to ruxolitinib treatment had reduced splenomegaly and improved blood counts after crossover. Rates of adverse effects decreased after the crossover, however an increase in infections was noted after induction of ruxolitinib (Kiladjian, et al., 2018). The exact mechanism by which IFN- α is able to improve disease-related symptoms and quality of life is not yet elucidated and evidence suggests that ruxolitinib in combination with IFN- α treatment may be superior to single treatment with either agent. A small clinical trial has complimented this theory by evaluating the use of IFN-a and ruxolitinib. The results show how patients displayed marked improvements in symptoms such as major reductions in splenomegaly and improved haematocrit. The authors suggest that combination therapies should be applied in the future (Bose & Verstovsek, 2017).

1.10. Fludarabine treatment in MPNs

Fludarabine is a STAT1 inhibitor used to treat chronic lymphocytic leukaemia (CLL), AML and some subtypes of Hodgkin's lymphoma (Egle, et al., 2018) (Zhang, et al., 2017) (Jackson, 2004). As an adenosine nucleoside analogue, fludarabine works by inhibiting DNA synthesis by competing with dATP as an alternative substrate and directly inhibiting DNA polymerases (Chun, et al., 1991) (Brockman, et al., 1977). Fludarabine is negatively charged at physiological pH and therefore acts as a pro-drug that is dephosphorylated before entering cells by facilitated transport (Barrueco, et al., 1987) (Plunkett, et al., 1980). Inside the cell, it is then re-phosphorylated to the triphosphate state, which is the major intracellular metabolite form of fludarabine and the only known metabolite to have cytotoxic activity. Mono- and diphosphate forms also exist in low concentrations within the cells (Ross, et al., 1993) (Plunkett, et al., 1993). Fludarabine triphosphate has also been shown to inhibit DNA primase, leading to inefficient synthesis of RNA primers required for the initiation of lagging strand synthesis (Catapano, et

al., 1993) (Parker & Cheng, 1987) and ribonuclease reductase, resulting in a reduction of deoxynucleoside pools within the cell (Parker, et al., 1988). Figure 7 shows the chemical structures of deoxyadenosine, a naturally occurring purine, and fludarabine and illustrates the similarities in structure between both purine analogues.



Deoxyadenosine

Fludarabine

Figure 7: Chemical structures of deoxyadenosine and fludarabine. Deoxyadenosine, the naturally occurring purine, and fludarabine have chemically similar structures and thus compete for the active sites of many enzymes involved in DNA synthesis and replication such as DNA polymerase, DNA primase and ribonuclease reductase. Image from (Sigmond & Peters, 2005).

Fludarabine treatment was approved in the US for medical use in 1991 (Oncology, 1991) and is part of the WHO's List of Essential Medicines, a list of the most effective and safe medicine needed in a health system (World Health Organisation, 2015). Fludarabine has been shown to be superior to chlorambucil (an alkylating agent) in the treatment of a multitude of haematological malignancies (Leblond, et al., 2013) (Rai & Hollweg, 2011) (Gandhi & Plunkett, 2002) and is also currently used in combination with cyclophosphamide, mitoxantrone, dexamethasone and rituximab (Thompson, et al., 2016) (Zinzani, et al., 2015) (Manoukian, et al., 2010) (Ma, et al., 2004). With respect to MPNs, fludarabine has been used in the treatment of elderly patients with MF (Matsubara, et al., 2016). Disadvantages of its use include side effects such as nausea, fever, pruritus, shortness of breath, with some severe side effects including

cytopenia and lung inflammation; some of these symptoms are dissimilar to the MPN symptoms themselves (Ding, et al., 2008).

It has been previously reported that fludarabine induces cell cycle arrest and apoptosis and is thought to act primarily through p53 activation (Baran-Marszak, et al., 2004). Since STAT1 has been shown to interact with p53 (Townsend, et al., 2004), fludarabine is able to inhibit the cytokine-induced activation of STAT1 and consequent target gene transcription (Frank, et al., 1999).

1.11. Combination of ruxolitinib and fludarabine in MPN treatment

Fludarabine has been previously used in combination with busulfan to decrease splenomegaly in patients with myeloid malignancies, including MF and AML prior to haematopoietic stem cell transplantation as the presence of splenomegaly has been associated with delayed engraftment, graft failure and poor survival (Gooptu, et al., 2018) (Khalil, et al., 2018) (Matsubara, et al., 2016). At present, there are no studies investigating a direct combinational treatment of ruxolitinib and fludarabine on the treatment of any myeloid malignancies, however one study has explored the use of ruxolitinib prior to a fludarabine/busulfan conditioning regimen as preparation for haematopoietic stem cell transplantation in MF patients. The outcome of this study confirmed that ruxolitinib was able to reduce splenomegaly and symptoms prior to conditioning and pre-treatment with ruxolitinib did not appear to negatively impact post-transplant outcomes (Gupta, et al., 2016).

1.12. Summary

To summarise the differences in these hyperproliferative MPNs, Table I outlines the disease phenotypes investigated in this study, their current treatment options and the cell lines representative of these diseases.

Table 1: MPN disease phenotype summary information. Information on the MPN disease phenotypes examined in this study, their molecular aberrations and frequency of disease in the populations, current treatment options numbered from first-line, low risk treatment option and increasing to high-risk patient options or options for non-responsive patients. Details of the cell lines representative of each disease phenotype and pertinent details are also included.

Type of MPN	Molecular aberrations	Treatment	Cell line used in this study	Origin of cell line
Essential thrombocythaemia	JAK2V617F (50-60% of cases) MPL exon 10 (3-4% of cases), CALR (15-25% of cases) nonmutated JAK2/CALR/MPL (10% of cases) (Imai, et al., 2017) (Nangalia, et al., 2013) (Rotunno, et al., 2014), (Pardanani, et al., 2006) (Rumi, et al., 2014)	<ol style="list-style-type: none"> 1. Aspirin once daily 2. Aspirin twice daily 3. Hydroxyurea (HU) and aspirin once daily 4. HU and aspirin twice daily 5. For HU resistant or unresponsive patients: pegylated IFN-α or busulfan and aspirin daily 	SET2	established from peripheral blood of a 71-year old female with ET at megakaryoblastic transformation, carries JAK2V617F mutation (Quentmeier, et al., 2006) (Uozumi, et al., 2000)
Polycythaemia vera	JAK2V617F (95-96% of cases) JAK2 exon 12 mutations (4-5% of cases) (Rumi, et al., 2014)	<ol style="list-style-type: none"> 1. Phlebotomy and aspirin daily 2. Phlebotomy and aspirin twice daily 3. Phlebotomy and aspirin and HU 4. For HU resistant or unresponsive patients: ruxolitinib, pegylated IFN-α or busulfan and aspirin daily 	HEL	established from peripheral blood of a 30-year old man with erythroleukemia (AML M6) in relapse (after treatment for Hodgkin lymphoma), carries JAK2V617F mutation (Quentmeier, et al., 2006) (Martin & Papayannopoulou, 1982)

This report will investigate the effects of JAK2 inhibition by ruxolitinib on cell proliferation and expression of downstream JAK/STAT signalling targets in ET- and PV-representative cell lines to elucidate the role of JAK2 signalling in the pathogenesis of these hyperproliferative MPNs. Ruxolitinib will also be used in combination with IFN- α , a STAT1 activator, and fludarabine, a selective STAT1 inhibitor, in both cell lines to investigate the role of STAT1 in the pathogenesis of each disease phenotype and identify potential molecular advantages of a dual therapy in the treatment of Ph- MPNs.

1.13. Aims and Objectives

The aims of this study were to investigate the effect of JAK2 inhibition via ruxolitinib on downstream signalling targets in cell lines representative of ET and PV (SET2 and HEL respectively) to help differentiate between the two disorders. In addition, a combination of ruxolitinib and IFN- α or fludarabine was used to investigate the effects of a dual agent therapy compared to ruxolitinib alone and evaluate the role of STAT1 in the pathogenesis of MPNs. The global proteome of SET2 cells was also investigated to identify key downstream targets of JAK2 which could be of interest to disease pathogenesis and progression. This was achieved via several objectives:

1. Investigate the effects of JAK2 inhibition by ruxolitinib on the proliferation of HEL and SET2 cells using MTS proliferation assays, Trypan Blue exclusion assays and growth curves
2. Examine the effect of ruxolitinib on the expression of downstream signalling targets SET2 cells using Q-RT-PCR, Western Blotting and mass spectrometry
3. Evaluate the effects of IFN- α , a STAT1 activator, and fludarabine, a selective STAT1 inhibitor, as a single and dual-agent therapy in combination with ruxolitinib in SET2 and HEL cells and measure the effects of combinational treatment on cellular proliferation and viability.

This report contains 3 hypotheses, as described below:

1. H0. Ruxolitinib will have no effect on cellular proliferation, viability or expression of downstream JAK2 targets in SET2 and HEL cells.

H1. Ruxolitinib will negatively affect cellular proliferation and viability. Expression of downstream JAK2 targets will also be decreased in SET2 and HEL cells treated with ruxolitinib.
2. H0. The combination of ruxolitinib and IFN- α or fludarabine will have no effect on SET2 and HEL cells and will not be superior to ruxolitinib treatment alone with respect to proliferation and viability.

H1. Ruxolitinib in combination with IFN- α or fludarabine will have a synergistic effect and be a more effective at inhibiting cellular proliferation and decreasing viability in SET2 and HEL cells.

3. H0. There will be no difference between the two cell lines, SET2 and HEL, in their response to ruxolitinib and a combination of ruxolitinib and IFN- α or fludarabine considering cell proliferation and viability.

H1. Treatment with ruxolitinib and dual treatment with IFN- α or fludarabine will have distinct cellular responses within SET2 and HEL cells, allowing better insights into the molecular and genetic pathogenesis of each disease phenotype.

2. Materials and Methods

All reagents, instrumentation, software and kits were supplied by Thermo Fisher Scientific (Paisley, UK), Sigma-Aldrich (Dorset, UK) or Bio-Rad Laboratories Ltd. (Hertfordshire, UK) unless specified otherwise. SET2 and HEL cells were incubated in NuAire TripleRed Laboratory Technology incubator (Buckinghamshire, UK). All statistical analysis was performed using GraphPad Prism v 7.04 (GraphPad Software Inc., California, USA).

2.1. Cell Culture

All cell culture was performed in a Class II MSC safety cabinet (NuAire LabGard ES NU-540 Class II, Type A2 Biosafety Cabinet). All cabinets and equipment were cleaned with 70% (v/v) industrial methylated spirits (IMS) made in distilled water prior to use. All cells were cultured at 37°C with 5% CO₂. Ruxolitinib and fludarabine powders (Selleckchem.com) were dissolved in sterile DMSO to create a final concentration of 25 and 50 mM respectively. Human Recombinant Interferon Alpha (IFN- α) 2A (Stem Cell Technologies) powder was dissolved in sterile Dulbecco Phosphate Buffered Saline (DPBS) (Lonza BioWhittaker) supplemented with 0.1% FBS to a concentration of 1 mg/ml. From these stock solutions, each treatment was further diluted using cell culture media to the required experimental concentrations. Cell viability was assessed to be greater than 95% before experiments were set up.

2.1.1. Cell lines and treatments

The SET2 cell line is a *JAK2V617F*+ line, established from the peripheral blood of a 71-year-old female with essential thrombocythaemia at the megakaryoblastic leukaemic transformation stage. Like the SET2 cell line, the polycythaemia vera-representative cell line (human erythroleukemia; HEL) also carries the *JAK2V617F* mutation. This line was established from the peripheral blood of a 30-year-old male with acute myeloid leukaemia subtype M6 (erythroleukemia), according to the French American British system and World Health Organisation classification. Both cell lines were purchased from DMSZ. SET2 and HEL cells were treated with 1 μ M ruxolitinib and cultured for up to 72 hours to investigate the effects of JAK2 inhibition on cell proliferation and viability.

1 μM ruxolitinib was chosen as this concentration has shown to have significant effects on cell proliferation and gene expression in previous studies (Waibel, et al., 2013) (Mazzacurati, et al., 2015) (Meyer, et al., 2015). Furthermore, it has been previously shown that the maximum concentration of ruxolitinib detected in the plasma of patients treated with currently licensed doses of ruxolitinib is 1 μM , as determined by mass spectrometry (Shilling, et al., 2010). IFN- α was used at a concentration of 1 $\mu\text{g}/\text{ml}$ in this study, whereas current literature shows that at a concentration of 2 $\mu\text{g}/\text{ml}$, the treatment is able to inhibit proliferation of HEL cells by 41% while the number of patient-derived EECs was reduced by 90% with this concentration (Verger, et al., 2018). In contrast, an in vivo study of IFN- α use report the maximum serum concentration at 0.0186 $\mu\text{g}/\text{ml}$ (Costa, et al., 2018). With respect to fludarabine, this molecule has previously been used as a synergistic drug to treat patients with relapsed leukaemias, including AML, and has been shown to achieve the most significant drug synergism with cytarabine at a concentration of 10 μM (Avramis, et al., 1998) (Gandhi, et al., 1998).

2.1.2. Culture of cell lines

Cell culture media for both cell lines was RPMI 1640 media supplemented with 25 mM HEPES and 2 mM L-glutamine (Lonza BioWhittaker), with 100 I.U./ml penicillin and 100 $\mu\text{g}/\text{ml}$ streptomycin at 1% (v/v) also added to the media. Foetal bovine serum (FBS) (Gibco) was added to SET2 media at a 20% (v/v) whereas 10% (v/v) FBS was added to HEL media. Cells were maintained at a concentration of $0.5-1 \times 10^5$ cells per ml and both cell lines were grown in suspension culture. After 48 hours of continued growth, or when cells reached 80% confluency, a single cell suspension was made, and cells were sub-cultured with fresh media.

2.1.3. Assessment of cell viability

Cell viability was assessed using the trypan blue exclusion assay. The dye is excluded from live cells as they possess an intact membrane however, dead cells do not and so take up the dye. Dead cells are therefore stained dark blue, which is visible under the microscope. To assess cell viability, a single cell suspension was made, and cells were transferred to a 15 ml centrifuge tube. Cells were collected by centrifugation at 1200 rpm (257 xg) for 3 minutes using a bench top centrifuge. The supernatant was discarded, and cell pellet resuspended in media pre-warmed to 37°C in a water bath. 50 μl cell suspension was removed and diluted 1:1 with Trypan Blue dye. 10 μl of this solution was loaded onto a

haemocytometer and cells were counted. The number of live and dead cells in the sample were counted and an average cell count was determined by the mean cell count of four 1 mm² areas. The total number of cells per ml cell suspension was calculated using the following equation: Cell count per ml = Average (mean) cell count x 2 (dilution factor with Trypan Blue) x 10⁴.

2.1.4. Assessment of cell proliferation by MTS assay

SET2 cells were cultured in media containing 1 µM ruxolitinib (referred to as RUX for the remainder of this report), 1 µg/ml IFN-α, 1 µM fludarabine (referred to as FLU) or a combination treatment (n=6) (1x10⁴ cells/96-well). Cells were incubated at 37°C 5% CO₂ for 72 hours and then MTS assay was performed as per the manufacturer's instructions using CellTitre 96 Aqueous MTS Reagent solution (Promega). 20 µl of MTS solution was added to each well and the plate left to incubate at 37°C in the dark for 3 hours before absorbance was read at 490 nm using a Synergy HT microplate reader (Vermont, USA). Live and dead cell controls and background fluorescence (media only) were also accounted for (n=3 for each).

2.2. Mass Spectrometry

2.2.1. Protein isolation and quantification

Cell pellets were collected and lysed in lysis buffer containing 0.5 M triethylammonium bicarbonate (TEAB), 0.05% SDS, 6.4 mM sodium pyrophosphate (SP) and 1 mM sodium orthovanadate (SO). Samples were sonicated twice for 15 seconds with a 15 second incubation on ice between sonication and then centrifuged at 21200 xg for 30 minutes. The lysate containing the total protein was removed and quantified by BCA assay (Thermo Fisher Scientific). Samples were made in 1:10 dilutions in lysis buffer and Pierce BCA Protein assay kit was used in accordance with the manufacturer's instructions. The plate was incubated at 37°C for 10 mins and the absorbance was read at 562 nm using a plate reader using a Synergy HT microplate reader (Vermont, USA).

2.2.2. Solution Digestion of Proteins

10 µg protein from each sample was made up to 15 µL with 100 mM TEAB. Reduction buffer was made with 45 µL 240 mM TCEP (pH 8) and 108 µL 120 mM iodoacetamide (IANH₂), and 85 µL of this buffer was

added to each sample. Samples were incubated in the dark for 1 hour at room temperature. 10 μL 0.01 $\mu\text{g}/\mu\text{L}$ Lys-C was added to each sample and left to digest at 37°C for 4 hours. 10 μL 0.05 $\mu\text{g}/\mu\text{L}$ Sequencing Grade Modified Trypsin Porcine (Promega) made in TEAB lysis buffer was added to samples and left to digest overnight at 37°C.

2.2.3. Peptide Recovery using Harvard Spin Column

Samples were acidified using 10% trifluoroacetic acid (TFA) and pH measured between 2-3 using pH sticks. 96-well Micro Spin Columns (Harvard Apparatus) were used as per the manufacturer's instructions. Briefly, 50% acetonitrile (AcN) constitution buffer was added to the spin columns. Two wash steps were performed before samples were loaded onto the columns. Samples were washed 3 times within the columns and eluted in 80% AcN solution containing 0.1% TFA. Eluted peptides were transferred to 1.5 mL Lo-Bind Eppendorf tubes and lyophilized by vacuum centrifugation for 3.5 hours. Peptides were reconstituted in 0.1% acetic acid in HPLC-grade water and loaded onto the LC-MS System.

2.2.4. SWATH-MS analysis

Data-independent acquisition (DIA) Sequential Window Acquisition of all Theoretical Fragment ions (SWATH) mass spectrometry was performed using a 5600 TripleTOF mass spectrometer (ABSciex, Warrington, UK) and an Eksigent 1D+ Nano LC systems (Eksigent, Dublin, CA). The LC gradient was produced using buffer A (2% AcN and 0.1% formic acid in HPLC water) and buffer B (2% water and 0.1% formic acid in AcN) with 0.1% iRT peptide samples of a known m/z ratio spiked-in. 3 μL containing 10 μg each sample was injected in triplicate and separated with a linear gradient of 2% buffer B to 35% buffer B over 180 min at a flow rate of 0.3 $\mu\text{L}/\text{min}$. Spectra autocalibration occurred after acquisition of every five samples using dynamic LC-MS and MS/MS acquisitions of 25 fmol β -galactosidase. The mass spectrometer was operated in a looped production mode; with the instrument tuned to allow a quadrupole resolution of 25 amu per mass selection.

2.2.5. Targeted Data Extraction and Bioinformatics

Spectral alignment and targeted data extraction of DIA samples were performed with the SWATH 2.0. Processing in Peakview (Version 2.2, AB Sciex) using an in-house plasma reference spectral library. Resulting SWATH .wiff files were analysed using Markerview (ABSciex). Peptides were identified with

99% confidence at a false discovery rate (FDR) below 1% and compared to a pan-human reference spectral library for target protein identification. Welch's t-test was used to detect differences between RUX-treated and untreated SET2 samples. The proteomic data set was then ordered by P-value and proteins with P-values less than 0.05 and below the FDR were considered for further analysis as this was the collection of proteins of interest differentially expressed upon RUX treatment in comparison to untreated cells. To identify significantly differentially expressed proteins upon JAK2 inhibition, the selected proteins of interest were ordered by fold change and proteins with a fold change >1.5 and $<1/1.5$, when comparing treated samples to untreated samples, were identified. Accession numbers of each protein were acquired through Uniprot database and protein-protein interactions were determined using the STRING database version 10.2. Volcano plots were produced using GraphPad Prism. This workflow allowed us to identify key downstream JAK2 targets which may contribute to the ET phenotype in SET2 cells and distinguish potential biomarkers of disease in ET and thus highlight future therapeutic targets.

2.3. Western Blotting

2.3.1. Protein extraction and quantification

Cell pellets were lysed on ice in lysis buffer containing 50 mM Tris, 150 mM NaCl, 1% NP-40 and 10% glycerol with one cOmplete Mini Protease Inhibitor Cocktail tablet (Roche Diagnostics, Mannheim, Germany) added per 20 ml lysis buffer. Samples were vortexed briefly before centrifugation at 21130 xg for 2 minutes at 4°C. The supernatant containing the protein was then transferred to a clean, chilled 0.5 mL Eppendorf tube and pellet discarded. Protein was quantified via BCA assay as previously described (see Section 2.2.1)

2.3.2. Protein analysis by SDS Polyacrylamide Gel Electrophoresis

Samples were mixed with 4X NuPAGE LDS sample loading buffer (Invitrogen by Thermo Scientific) in 0.5 mL Eppendorfs and heated 99°C for 2 minutes on a digital heat block. Two 5-10% Tris-Glycine SDS gels were prepared as described previously (Harlow & Lane, 1988). The gels were assembled within the electrophoresis tank and the tank filled with SDS running buffer (25 mM Tris, 192 mM Glycine, 0.1% w/v SDS). Lysates were loaded onto the gels along with 5 µL Spectra Multicolor Broad Range Protein Ladder molecular weight marker (Thermo Fisher Scientific). Proteins were separated by electrophoresis at 100 V

for 100 minutes in a Mini-Protean Tetra System electrophoresis tank. Transfer to Trans-Blot Turbo Transfer 0.2 μ L nitrocellulose membranes was performed using a semi-dry automated transfer system (Trans-Blot Turbo Transfer System) as per the manufacturer's instructions and using Trans Blot Transfer Solution (Bio-Rad). Parameters for the automated transfer are as follows: 25 V, 2.5 A, 7 minutes. The membrane was blocked for 1 hour at room temperature on a rocker in 5% BSA made in TBS-Tween (20 mM Tris, 100 mM NaCl, 0.1% Tween, pH 7.5). Primary antibody solution was added to the membrane and incubated overnight at 4°C on a rocking platform shaker. Primary antibody concentrations are found within Table II.

Table II: Details of Western Blot antibodies used in this report. All primary antibodies were diluted in 2.5% BSA in TBS-Tween.

Monoclonal Primary Antibody Target	Dilution	Organism of origin	Manufacturer	Phosphorylated residue	Antibody Clone
STAT1	1:10,000	Rabbit	Cell Signalling Technology	-	-
Phospho-STAT1	1:1000	Rabbit	Cell Signalling Technology	Y701	D4A7
STAT5	1:5000	Rabbit	Cell Signalling Technology	-	-
HSP70	1:2000	Rabbit	Cell Signalling Technology	-	-
α -Tubulin	1:10000	Mouse	Merck (formerly Sigma Aldrich)	-	DM1A

Blots were then washed 5 times for 5 minutes per wash in TBS-Tween. HRP-linked polyclonal secondary antibody (Dako) was added at a concentration of 1:10,000 (made in TBS). Incubation of the secondary antibody took place at room temperature on a rocking platform shaker for 1 hour. The membrane was again washed 5 times for 5 minutes each in TBS-Tween. The Radiance Plus High Sensitivity Chemiluminescent HRP Substrate kit (Azure Biosystems) was used as per the manufacturer's instructions, with both kit reagents being mixed at a 1:1 ratio to make the ECL reagent. 0.5 mL reagent was then added to the membrane and protein bands were detected using chemiluminescence via the ChemiDoc Gel Imaging System. The protein of interest was identified using a molecular weight marker

which was run in the first lane of each gel. Densitometry analysis was performed using ImageLab 6.0 software (Bio-Rad) and showed the relative density of each protein in each sample to quantify the expression of target protein. Target protein expression was normalized to the expression of α -tubulin in each sample.

2.4. Q-RT-PCR

2.4.1. RNA Isolation

Total RNA was isolated from cells using an RNA Mini-Prep kit (Zymo Research) as per the manufacturer's instructions. Briefly, cells were lysed in buffer before being transferred to a spin column and filtered by centrifugation. 0.8% (v/v) ethanol was added to the filtrate before being passed through another filtered spin column. Samples were washed before incubation with RNase-Free DNase (Qiagen) for 15 minutes at room temperature. Cells were washed twice, and RNA was eluted in RNase-free water. The concentration of RNA in each sample was measured using a Nanodrop 1000 Spectrophotometer and One Viewer software (Thermo Scientific).

2.4.2. RNA to cDNA conversion

1000 μ g RNA from each sample was diluted in nuclease-free water and reverse transcribed using the iScript cDNA synthesis kit (Bio-Rad) as per the manufacturer's instructions. 15 μ L isolated RNA was mixed with 1 μ L MMLV reverse transcriptase (RT) and 4 μ L 5x reaction mix containing both oligo(DT) and random hexamer primers in 0.2 mL Eppendorf tubes (20 μ L total volume). For each sample, a negative control was made using 1 μ L nuclease-free water in place of the reverse transcriptase. A no-template control containing 15 μ L RNase-free water was also made. All samples were placed on a SureCycler 8800 thermocycler (Agilent Technologies Ltd., Cheshire, UK) with parameters as follows (see Table III). After reverse transcription, all samples were stored at -20°C.

Table III: Thermal cycler parameters for reverse transcription of RNA.

RT Step	Temperature (°C)	Time (minutes)
Priming	25	5
Reverse Transcription	46	20
RT Inactivation	95	1
Storage	4	∞

2.4.3.Q-RT-PCR

Samples were diluted 1:50 with molecular-grade water and SYBR Green forward and reverse primers were made to 10 mM, also with molecular-grade water. Primers were then combined with SensiFast SYBR Lo-ROX Master mix (Bioline) at a 1:11 ratio respectively. 5.5 µL of SYBR Green/primer solution was added to each well along with 90 µg cDNA (suspended in 4.5 µL) to give a total volume of 10 µL per well. Each SYBR Green reaction was performed in duplicate on a 96-well PCR plate. The plate was centrifuged at 100 xg for 1 minute before being loaded onto the StepOnePlus Real-Time qPCR System (Applied Biosystems). qPCR conditions were input into the StepOne Software (v2.3) and were: 95°C for 10 minutes then 40 cycles of 95°C for 15 seconds and 60°C for 1 minute. A dissociation curve was added to each reaction to determine the accuracy of primers used. Dissociation curve parameters were: 95°C for 15 seconds, 60°C for 1 minute and +0.3°C/second increasing temperature up to 95°C. The cycle threshold (CT) values for each sample were normalised to GAPDH CTs and the comparative CT method ($2^{-\Delta\Delta CT}$) was used to calculate the relative quantities of target mRNAs. A list of primer sequences can be found in Table IV.

Table IV: List of primer sequences used in this report. Forward and reverse primer sequences used in Q-RT-PCR experiments.

Gene	Primer Sequences (5'-3')
STAT1	F: ATCAGGCTCAGTCGGGGAATA R: TGGTCTCGTGTCTCTGTTCT
STAT3	F: GGTACATCATGGGCTTTATC R: TTTGCTGCTTTCACTGAATC

STAT5B	F: ATGGGACTCAGTAGATCTTG R: CTTCAGTAAAACCCATCTTCC
SOCS1	F: TTTTCGCCCTTAGCGTGAAG R: CATCCAGGTGAAAGCGGC
SOCS3	F: AGCAGCGATGGAATTACCTGGAAC R: TCCAGCCCAATACCTGACACAGAA
HSP90AB1	F: AGAAATTGCCCAACTCATGTCC R: ATCAACTCCCGAAGGAAAATCTC
HSPA8	F: ACCTACTCTTGTGTGGGTGTT R: GACATAGCTTGGAGTGGTTCG
HSPA5B	F: CATCACGCCGTCCTATGTGCG R: CGTCAAAGACCGTGTTCG
HLA-A	F: CTTGTAAAGTGTGAGACAGC R: CTTCAAGTCACAAAGGGAAG
CALR	F: AGTCCGGCAAGTTCTACGG R: ACAGAGCATAAAAGCGTGCAT
CANX	F: GGCCAAGCATCATGCCATCT R: TGATCCAGGTTGAGTTCTGGT
MCL1	F: TGCTTCGGAACTGGACATCA R: TAGCCACAAAGGCACCAAAAG
IRF1	F: CTGTGCGAGTGTACCGGATG R: ATCCCCACATGACTTCCTCTT
DDX3X	F: ACGAGAGAGTTGGCAGTACAG R: ATAAACCACGCAAGGACGAAC
ISG15	F: CGCAGATCACCCAGAAGATCG R: TTCGTGCGATTTGTCCACCA
TAP-1	F: CTGGGGAAGTCACCCTACC R: CAGAGGCTCCCAGTTTGTG
GAPDH	F: TGCACCACCAACTGCTTAGC R: GGCATGGACTGTGGTCATGAG

2.5. Statistical Analysis

Results are presented as mean \pm standard deviation (SD). To assess statistical analysis of growth curves and Trypan Blue exclusion assays comparing each treatment (ruxolitinib alone and the combination of ruxolitinib and IFN α or fludarabine) over 72 hours, a two-way analysis of variance (ANOVA) was performed with subsequent Bonferroni post-hoc analysis test. MTS assays comparing ruxolitinib alone with untreated cells were analysed by unpaired T-tests, whereas MTS assay results assessing the combination of ruxolitinib with IFN α or fludarabine were assessed by one-way ANOVA with Tukey's multiple comparison post-hoc test. For RNA expression analysis by Q-RT-PCR, unpaired T-test were performed for 24-hour experiments whereas for 72-hour experiments, two-way ANOVA with Bonferroni's post-hoc test was performed as expression was normalised to the expression of each target of untreated cells at 24 hours. Differential protein expression analysed by Western Blot and SWATH-MS was also analysed by unpaired T-tests. For mass spectrometry experiments, Welch's T-test was performed for comparison of differential protein expression in SET2 cells upon 24-hour ruxolitinib treatment. All of this statistical analysis was performed in GraphPad Prism v5.0. Results were considered statistically significant when the P value was less than or equal to 0.05. Stars representing p values are indicated as follows: $p > 0.05$ not significant; $p < 0.05$ *; $p < 0.01$ **; $p < 0.001$ ***; $p < 0.0001$.

3. Results

3.1. The effect of 1 μ M RUX on cellular proliferation and viability

To investigate the effect of RUX on SET2 and HEL, cells were seeded at a density of 2.5×10^4 cells/ml in 6-well plates. Cells were grown in the presence or absence of 1 μ M RUX and cultured for a total of 72 hours at 37°C 5% CO₂. Every 24 hours, a single cell suspension was made and 50 μ L was removed for counting. Cells were mixed at a 1:1 (v/v) ratio with Trypan Blue and counted as per Section 2.1.3.

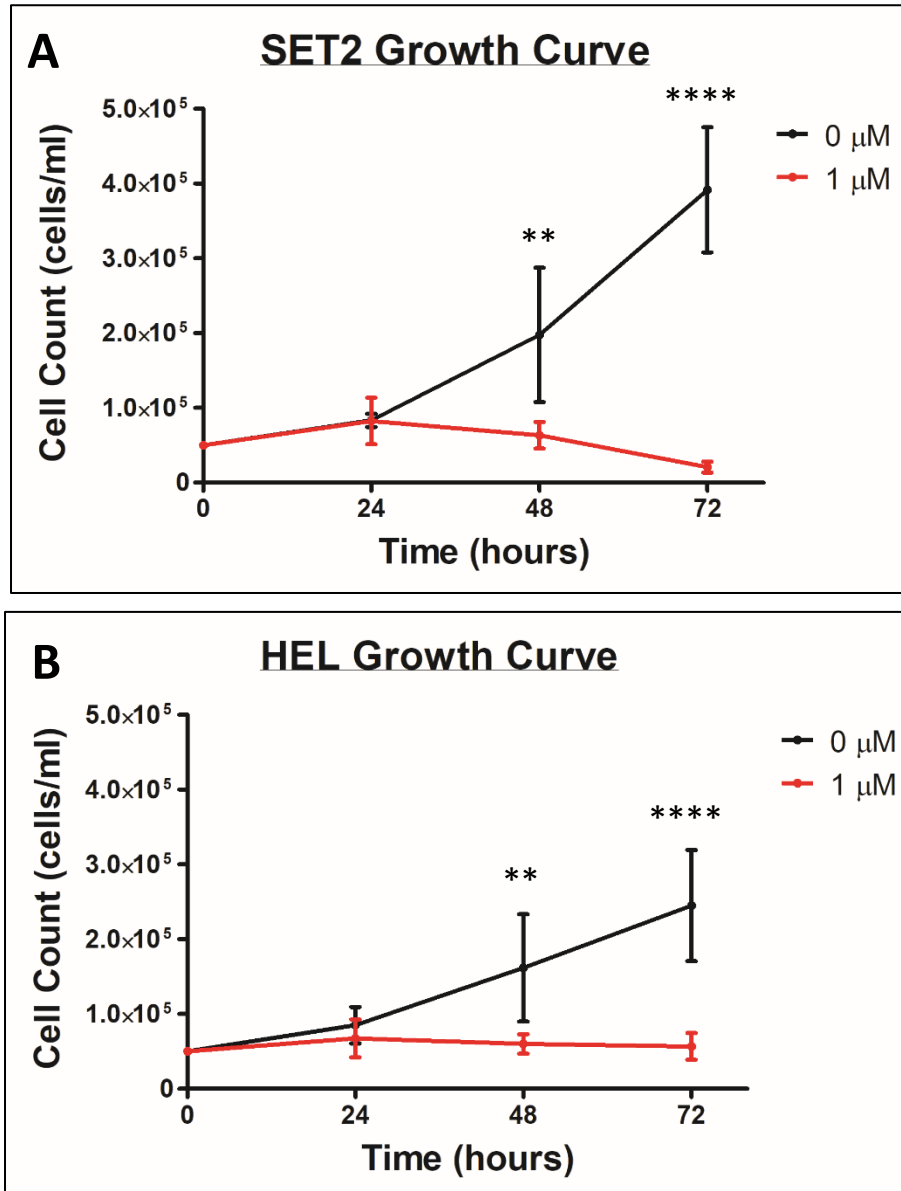


Figure 8: A) SET2 and B) HEL cells grown in the presence or absence of 1 μ M RUX over 72 hours and cells counted at 24-hour intervals ($n=4$). Each point represents the mean of the biological repeats with error bars indicating the standard deviation. Two-way ANOVA: SET2: $p < 0.0001$. HEL: $p = 0.0135$.

Figure 8 shows the total number of SET2 and HEL cells at each time point when treated with 1 μ M RUX or vehicle control (DMSO). The graph illustrates that cellular proliferation is negatively affected by RUX treatment in both cell lines. Two-way ANOVA repeated measures analysis of SET2 results shown in Figure 8A shows a significant difference in cell proliferation between treated and untreated SET2 cells ($p < 0.0001$). A similar pattern was observed with HEL cells in Figure 8B ($p = 0.0135$). Bonferroni multiple comparisons analysis indicates no significant differences comparing treated to untreated cells at 24 hours however a statistically significant difference at 48 and 72 hours was observed in SET2 cells ($p < 0.01$ and $p < 0.0001$ respectively). In HEL cells, Bonferroni multiple comparison showed the same pattern, with no significant difference in cell proliferation at 24 hours but a significant difference at 48 and 72 hours ($p < 0.01$ and $p < 0.0001$ respectively).

Alongside the production of growth curves, the sample of cells removed for counting at each time point were subject to Trypan Blue exclusion assay to assess cell viability in SET2 and HEL cell treated with 1 μ M RUX. The Trypan Blue data shown below in Figure 9 is coupled with the growth curve data shown in Figure 8.

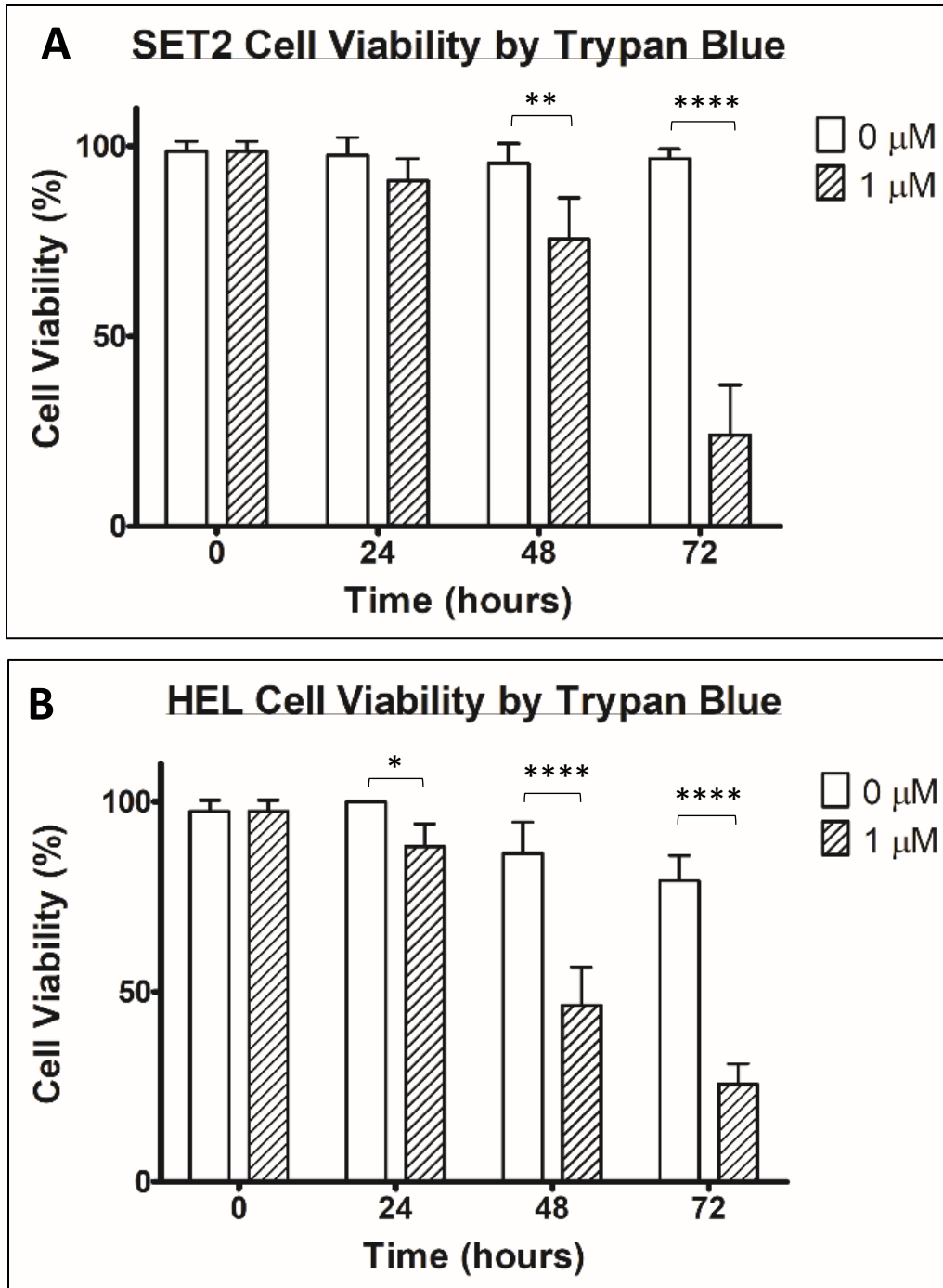


Figure 9: A) SET2 and B) HEL cells grown in the presence or absence of 1 μM RUX over 72 hours and cells viability determined by Trypan Blue every 24 hours ($n=4$). Each bar represents the mean of the biological repeats with error bars indicating the standard deviation. Two-way ANOVA: SET2: $p=0.0001$. HEL: $p<0.0001$.

Trypan Blue exclusion assay results shown in Figure 9 illustrate that the viability of both SET2 and HEL cells was decreased with RUX treatment after 24, 48 and 72 hours compared to untreated cells. Two-way ANOVA repeated measures analysis shows a significant difference in cell proliferation between treated and untreated SET2 cells ($p=0.0001$), shown in Figure 9A. A similar pattern was observed with HEL cells in Figure 9B ($p<0.0001$). Bonferroni multiple comparisons analysis of SET2 results indicates no significant differences comparing treated to untreated cells at 24 hours however a statistically significant difference was observed at both 48 and 72 hours in SET2 cells ($p<0.01$ and $p<0.0001$ respectively). In HEL cells, Bonferroni multiple comparison showed a significant decrease in cellular proliferation at all three time-points ($p<0.05$, $p<0.0001$ and $p<0.0001$ respectively), suggesting that HEL cells may be more sensitive to ruxolitinib treatment.

Cell proliferation was also determined by MTS assay. 1×10^4 cells were grown in a 96-well plate in the presence or absence of $1 \mu\text{M}$ RUX and cultured for 72 hours at 37°C 5% CO_2 .

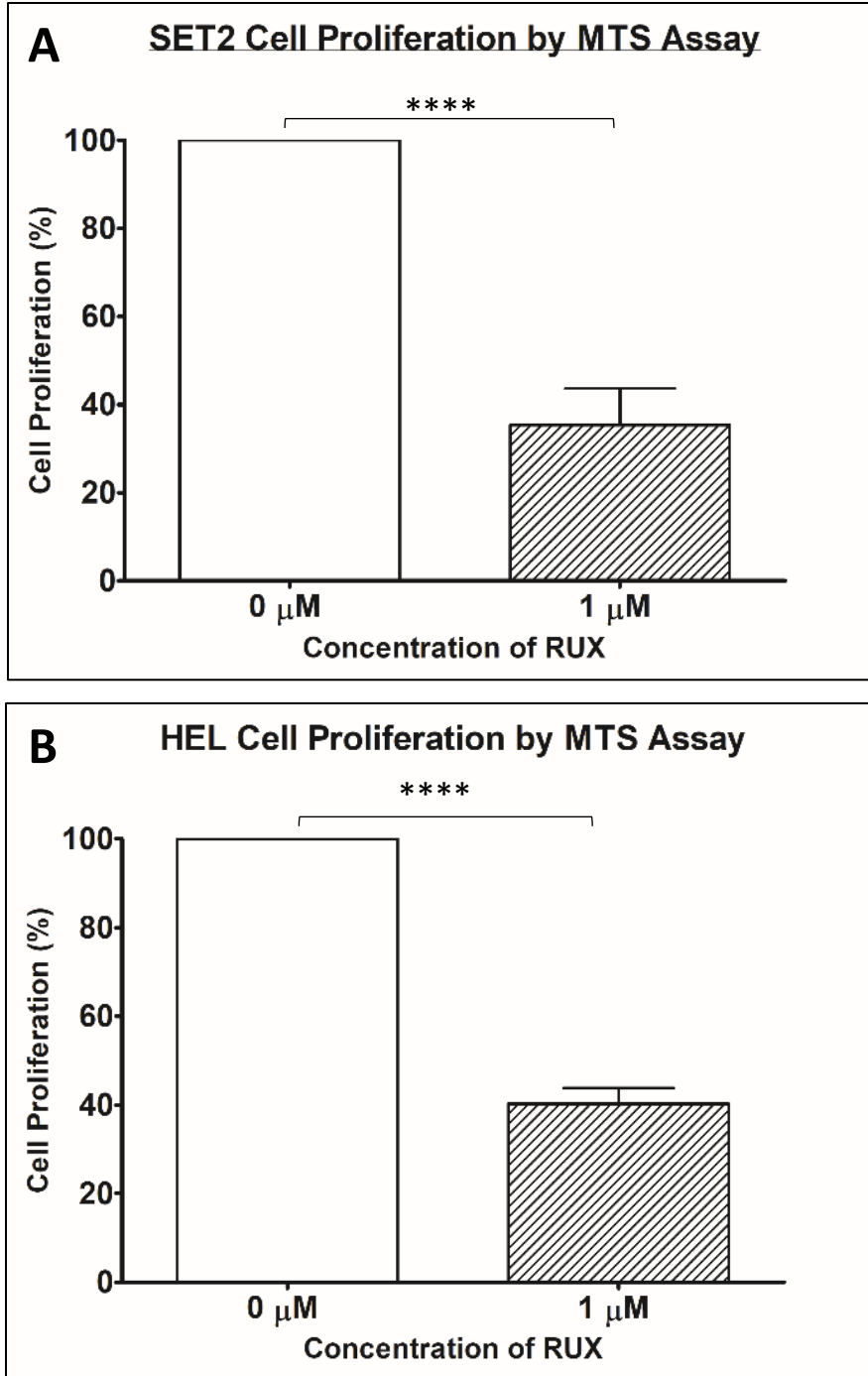


Figure 10: Cell proliferation in A) SET2 and B) HEL cells determined by MTS assay 72 hours post-treatment with 1 μ M RUX, normalised to untreated controls (n=6 and n=7 respectively). Each bar represents the mean of the biological repeats with error bars indicating the standard deviation. Unpaired T-test: SET2: $p < 0.0001$. HEL: $p < 0.0001$.

Figure 10 shows the percentage proliferation of SET2 and HEL cells treated with 1 μ M RUX or VC (DMSO), with results normalized to the VC, determined by MTS assay. This experiment shows that cellular proliferation is negatively affected by RUX treatment in both SET2 (Figure 10A) and HEL cells (Figure 10B). Unpaired T-Tests were performed and show a significant decrease in cell proliferation was observed when comparing RUX-treated cells to untreated cells in both cell lines after 72 hours (SET2: $p < 0.0001$. HEL: $p < 0.0001$.)

3.2. The effect of 1 μ M ruxolitinib on global protein expression in ET

To investigate the changes in global protein expression upon JAK2 inhibition with RUX, Sequential Windowed Acquisition of All Theoretical Fragment Ion Mass Spectra (SWATH-MS) was performed in SET2 cells subject to 1 μ M ruxolitinib treatment and cultured for 24 hours. SWATH-MS generates a digital proteomic map of the biological sample is then compared to an existing pan-human database for protein identification. SWATH-MS was performed in triplicate on ruxolitinib-treated cells to identify molecules of importance to JAK2 with respect to the global signalling pathways in ET. Three biological repeats of SET2 cells treated with 1 μ M RUX and cultured for 24 hours were processed for SWATH-MS analysis, as per Section 2.2. HEL cell samples were not analysed by SWATH-MS due to problems with cell viability when conducting this experiment.

During mass spectrometry analysis, 4467 proteins were identified at a 99% confidence and 1% false discovery rate. Figure 11 below shows the volcano plot of proteins differentially expressed 24-hours after ruxolitinib treatment in SET2 cells and identified through mass spectrometry analysis.

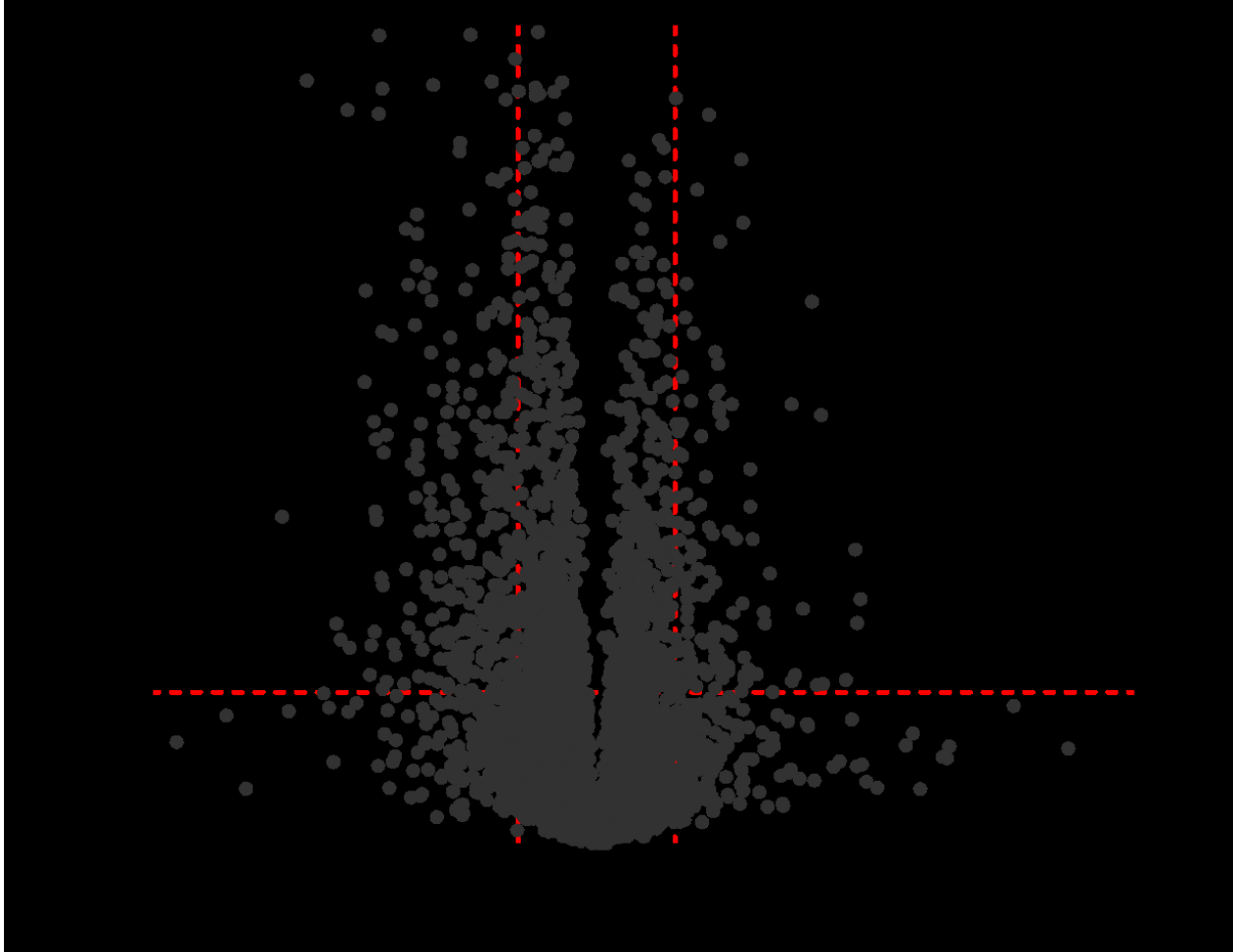


Figure 11: Volcano plot of the clustering of differentially expressed proteins in SET2 cells upon treatment with and without 1 μ M RUX for 24 hours, identified by SWATH-MS (n=3). Each plot indicates a different protein identified by mass spectrometry. Red dotted lines indicate the cut-off points for the proteins considered up- and downregulated in response to RUX, with fold change values of greater than 1.5 and less than 0.667. The horizontal red dotted line indicates the cut-off point for protein expression to be significantly altered by RUX treatment, as determined by Welch's T-test ($p < 0.05$).

To investigate changes in protein expression in SET2 cells in response to RUX treatment, the 4467 proteins identified to be differentially expressed were stratified to highlight significantly up- and downregulated proteins. Upregulated proteins were considered as those with a fold change of greater than 1.5 whereas downregulated proteins had a fold change of less than 1/1.5 (0.667) with respect to untreated cells. Further stratification was required to select only the proteins with significant changes in expression when comparing treated to untreated cells ($p < 0.05$, as determined by Welch's two-tailed t -test).

Of the 4467 proteins identified to be differentially expressed in response to RUX treatment, 305 proteins were recognised as significantly downregulated in response to RUX. A comprehensive list of all significantly downregulated proteins, as determined by Welch's T-test, can be found below in Table V.

Table V: List of significantly downregulated proteins in SET2 cells upon 1 μ M RUX treatment for 24 hours, detected by SWATH-MS. Details of all significantly downregulated proteins in SET2 cells in response to 24hr RUX treatment. Information on the protein and associated UniProt ID, function (as described within the UniProt database), fold change and p-values comparing treated to untreated cells, as determined by Welch's T-test, are included.

Uniprot ID	Protein Identity	Protein Name	Function	p-value	Fold Change
Q8N0X7	SPG20	Spartin	May be implicated in endosomal trafficking, or microtubule dynamics, or both. Participates in cytokinesis	0.00075	0.663
Q9Y2K7	KDM2A	Lysine-specific demethylase 2A	Important in the histone code as it specifically demethylates 'Lys-36' of histone H3	0.04307	0.661
P46060	RAGP1	Ran GTPase-activating protein 1	Converts cytoplasmic GTP-bound RAN to GDP-bound RAN, which is essential for RAN-mediated nuclear import and export	6.75E-06	0.66
Q9UHD1	CHRD1	Cysteine and histidine-rich domain-containing protein 1	Inhibits the kinase activity of ROCK2 and regulates centrosome duplication. Also acts as co-chaperone for HSP90.	7.90E-05	0.659
Q02809	PLOD1	Procollagen-lysine,2-oxoglutarate 5-dioxygenase 1	Catalyses the hydroxylation of lysine residues in collagen alpha chains as part of a complex with PLOD1, P3H3 and P3H4. Also required for normal assembly and cross-linking of collagen fibrils	0.00059	0.658
P67809	YBOX1	Nuclease-sensitive element-binding protein 1	Regulates splice site selection by binding to splice sites in pre-mRNA. Also binds to and stabilizes cytoplasmic mRNA	1.90E-07	0.657
P62266	RS23	40S ribosomal protein S23	Component of the ribosome, a large ribonucleoprotein complex responsible for the synthesis of proteins in the cell	0.00035	0.657
Q5UIP0	RIF1	Telomere-associated protein RIF1	Regulates the activity of TP53BP1 that promotes non-homologous end joining mediated repair of double stranded DNA breaks in response to DNA damage	3.02E-06	0.655
Q92925	SMRD2	SWI/SNF-related matrix-associated actin-dependent regulator of chromatin subfamily D member 2	Chromatin remodelling protein involved in complexes to change chromatin structure and DNA-histone contacts within the nucleosome Also controls the transcriptional activation and repression of chromatin remodelling genes	0.00527	0.655
Q0VDF9	HSP7E	Heat shock 70 kDa protein 14	Component of the ribosome-associated complex (RAC) involved in folding or maintaining nascent polypeptides in a folded state	0.00874	0.653
O00571	DDX3X	ATP-dependent RNA helicase DDX3X	Multifunctional protein involved in several steps of gene expression, for example transcription, translation, mRNA maturation and export	6.78E-08	0.651

Q13232	NDK3	Nucleoside diphosphate kinase 3	Synthesises nucleoside triphosphates. Also plays a role in haematopoiesis by inhibiting granulocyte differentiation and inducing apoptosis	0.00264	0.651
Q96SL4	GPX7	Glutathione peroxidase 7	Protects against oxidative DNA damage and double-strand breaks	0.01012	0.651
P39656	OST48	Dolichyl-diphosphooligosaccharide--protein glycosyltransferase 48 kDa subunit	Required for efficient N-glycosylation. Essential subunit of the N-oligosaccharyl transferase (OST) complex	0.00011	0.65
Q9BQ67	GRWD1	Glutamate-rich WD repeat-containing protein 1	Binds to histones to regulate chromatin dynamics and maintain minichromosome loading at replication origins by promoting the opening of chromatin	0.00012	0.65
O00182	LEG9	Galectin-9	Binds galactosides. Acts as an eosinophil chemoattractant. Also inhibits angiogenesis	0.0402	0.649
O95456	PSMG1	Proteasome assembly chaperone 1	Chaperone protein which promotes assembly of the 20S proteasome as part of a heterodimer with PSMG2	0.00013	0.648
Q8IY22	CMIP	C-Maf-inducing protein	Plays a role in T-helper 2 signalling	0.00876	0.648
Q96SB4	SRPK1	SRSF protein kinase 1	Involved in the regulation of splicing and phosphorylation of SR splicing factors. Also controls the distribution of splicing factors in the nucleus of interphase cells and the reorganization of nuclear speckles during mitosis	0.03978	0.648
Q9BX40	LS14B	Protein LSM14 homolog B	Controls mRNA translation	0.00817	0.647
P57088	TMM33	Transmembrane protein 33	Helps regulate the tubular endoplasmic reticulum (ER) network. Suppresses the RTN3/4-induced formation of the ER tubules. Positively regulates PERK-mediated and IRE1-mediated unfolded protein response signalling	0.03094	0.647
P62633	CNBP	Cellular nucleic acid-binding protein	Single-stranded DNA-binding protein that specifically binds to the sterol regulatory element (SRE). Involved in cholesterol balance in mammalian cells by lowering levels of low-density lipoprotein receptor and enzymes in the cholesterol biosynthesis pathway	2.03E-08	0.644
P07919	QCR6	Cytochrome b-c1 complex subunit 6, mitochondrial	Component of the ubiquinol-cytochrome c reductase complex (complex III or cytochrome b-c1 complex), which is part of the mitochondrial respiratory chain	0.03901	0.643
Q15843	NEDD8	NEDD8	Ubiquitin-like protein which plays an important role in cell cycle control	0.04136	0.643

Q9UN86	G3BP2	Ras GTPase-activating protein-binding protein 2	Probable scaffold protein that may be involved in mRNA transport	1.30E-08	0.642
Q96KB5	TOPK	Lymphokine-activated killer T-cell-originated protein kinase	Protein that phosphorylates MAP kinase p38. Seems to be active only in mitosis but may also be involved in the activation of lymphoid cells	0.00957	0.642
Q8WXE9	STON2	Stonin-2	Adapter protein involved in endocytic machinery and synaptic vesicle recycling. May also facilitate the uncoating of clathrin-coated vesicles	0.02954	0.642
Q8TDB6	DTX3L	E3 ubiquitin-protein ligase DTX3L	E3 ubiquitin-protein ligase which, in association with ADP-ribosyltransferase PARP9, plays a role in DNA damage repair and in interferon-mediated antiviral responses	0.00061	0.641
P49327	FAS	Fatty acid synthase	An acyl carrier protein that catalyses the formation of long-chain fatty acids from acetyl-CoA, malonyl-CoA and NADPH	7.42E-13	0.639
O43156	TTI1	TELO2-interacting protein 1 homolog	Involved in the cellular resistance to DNA damage stresses. May participate in the proper folding of newly synthesized PIKKs with the TTT complex and HSP90. Promotes the maintenance, assembly and stabilisation of mTORC1 and 2 complexes which regulate cellular growth and survival in response to hormone and nutrient signals	0.00061	0.638
Q00341	VIGLN	Vigilin	Potentially involved in cell sterol metabolism by protecting cells from over-accumulating cholesterol	0.00123	0.638
Q9UHI6	DDX20	Probable ATP-dependent RNA helicase DDX20	Part of the SMN complex that catalyses the assembly of small nuclear ribonucleoproteins (snRNPs), the building blocks of the spliceosome.	0.00048	0.637
O60427	FADS1	Fatty acid desaturase 1	Involved in the catalysis of highly unsaturated fatty acids from precursor polyunsaturated fatty acids	0.00378	0.637
Q14558	KPRA	Phosphoribosyl pyrophosphate synthase-associated protein 1	Seems to play a negative regulatory role in 5-phosphoribose 1-diphosphate synthesis	0.0337	0.637
O94966	UBP19	Ubiquitin carboxyl-terminal hydrolase 19	Deubiquitinating enzyme that regulates the degradation of various proteins	0.02221	0.636
Q8NHQ9	DDX55	ATP-dependent RNA helicase DDX55	Probable ATP-binding RNA helicase	0.0414	0.636
P26358	DNMT1	DNA (cytosine-5)-methyltransferase 1	Methylates CpG residues. Maintains the methylation pattern in newly synthesised DNA strands by associating with DNA replication sites in S phase. This is essential for epigenetic inheritance	7.14E-06	0.635

O14933	UB2L6	Ubiquitin/ISG15-conjugating enzyme E2 L6	Catalyses the covalent attachment of ubiquitin or ISG15 to other proteins.	1.18E-05	0.633
Q8TB61	S35B2	Adenosine 3'-phospho 5'-phosphosulfate transporter 1	Controls the transport of adenosine 3'-phospho 5'-phosphosulfate (PAPS) from the cytosol to the Golgi	0.00077	0.633
Q99873	ANM1	Protein arginine N-methyltransferase 1	The main enzyme that controls the monomethylation and asymmetric dimethylation of histone H4 'Arg-4', a specific tag for epigenetic transcriptional activation	0.00014	0.632
Q99653	CHP1	Calcineurin B homologous protein 1	Calcium-binding protein involved in a number of cellular processes: regulation of vesicular trafficking; gene transcription; co-factor in cellular pH control; mediates the association between microtubules and membrane-bound organelles of the ER and Golgi apparatus; inhibits rRNA transcription	0.00312	0.632
Q14807	KIF22	Kinesin-like protein KIF22	Involved in spindle formation and subsequent movements of chromosomes during mitosis and meiosis by binding to microtubules and DNA	0.05361	0.632
P55209	NP1L1	Nucleosome assembly protein 1-like 1	May be involved in modulating chromatin formation and contribute to regulation of cell proliferation.	0.00017	0.631
Q9NR30	DDX21	Nucleolar RNA helicase 2	Senses the transcriptional status of RNA polymerase (Pol) I and II. Also promotes ribosomal RNA (rRNA) processing and transcription from polymerase II (Pol II)	8.33E-10	0.63
P11940	PABP1	Polyadenylate-binding protein 1	Binds the poly(A) tail of mRNA. May be involved in cytoplasmic regulatory processes such as pre-mRNA splicing	1.83E-06	0.628
P56182	RRP1	Ribosomal RNA processing protein 1 homolog A	Plays a critical role in the generation of 28S rRNA.	2.65E-05	0.628
O00232	PSD12	26S proteasome non-ATPase regulatory subunit 12	Component of the 26S proteasome. Important in maintaining protein homeostasis by removing proteins whose functions are no longer required and moving misfolded or damaged proteins	0.00094	0.627
Q5TA45	INT11	Integrator complex subunit 11	Involved in the transcription of small nuclear RNA U1 and U2	0.01202	0.627
Q9NRW3	ABC3C	DNA dC-dU-editing enzyme APOBEC-3C	DNA deaminase (cytidine deaminase) that may play a role in the epigenetic regulation of gene expression through the process of active DNA demethylation	0.0194	0.627

Q6UB35	C1TM	Monofunctional C1-tetrahydrofolate synthase, mitochondrial	Thought to provide the missing metabolic reaction linking the mitochondria and the cytoplasm in one-carbon folate metabolism	4.24E-07	0.626
Q99615	DNJC7	DnaJ homolog subfamily C member 7	Acts as recycling co-chaperone to HSP70 and HSP90 in folding of steroid receptors	0.00248	0.626
Q9Y314	NOSIP	Nitric oxide synthase-interacting protein	Negatively regulates nitric oxide production by inducing the translocation of NOS1 and NOS3 to the actin cytoskeleton and inhibiting their activity	0.00625	0.626
O75607	NPM3	Nucleoplasmin-3	May act as a chaperone	0.0002	0.625
P46783	RS10	40S ribosomal protein S10	Component of the 40S ribosomal subunit	0.01142	0.621
Q5PRF9	SMAG2	Protein Smaug homolog 2	Transcriptional repressor protein. Overexpression inhibits the transcriptional activities of AP-1, p53/TP53 and CDKN1A	0.05348	0.619
P08195	4F2	4F2 cell-surface antigen heavy chain	Required by light chain amino-acid transporters. Involved in the transport of large neutral amino acids	0.0043	0.618
P12004	PCNA	Proliferating cell nuclear antigen	Helps control DNA replication by increasing DNA polymerase delta's processability during elongation of the leading strand. Plays a key role in DNA repair and damage response pathways	3.12E-09	0.614
Q01650	LAT1	Large neutral amino acids transporter small subunit 1	Sodium-independent, high-affinity transport of large neutral amino acids. Involved in cellular amino acid uptake	0.04554	0.614
Q9BVJ6	UT14A	U3 small nucleolar RNA-associated protein 14 homolog A	May be required for ribosome biogenesis	0.00106	0.613
P24941	CDK2	Cyclin-dependent kinase 2	Serine/threonine-protein kinase involved cell cycle control at the point of G1-S transition/ Promotes DNA synthesis and regulates G2 progression	0.0002	0.61
Q15397	PUM3	Pumilio homolog 3	Inhibits the poly(ADP-ribosylation) activity of PARP1 and the degradation of PARP1 by CASP3 following genotoxic stress	0.00032	0.61
Q9NRN7	ADPPT	L-aminoadipate-semialdehyde dehydrogenase-phosphopantetheinyl transferase	Catalyses the post-translational modification of target proteins by phosphopantetheine.	0.0045	0.609
P57678	GEMI4	Gem-associated protein 4	Catalyses the assembly of small nuclear ribonucleoproteins (snRNPs), essential components of the spliceosome	0.00788	0.609

Q9UKD2	MRT4	mRNA turnover protein 4 homolog	Component of the ribosome assembly machinery	7.28E-05	0.608
Q8TF42	UBS3B	Ubiquitin-associated and SH3 domain-containing protein B	Inhibits the downregulation and degradation of receptor tyrosine kinases and promotes the accumulation of activated target receptors on the cell surface	0.01355	0.608
Q9UNL2	SSRG	Translocon-associated protein subunit gamma	Part of a complex that binds calcium to the ER membrane and regulates the retention of ER resident proteins	0.006	0.606
P78346	RPP30	Ribonuclease P protein subunit p30	Part of the ribonuclease P complex that generates mature tRNA molecules by cleaving their 5'-ends	0.03405	0.606
P40429	RL13A	60S ribosomal protein L13a	Component of the GAIT (gamma interferon-activated inhibitor of translation) complex which mediates translation inhibition in the inflammation processes	2.34E-05	0.605
Q13685	AAMP	Angio-associated migratory cell protein	Plays a role in angiogenesis and cell migration	0.00096	0.604
Q9NY61	AATF	Protein AATF	General inhibitor of histone deacetylase HDAC1 and therefore involved in cell cycle progression	0.01019	0.604
P23921	RIR1	Ribonucleoside-diphosphate reductase large subunit	Provides the precursors for DNA synthesis. Catalyses the biosynthesis of deoxyribonucleotides from the corresponding ribonucleotides.	2.10E-06	0.602
Q8NCA5	FA98A	Protein FAM98A	Involved in skeletal homeostasis by stimulating PRMT1-induced protein arginine methylation	0.01081	0.601
Q9HCN4	GPN1	GPN-loop GTPase 1	Small GTPase required for nuclear import of RNA polymerase II	0.01265	0.601
O95714	HERC2	E3 ubiquitin-protein ligase HERC2	Regulates ubiquitin-dependent retention of repair proteins on damaged chromosomes	0.00069	0.6
P35625	TIMP3	Metalloproteinase inhibitor 3	Creates a complex with metalloproteinases and binds to their catalytic zinc cofactor, irreversibly inactivating them	0.00443	0.6
P68402	PA1B2	Platelet-activating factor acetylhydrolase IB subunit beta	Inactivates platelet activating factor (PAF) and involved in lipid metabolism and positive regulation of macroautophagy	0.01239	0.598
Q9NZA1	CLIC5	Chloride intracellular channel protein 5	Inserts into membranes and forms ion channels with poor selectivity. May also transport chloride ions	0.00391	0.597
Q12899	TRI26	Tripartite motif-containing protein 26	Regulates IFN-beta production and antiviral response downstream of pattern-recognition receptors (PRRs). Also encourages nuclear IRF3 ubiquitination and proteasomal degradation	0.02327	0.595

Q99496	RING2	E3 ubiquitin-protein ligase RING2	Plays a central role in histone code and gene regulation by mediation of monoubiquitination of 'Lys-119' of histone H2A (H2AK119Ub)	0.00108	0.593
Q13501	SQSTM	Sequestosome-1	Receptor required for selective macroautophagy. Bridges the link between polyubiquitinated cargo and autophagosomes	8.36E-05	0.592
P60602	ROMO1	Reactive oxygen species modulator 1	Promotes the production of reactive oxygen species (ROS) necessary for cell proliferation. May be involved in the induction of oxidative DNA damage and replicative senescence.	0.01431	0.592
P46013	KI67	Antigen KI-67	Important in the maintenance of individual mitotic chromosomes dispersed in the cytoplasm following nuclear envelope disassembly	6.42E-05	0.591
Q8WV99	ZFN2B	AN1-type zinc finger protein 2B	Regulates the translocation and ubiquitin-mediated proteasomal degradation of nascent proteins at the ER, controlling protein homeostasis	0.00595	0.591
P57721	PCBP3	Poly(rC)-binding protein 3	Single-stranded nucleic acid binding protein that binds to oligo dC	0.00417	0.59
O00566	MPP10	U3 small nucleolar ribonucleoprotein protein MPP10	Component of the 60-80S U3 small nucleolar ribonucleoprotein (U3 snoRNP). Required for cleaving during pre-18S rRNA processing	0.03856	0.589
O43716	GATC	Glutamyl-tRNA(Gln) amidotransferase subunit C, mitochondrial	Promotes the formation of correctly charged Gln-tRNA(Gln) through the transamination of misacylated Glu-tRNA(Gln) in the mitochondria during mitochondrial translation	0.02098	0.587
Q8IWZ3	ANKH1	Ankyrin repeat and KH domain-containing protein 1	May function as a scaffolding protein that associates with the abnormal phenotype of leukaemia cells. Isoform 2 is thought to possess antiapoptotic effects and regulate caspase activity	0.00158	0.585
Q13422	IKZF1	DNA-binding protein Ikaros	Transcription regulator of hematopoietic cell differentiation. Regulates transcription through association with both HDAC-dependent and HDAC-independent complexes.	0.01651	0.585
P61289	PSME3	Proteasome activator complex subunit 3	Subunit of the 11S REG-gamma proteasome regulator. Involved in the promotion of ubiquitination and proteasomal degradation of p53/TP53, resulting in inhibited apoptosis	2.05E-06	0.584
P52732	KIF11	Kinesin-like protein KIF11	Motor protein required for establishing a bipolar spindle during mitosis	2.96E-07	0.583
Q14331	FRG1	Protein FRG1	May function in the regulation of pre-mRNA splicing or assembly of rRNA into ribosomal subunits.	0.00781	0.583

P30305	MPIP2	M-phase inducer phosphatase 2	Dose-dependently induces mitotic progression through its tyrosine protein phosphatase activity. Required for G2/M progression during the cell cycle	0.04785	0.583
P42224	STAT1	Signal transducer and activator of transcription 1-alpha/beta	Mediates the cellular response to interferons, cytokines and other growth factors	7.36E-08	0.582
O95793	STAU1	Double-stranded RNA-binding protein Staufen homolog 1	Binds double-stranded RNA and tubulin and forms cross-links between the cytoskeleton and RNA components to affect the positioning of mRNAs and stimulate their translation	0.00175	0.582
Q92598	HS105	Heat shock protein 105 kDa	Acts as a nucleotide-exchange factor for HSPA1A and HSPA1B chaperone proteins, promoting the release of ADP and stimulating client/substrate protein release. Also inhibits HSPA8 and HSC70 activity	5.07E-08	0.581
Q9UI30	TR112	Multifunctional methyltransferase subunit TRM112-like protein	Acts as an activator of both rRNA/tRNA and protein methyltransferases	2.80E-05	0.58
Q9P287	BCCIP	BRCA2 and CDKN1A-interacting protein	Isoform 2/alpha is particularly important for the regulation of microtubule anchoring and stability, and spindle architecture and orientation during interphase. May promote cell cycle arrest by enhancing the inhibition of CDK2 activity by CDKN1A.	0.00078	0.58
Q9H4B7	TBB1	Tubulin beta-1 chain	Major component of microtubules	0.00832	0.579
Q14444	CAPR1	Caprin-1	Regulates the transport and translation of mRNAs of proteins involved in proliferation and migration	4.67E-10	0.578
Q9Y5A9	YTHD2	YTH domain-containing family protein 2	Regulates RNA stability, processing and degradation by binding N6-methyladenosine (m6A)-containing RNAs	0.00351	0.575
P62310	LSM3	U6 snRNA-associated Sm-like protein LSM3	Binds specifically to the 3'-terminal U-tract of U6 snRNA	0.00382	0.574
Q03518	TAP1	Antigen peptide transporter 1	Involved in the transport of antigens from the cytoplasm to the endoplasmic reticulum for association with MHC class I molecules	0.00089	0.573
Q9Y3D7	TIM16	Mitochondrial import inner membrane translocase subunit TIM16	Regulates ATP-dependent protein translocation into the mitochondrial matrix	0.02513	0.573
P49005	DPOD2	DNA polymerase delta subunit 2	Component of Pol-delta3 and Pol-delta4 (DNA polymerase complexes)and is involved in lagging strand synthesis and repair	0.00029	0.572

Q07864	DPOE1	DNA polymerase epsilon catalytic subunit A	Participates in DNA repair and in chromosomal DNA replication.	0.02186	0.572
Q5K651	SAMD9	Sterile alpha motif domain-containing protein 9	May play a role in the inflammatory response to tissue injury and the control of extra-osseous calcification, acting as a downstream target of TNF-alpha signalling. May be involved in endosome fusion	0.05455	0.572
Q9Y289	SC5A6	Sodium-dependent multivitamin transporter	Transports pantothenate, biotin and lipoate in the presence of sodium	0.01021	0.57
O14662	STX16	Syntaxin-16	SNARE protein involved in vesicular transport from the late endosomes to the trans-Golgi network	0.02708	0.569
Q13907	IDI1	Isopentenyl-diphosphate Delta-isomerase 1	Part of the isoprenoid biosynthesis pathway	0.0012	0.568
P17844	DDX5	Probable ATP-dependent RNA helicase DDX5	Regulates pre-mRNA splicing and transcription. Transcriptional coactivator for p53. Also involved in p53's response to DNA damage and apoptosis	8.81E-10	0.567
P37198	NUP62	Nuclear pore glycoprotein p62	Essential component of the nuclear pore complex. Plays a role in the M phase of the cell cycle by regulating centrosome segregation, centriole maturation and spindle orientation	0.01731	0.565
Q8NB16	MLKL	Mixed lineage kinase domain-like protein	Pseudokinase that plays a key role in TNF-induced necroptosis, a programmed cell death process.	0.03507	0.565
P01033	TIMP1	Metalloproteinase inhibitor 1	Forms one-to-one complexes with target metalloproteinases and binds to their catalytic zinc cofactor, irreversibly inactivating them	0.00041	0.564
Q9NQT8	KI13B	Kinesin-like protein KIF13B	Associated with the reorganisation of the cortical cytoskeleton. Regulates axon formation	0.01251	0.562
O14579	COPE	Coatomer subunit epsilon	Cytosolic protein complex that binds to dilysine motifs and reversibly associates with Golgi non-clathrin-coated vesicles, which further mediate biosynthetic protein transport from the ER, via the Golgi up to the trans Golgi network	0.00031	0.56
Q6DD88	ATLA3	Atlastin-3	Involved in endoplasmic reticulum tubular network biogenesis	0.01071	0.56
Q9H2J4	PDCL3	Phosducin-like protein 3	Acts as a chaperone for the angiogenic VEGF receptor KDR/VEGFR2, controlling its abundance and inhibiting its ubiquitination and degradation.	0.0002	0.559
P17813	EGLN	Endoglin	Vascular endothelium glycoprotein that plays an important role in the regulation of angiogenesis. Acts as TGF-beta coreceptor and is involved in	3.12E-05	0.558

			the TGF-beta/BMP signalling cascade that ultimately leads to the activation of SMAD transcription factors		
Q16850	CP51A	Lanosterol 14-alpha demethylase	Catalyses C14-demethylation of lanosterol to convert into zymosterol in the cholesterol biosynthesis pathway	3.51E-05	0.558
Q53GQ0	DHB12	Very-long-chain 3-oxoacyl-CoA reductase	Catalyses the second of four reactions within the long-chain fatty acids elongation cycle	0.00204	0.558
Q9NP97	DLRB1	Dynein light chain roadblock-type 1	Acts as a motor for the intracellular retrograde motility of vesicles and organelles along microtubules	0.02364	0.557
Q7Z7L1	SLN11	Schlafen family member 11	Inhibitor of DNA replication that promotes cell death in response to DNA damage. Acts as a guardian of the genome by killing cells with defective replication	0.02595	0.554
Q6PD62	CTR9	RNA polymerase-associated protein CTR9 homolog	Component of the PAF1 complex which has multiple functions during transcription by RNA polymerase II. Involved in haematopoiesis and histone modification e.g. ubiquitination of histone H2B and methylation on histone H3 'Lys-4'	0.00042	0.553
Q9NY65	TBA8	Tubulin alpha-8 chain	Major component of microtubules	0.00984	0.552
Q9UBC5	MYO1A	Unconventional myosin-Ia	Involved in directing the movement of organelles along actin filaments	0.01681	0.551
Q9NVP2	ASF1B	Histone chaperone ASF1B	Histone chaperone that facilitates histone deposition, exchange and removal during nucleosome assembly and disassembly	0.00071	0.548
Q13627	DYR1A	Dual specificity tyrosine-phosphorylation-regulated kinase 1A	Involved in the signalling pathway which regulates nuclear functions of cellular proliferation. Also modulates alternative splicing by phosphorylating SRSF6 splice factor	0.00469	0.543
Q9Y6A5	TACC3	Transforming acidic coiled-coil-containing protein 3	Plays a role in the microtubule-dependent coupling of the nucleus and the centrosome	0.0532	0.542
O75794	CD123	Cell division cycle protein 123 homolog	Required for S phase entry of the cell cycle	0.00686	0.541
Q9UL25	RAB21	Ras-related protein Rab-21	Regulates cell adhesion and migration by regulation of integrin internalisation and recycling	0.01728	0.54
Q9ULX3	NOB1	RNA-binding protein NOB1	May play a role in mRNA degradation.	8.83E-05	0.538
Q05397	FAK1	Focal adhesion kinase 1	Non-receptor protein-tyrosine kinase that has a critical function in many cellular processes, including regulating cell migration, adhesion,	0.00712	0.537

			reorganization of the actin cytoskeleton, cell cycle progression, proliferation and apoptosis		
P34931	HS71L	Heat shock 70 kDa protein 1-like	Molecular chaperone involved in a multitude of cellular processes including protecting the proteome from stress, folding and transport of newly synthesized polypeptides and activates the proteolysis of misfolded proteins	0.01529	0.536
P98179	RBM3	RNA-binding protein 3	Enhances global protein synthesis at both physiological and mild hypothermic temperatures. Promotes the phosphorylation of translation initiation factors	1.22E-05	0.527
Q05639	EF1A2	Elongation factor 1-alpha 2	Promotes GTP-dependent binding of aminoacyl-tRNA to the A-site of ribosomes during protein biosynthesis	0.00667	0.525
Q92667	AKAP1	A-kinase anchor protein 1, mitochondrial	Binds to type I and II regulatory subunits of protein kinase A and stabilises them to the mitochondrial outer membrane.	0.04689	0.525
Q9ULW3	ABT1	Activator of basal transcription 1	Could be a novel TATA-binding protein (TBP) which can function as a basal transcription activator	0.05047	0.525
O75153	CLU	Clustered mitochondria protein homolog	Involved in mitochondrial biogenesis. Binds to and regulates the transport or translation of mRNAs of nuclear-encoded mitochondrial proteins in the cytoplasm	2.27E-09	0.524
Q5SYB0	FRPD1	FERM and PDZ domain-containing protein 1	Involved in protein localisation to membranes and regulates G-protein coupled receptor signalling through stabilisation of membrane-bound GPSM1	0.01212	0.524
Q13283	G3BP1	Ras GTPase-activating protein-binding protein 1	Unwinds partial DNA and RNA duplexes. ATP- and magnesium-dependent	1.18E-07	0.522
P41227	NAA10	N-alpha-acetyltransferase 10	Catalytic subunit of NatA complex which has alpha acetyltransferase activity	0.00863	0.522
O75494	SRS10	Serine/arginine-rich splicing factor 10	Functions as a repressor of pre-mRNA splicing in its dephosphorylated form. Required for splicing repression in M-phase cells and after heat shock	0.00014	0.521
Q5VWQ8	DAB2P	Disabled homolog 2-interacting protein	Scaffold protein involved in the reduction of G1 phase cyclin levels, resulting in G0/G1 cell cycle arrest. Also involved in multiple intracellular processes such as apoptosis, cell survival, angiogenesis, cell migration and maturation	0.05331	0.521

Q9Y6H1	CHCH2	Coiled-coil-helix-coiled-coil-helix domain-containing protein 2	Transcription factor involved in oxygen response. Activates the transcription of COX4I2 (cytochrome c oxidase) under hypoxic conditions	0.00278	0.52
Q96D46	NMD3	60S ribosomal export protein NMD3	Adapter protein for XPO1/CRM1-mediated export of the 60S ribosomal subunit	0.00603	0.52
Q9NRZ9	HELLS	Lymphoid-specific helicase	Required for de novo or maintenance DNA methylation. May be involved in the formation and organization of heterochromatin, which consequently regulates transcription and mitosis	0.00462	0.519
P15104	GLNA	Glutamine synthetase	Plays an essential role in the metabolism of nitrogen by catalysing the condensation of glutamate and ammonia to form glutamine	3.69E-06	0.518
O75676	KS6A4	Ribosomal protein S6 kinase alpha-4	Required for the mitogen- or stress-induced phosphorylation of the CREB1, ATF1 and RELA transcription factors, thus contributes to gene activation by histone phosphorylation and regulation of inflammatory genes	0.01988	0.518
Q9BRT9	SLD5	DNA replication complex GINS protein SLD5	Initiates DNA replication and progression of DNA replication forks	0.00318	0.517
Q30154	DRB5	HLA class II histocompatibility antigen, DR beta 5 chain	Binds antigens produced as a result of endocytosis of antigen presenting cells (APC). Presents these antigens on the cell surface for recognition by T-cells	0.01429	0.516
O15091	MRRP3	Mitochondrial ribonuclease P protein 3	Removes the 5'-extranucleotides from tRNA precursor via its endonucleolytic activity	0.02412	0.515
Q9UBV2	SE1L1	Protein sel-1 homolog 1	Important in endoplasmic reticulum-associated degradation (ERAD) and involved in ubiquitin-dependent degradation of misfolded ER proteins	0.0028	0.513
Q9NVE7	PANK4	Pantothenate kinase 4	Regulates intracellular CoA concentration	0.01189	0.511
Q969Z3	Mar-02	Mitochondrial amidoxime reducing component 2	As a component of the benzamidoxime prodrug-converting complex required to reduce N-hydroxylated prodrugs, such as benzamidoxime	0.03071	0.511
Q9H223	EHD4	EH domain-containing protein 4	ATP- and membrane-binding protein involved in the control of membrane reorganization and tubulation upon ATP hydrolysis. Also involved in early endosomal transport	1.78E-05	0.509
Q13112	CAF1B	Chromatin assembly factor 1 subunit B	Part of a complex thought to assist in the assembly of histone octamers onto replicating DNA, therefore mediating chromatin assembly in DNA replication and repair	0.00149	0.506

Q9Y4C8	RBM19	Probable RNA-binding protein 19	Plays a role in embryo pre-implantation development	0.03056	0.505
P49642	PRI1	DNA primase small subunit	Polymerase enzyme that synthesizes small RNA primers for the Okazaki fragments that form during DNA replication	0.0002	0.503
O94919	ENDD1	Endonuclease domain-containing 1 protein	Acts as a DNase and RNase	0.01993	0.499
Q8IWR0	Z3H7A	Zinc finger CCCH domain-containing protein 7A	May be a specific regulator of miRNA biogenesis.	0.01438	0.498
Q96GD4	AURKB	Aurora kinase B	Serine/threonine-protein kinase that forms part of the chromosomal passenger complex that regulates mitosis	0.04832	0.496
P13693	TCTP	Translationally-controlled tumour protein	Involved in calcium binding and microtubule stabilization.	9.88E-07	0.495
O95478	NSA2	Ribosome biogenesis protein NSA2 homolog	Involved in the biogenesis and quality control of pre-60S ribosomal subunits	1.17E-06	0.493
Q92643	GPI8	GPI-anchor transamidase	Involved in glycolipid biosynthesis by mediating GPI anchoring in the ER	0.00548	0.493
Q9NYY8	FAKD2	FAST kinase domain-containing protein 2, mitochondrial	Plays an important role in assembly of the mitochondrial large ribosomal subunit	0.00193	0.492
Q8WWK9	CKAP2	Cytoskeleton-associated protein 2	Stabilises microtubules. Also involved in regulating p53/TP53-dependent aneuploidy and cell death	0.00197	0.492
O14802	RPC1	DNA-directed RNA polymerase III subunit RPC1	Largest and catalytic core component of RNA polymerase III which synthesizes 5S rRNA and tRNAs. Catalyses the transcription of DNA to RNA	0.00761	0.49
Q8TDN6	BRX1	Ribosome biogenesis protein BRX1 homolog	Required for biogenesis of the 60S ribosomal subunit	0.00136	0.489
Q6UW68	TM205	Transmembrane protein 205	Involved in the resistance to cisplatin in cancerous cells	0.0048	0.489
Q9HA92	RSAD1	Radical S-adenosyl methionine domain-containing protein 1, mitochondrial	May be involved in porphyrin cofactor biosynthesis	0.02223	0.489
Q16625	OCLN	Occludin	Important in the formation and regulation of the tight junction paracellular permeability barriers by inducing adhesion when expressed in cells lacking tight junctions	0.03281	0.488

O00264	PGRC1	Membrane-associated progesterone receptor component 1	Component of a progesterone-binding protein complex	0.00123	0.487
Q96R06	SPAG5	Sperm-associated antigen 5	Essential mitotic spindle component required for chromosomal segregation and alignment, anaphase progression and maintenance of spindle pole structure	0.00762	0.487
Q8NG66	NEK11	Serine/threonine-protein kinase Nek11	Involved in the G2/M checkpoint response to DNA damage. Controls degradation of CDC25A (M-phase inducer phosphate 1).	0.00269	0.485
Q9C037	TRIM4	E3 ubiquitin-protein ligase TRIM4	Controls 'Lys-63'-linked polyubiquitination of DDX58 innate immune receptor which enhances IFN induction	0.02397	0.484
P52292	IMA1	Importin subunit alpha-1	Functions as an adapter protein for nuclear receptor KPNB1, which is involved in the Ran nuclear import pathway	2.27E-08	0.482
Q6NYC1	JMJD6	Bifunctional arginine demethylase and lysyl-hydroxylase JMJD6	Dioxygenase that regulates RNA splicing by mediating the activity of U2AF2/U2AF65	0.00473	0.482
Q9NZQ3	SPN90	NCK-interacting protein with SH3 domain	Has an important role in stress fibre formation induced by active diaphanous protein homolog 1 (DRF1)	0.01564	0.479
O15496	PA2GX	Group 10 secretory phospholipase A2	Catalyses the calcium-dependent hydrolysis of the 2-acyl groups in 3-sn-phosphoglycerides	0.03072	0.479
P40692	MLH1	DNA mismatch repair protein Mlh1	Heterodimerizes with PMS2 to form MutL alpha which is involved in the DNA mismatch repair system	0.00091	0.477
P78316	NOP14	Nucleolar protein 14	Involved in pre-18S ribosomal RNA nucleolar processing and nuclear export of 40S pre-ribosomal subunits into the cytoplasm	0.00012	0.476
P23258	TBG1	Tubulin gamma-1 chain	Major constituent of microtubules. The gamma chain is found at microtubule organizing centres (MTOC) such as the spindle poles or the centrosome	0.00201	0.473
Q99661	KIF2C	Kinesin-like protein KIF2C	Forms the major microtubule plus-end depolymerizing complex in mitotic cells when in complex with KIF18B. Important in mitosis for the regulation of microtubule turnover at the kinetochore and chromosome segregation	0.00044	0.472
O60566	BUB1B	Mitotic checkpoint serine/threonine-protein kinase BUB1 beta	Mitotic checkpoint protein required for progression of mitosis	0.00793	0.472

P62847	RS24	40S ribosomal protein S24	Critical role in the processing of pre-rRNA and maturation of 40S ribosomal subunits	4.57E-05	0.47
P36639	8ODP	7,8-dihydro-8-oxoguanine triphosphatase	Antimutagenic protein that acts as a sanitising enzyme for oxidized nucleotide pools and suppresses cell dysfunction and death-induced oxidative stress. Prevents misincorporation of oxidised purine nucleoside triphosphates into DNA	0.00667	0.468
Q9NUU7	DD19A	ATP-dependent RNA helicase DDX19A	Involved in mRNA export from the nucleus	0.01513	0.465
P51580	TPMT	Thiopurine S-methyltransferase	Catalyses the S-methylation of thiopurine drugs. TPMT activity modulates the cytotoxic effects of thiopurine pro-drugs	0.0187	0.465
Q9BYE9	CDHR2	Cadherin-related family member 2	Plays a role in cell-cell adhesion and contact inhibition in epithelial cells	0.04553	0.465
Q58FF6	H90B4	Putative heat shock protein HSP 90-beta 4	Chaperonin that promotes the maturation, maintenance and regulation of target proteins	0.00076	0.464
P09486	SPRC	SPARC	Interacts with extracellular matrix proteins and cytokines to regulate cell growth	0.04161	0.464
O75534	CSDE1	Cold shock domain-containing protein E1	RNA-binding protein involved in translationally coupled mRNA turnover	6.51E-11	0.463
Q9H2D6	TARA	TRIO and F-actin-binding protein	Directly binds and stabilises filamentous F-actin to regulate actin cytoskeleton organization and cell contraction	0.0002	0.462
P61619	S61A1	Protein transport protein Sec61 subunit alpha isoform 1	Important in the insertion of secretory and membrane polypeptides into the ER. Required for assembly of membrane and secretory proteins.	0.02559	0.462
Q9BZL1	UBL5	Ubiquitin-like protein 5	Positively regulates chaperone gene expression in the mitochondrial unfolded protein response. Induction of cellular stress promotes the accumulation of UBL-5	6.12E-10	0.461
Q12834	CDC20	Cell division cycle protein 20 homolog	Essential to provide full ubiquitin ligase activity within the anaphase promoting complex/cyclosome	0.00028	0.455
O75843	AP1G2	AP-1 complex subunit gamma-like 2	Involved in protein sorting in late endosomes or multivesicular bodies	0.00718	0.455
Q49A26	GLYR1	Putative oxidoreductase GLYR1	Putative oxidoreductase that is recruited on chromatin and promotes KDM1B demethylase activity	0.00153	0.454

Q9Y5J9	TIM8B	Mitochondrial import inner membrane translocase subunit Tim8 B	Imports and inserts of multi-pass transmembrane proteins into the l inner membrane of the mitochondria	0.01069	0.454
Q9BZX2	UCK2	Uridine-cytidine kinase 2	Phosphorylates uridine and cytidine to uridine monophosphate and cytidine monophosphate	0.00515	0.449
O14653	GOSR2	Golgi SNAP receptor complex member 2	Involved in transport of proteins from the cis/medial-Golgi to the trans-Golgi network	0.01577	0.447
Q8N9F7	GDPD1	Glycerophosphodiester phosphodiesterase domain-containing protein 1	Involved in the phospholipid metabolic process. Hydrolyses lysoglycerophospholipids to produce lysophosphatidic acid (LPA) and the corresponding amines	0.02574	0.446
Q9BW19	KIFC1	Kinesin-like protein KIFC1	Required for bipolar spindle formation	0.00327	0.445
O00165	HAX1	HCLS1-associated protein X-1	Interacts with KCNC3 and the Arp2/3 complex to regulate and reorganise the cortical actin cytoskeleton	0.04004	0.441
Q9H6U8	ALG9	Alpha-1,2-mannosyltransferase ALG9	Involved in the protein glycosylation pathway. Catalyses the transfer of mannose from Dol-P-Man to lipid-linked oligosaccharides	0.0171	0.437
Q9HAH7	FBRS	Probable fibrosin-1	May be a fibrogenic lymphokine involved in fibroblast growth	0.00726	0.436
Q13895	BYST	Bystin	Required for the biogenesis of 40S ribosomal subunits and processing of 20S pre-rRNA precursors	0.00013	0.432
O14530	TXND9	Thioredoxin domain-containing protein 9	Significantly decreases the ATPase activity of chaperonin TCP1 complex to negatively regulate protein folding of actin and tubulin	3.17E-07	0.431
Q2VIR3	IF2GL	Putative eukaryotic translation initiation factor 2 subunit 3-like protein	Molecular subunit of eukaryotic initiation factor 2 (eIF2), involved in the early stages of protein synthesis	0.00203	0.429
Q10469	MGAT2	Alpha-1,6-mannosyl-glycoprotein 2-beta-N-acetylglucosaminyltransferase	Involved in protein glycosylation and modification. Catalyses an essential step in the conversion of oligo-mannose to complex N-glycans.	0.01187	0.429
Q9BV57	MTND	1,2-dihydroxy-3-keto-5-methylthiopentene dioxygenase	Down-regulates cell migration mediated by MMP14	2.22E-05	0.427
P31350	RIR2	Ribonucleoside-diphosphate reductase subunit M2	Provides the precursors for DNA synthesis. Catalyses the biosynthesis of deoxyribonucleotides from the corresponding ribonucleotides. Inhibits Wnt signalling	6.17E-05	0.426

O43324	MCA3	Eukaryotic translation elongation factor 1 epsilon-1	Positive modulator of ATM response to DNA damage	0.00119	0.425
P27635	RL10	60S ribosomal protein L10	Component of the large ribosomal subunit. Plays a role in the formation of actively translating ribosomes	1.29E-05	0.424
Q9HCG8	CWC22	Pre-mRNA-splicing factor CWC22 homolog	Required for nonsense-mediated decay, pre-mRNA splicing and exon-junction complex assembly.	0.03759	0.424
Q9UBI1	COMD3	COMM domain-containing protein 3	Modulates the activity of cullin-RING E3 ubiquitin ligase (CRL) complexes. May also be involved in the downregulation of NF-kappa-B activity	0.00089	0.423
P01892	1A02	HLA class I histocompatibility antigen, A-2 alpha chain	Involved in the presentation of foreign antigens to the immune system	0.00632	0.418
Q8IZQ1	WDFY3	WD repeat and FYVE domain-containing protein 3	Adapter protein involved in selective macroautophagy by linking proteins destined for degradation to the core autophagic machinery members	0.00505	0.416
P53350	PLK1	Serine/threonine-protein kinase PLK1	Serine/threonine-protein kinase that performs several important functions throughout M phase of the cell cycle, including the regulation of centrosome maturation and spindle assembly and removal of cohesins from chromosome arms	1.70E-05	0.411
Q7L7X3	TAOK1	Serine/threonine-protein kinase TAO1	Serine/threonine-protein kinase involved in a number of intracellular pathways such as p38/MAPK14 stress-activated MAPK cascade, DNA damage response and the regulation of cytoskeleton stability	0.02141	0.408
P60520	GBRL2	Gamma-aminobutyric acid receptor-associated protein-like 2	Ubiquitin-like modifier. Modulates intra-Golgi transport through coupling between NSF activity and SNAREs activation. Involved in autophagy	0.00025	0.404
Q14CZ7	FAKD3	FAST kinase domain-containing protein 3, mitochondrial	Required for mitochondrial respiration by increasing the steady-state levels and half-lives of some mature mitochondrial mRNAs	0.00207	0.403
P33121	ACSL1	Long-chain-fatty-acid--CoA ligase 1	Activates long-chain fatty acids for lipid synthesis and degradation via beta-oxidation	0.03623	0.401
Q07817	B2CL1	Bcl-2-like protein 1	Potent inhibitor of cell death and inhibits activation of caspases. Also acts as a regulator of G2 checkpoint and progression to cytokinesis during mitosis	0.00062	0.398
Q96PP9	GBP4	Guanylate-binding protein 4	Plays a role in erythroid differentiation. Hydrolyses GTP	0.01673	0.398
Q01581	HMCS1	Hydroxymethylglutaryl-CoA synthase, cytoplasmic	Enzyme that condenses acetyl-CoA with acetoacetyl-CoA to form HMG-CoA. This step is involved in mevalonate synthesis	5.97E-06	0.397

Q6PL18	ATAD2	ATPase family AAA domain-containing protein 2	Transcriptional coactivator of ESR1 (Estrogen receptor alpha) which regulates gene expression patterns	4.05E-06	0.396
Q13509	TBB3	Tubulin beta-3 chain	Major constituent of microtubules. TUBB3 plays a critical role in proper axon guidance and maintenance	0.00107	0.393
Q96EK9	KTI12	Protein KTI12 homolog	Chromatin-associated protein which interacts with the Elongator complex, a component of the elongating form of RNA polymerase II	3.58E-05	0.392
Q9BUN8	DERL1	Derlin-1	Part of the endoplasmic reticulum-associated degradation (ERAD) for misfolded luminal proteins. Forms a channel that allows misfolded proteins into the cytosol for ubiquitination and degraded by the proteasome	0.00055	0.385
Q9NQZ5	STAR7	StAR-related lipid transfer protein 7, mitochondrial	Plays a protective role in mucosal tissues by preventing exaggerated allergic response	0.00953	0.382
P31689	DNJA1	DnaJ homolog subfamily A member 1	Co-chaperone for HSPA8/Hsc70 and HSPA1B for protein transport into mitochondria. Also protects cells from apoptosis by negatively regulating the translocation of BAX from the cytosol to the mitochondria in response to cellular stress	1.69E-10	0.379
P20290	BTF3	Transcription factor BTF3	Binds to newly synthesised polypeptide chains as they emerge from the ribosome and blocks their interaction with the signal recognition particle, inhibiting them from being targeted for secretion	1.62E-05	0.379
P08473	NEP	Nepilysin	Cleaves a Gly-Phe bond in opioid peptides such as Met- and Leu-enkephalins, causing their destruction	0.01377	0.378
Q9UBB6	NCDN	Neurochondrin	Positively regulates the expression of GRM5 and increases its cell surface localisation of GRM5 to promote signal transduction within the nervous system	5.41E-06	0.374
Q9H4A5	GLP3L	Golgi phosphoprotein 3-like	Phosphatidylinositol-4-phosphate-binding protein. Antagonises the action of GOLPH3 required for vesicle budding at the Golgi	0.0044	0.374
Q9ULJ3	ZBT21	Zinc finger and BTB domain-containing protein 21	Acts as a transcription repressor	0.04207	0.371
P06732	KCRM	Creatine kinase M-type	Reversibly catalyses the transfer of phosphate between ATP and various phosphogens (e.g. creatine phosphate).	0.05299	0.356
O43561	LAT	Linker for activation of T-cells family member 1	Involved in TCR (T-cell antigen receptor)- and pre-TCR-mediated signalling in mature T-cells and during their development	0.02382	0.354

P08243	ASNS	Asparagine synthetase [glutamine-hydrolysing]	Part of the amino acid biosynthesis pathway. Involved in the synthesis of L-asparagine from L-aspartate	0.01926	0.35
P33908	MA1A1	Mannosyl-oligosaccharide 1,2-alpha-mannosidase IA	Involved in the maturation of Asn-linked oligosaccharides, as part of protein glycosylation	4.38E-05	0.347
P41440	S19A1	Folate transporter 1	Transporter for the intake of folate	0.04008	0.339
P22392	NDKB	Nucleoside diphosphate kinase B	Major role in the synthesis of nucleoside triphosphates other than ATP.	0.00031	0.338
Q9NRL2	BAZ1A	Bromodomain adjacent to zinc finger domain protein 1A	Component of the ACF complex, an ATP-dependent chromatin remodelling complex, that regulates spacing of nucleosomes using ATP to generate evenly spaced nucleosomes along the chromatin	0.00044	0.334
Q9BU89	DOHH	Deoxyhypusine hydroxylase	Plays a role in the post-translational modification of lysine into hypusine in the eukaryotic translation initiation factor 5A, essential for its maturity and function	0.00602	0.332
Q7LGA3	HS2ST	Heparan sulphate 2-O-sulfotransferase 1	Catalyses the transfer of sulphate to the C2-position of selected hexuronic acid residues within the maturing heparan sulphate (HS) which is essential for HS to participate in a variety of high-affinity ligand-binding interactions and signalling processes	4.07E-05	0.331
Q92692	NECT2	Nectin-2	Modulates T-cell activation and signalling by co-stimulating or co-inhibiting T-cell function, depending on the receptor it binds to	0.00516	0.329
P04183	KITH	Thymidine kinase, cytosolic	Phosphotransferase enzyme that has a key role in the synthesis of DNA.	1.20E-07	0.326
P16070	CD44	CD44 antigen	Receptor for hyaluronic acid (HA). Mediates cell-cell and cell-matrix interactions through its affinity for HA. Adhesion with HA plays an important role in cell migration, tumour growth and progression and haematopoiesis	5.62E-07	0.325
O60232	SSA27	Sjogren syndrome/scleroderma autoantigen 1	Antigenic molecule which may play a role in mitosis. Could be a centromere-associated protein. May induce anti-centromere antibodies.	0.00165	0.321
O43318	M3K7	Mitogen-activated protein kinase 7	Serine/threonine kinase involved in the MAPK signal transduction pathway. Mediates signal transduction of TRAF6, various cytokines	0.0014	0.32
O14965	AURKA	Aurora kinase A	Involved in several events during mitosis by association with the centrosome and spindle microtubules. Events include establishing mitotic	0.01501	0.318

			spindles, centrosome duplication, centrosome separation, chromosomal alignment, spindle assembly checkpoint, and cytokinesis		
Q9NPD8	UBE2T	Ubiquitin-conjugating enzyme E2 T	Accepts ubiquitin from the E1 complex and catalyses its covalent attachment to other proteins.	0.00024	0.317
Q5XPI4	RN123	E3 ubiquitin-protein ligase RNF123	Required during G1 phase of the cell cycle for polyubiquitination and proteasome-mediated degradation of CDKN1B	0.01952	0.313
P02533	K1C14	Keratin, type I cytoskeletal 14	Promotes the self-organisation of KRT5-KRT14 filaments into large bundles	0.03506	0.31
Q8IYD1	ERF3B	Eukaryotic peptide chain release factor GTP-binding subunit ERF3B	Involved in translation termination in response to the termination codons UAA, UAG and UGA	1.82E-05	0.304
Q16763	UBE2S	Ubiquitin-conjugating enzyme E2	Accepts ubiquitin from the E1 complex and catalyses its covalent attachment to other proteins	0.00011	0.302
Q15758	AAAT	Neutral amino acid transporter B(0)	Sodium-dependent amino acids transporter for a broad range of amino acid substrates	3.24E-10	0.299
Q8NCG7	DGLB	Sn1-specific diacylglycerol lipase beta	Catalyses the hydrolysis of diacylglycerol (DAG) to 2-arachidonoyl-glycerol (2-AG)	0.02049	0.28
O95864	FADS2	Fatty acid desaturase 2	Catalyses the biosynthesis of highly unsaturated fatty acids from precursor essential polyunsaturated fatty acids in the lipid metabolism pathway	5.18E-07	0.277
P13929	ENOB	Beta-enolase	Involved in the synthesis of pyruvate from D-glyceraldehyde 3-phosphate	0.01749	0.267
P04818	TYSY	Thymidylate synthase	Mitochondrial protein involved in the dTTP biosynthesis pathway which is part of Pyrimidine metabolism	2.70E-11	0.252
Q9H2V7	SPNS1	Protein spinster homolog 1	Sphingolipid transporter. May be involved in necrotic or autophagic cell death	0.05051	0.245
Q99595	TI17A	Mitochondrial import inner membrane translocase subunit Tim17-A	Mediates the translocation of transit peptide-containing proteins across the mitochondrial inner membrane as part of the TIM23 complex	2.90E-07	0.224
Q9ULW0	TPX2	Targeting protein for Xklp2	Spindle assembly factor essential in apoptosis for the assembly of mitotic spindles and microtubules	0.00156	0.197
Q15004	PAF15	PCNA-associated factor	PCNA-binding protein that regulates DNA repair during replication	1.07E-08	0.126

All significantly downregulated proteins were then mapped using STRING-DB, an online biological database of known and predicted protein-protein interactions. The protein map below was generated using this web resource and indicates the relationship between proteins to form clusters of similar function and structure. In the STRING-DB images, interactions from curated databases and experimentally determined interactions are assigned light blue and pink connections respectively while predicted interactions through gene neighbourhood, gene fusion or gene co-occurrence relate to green, red or dark blue connections respectively. White connections represent protein homology, black connections indicate co-expression while yellow connections indicate text mining. Empty nodes indicate proteins of unknown 3D structure while filled nodes show proteins with some known or predicted 3D structure.

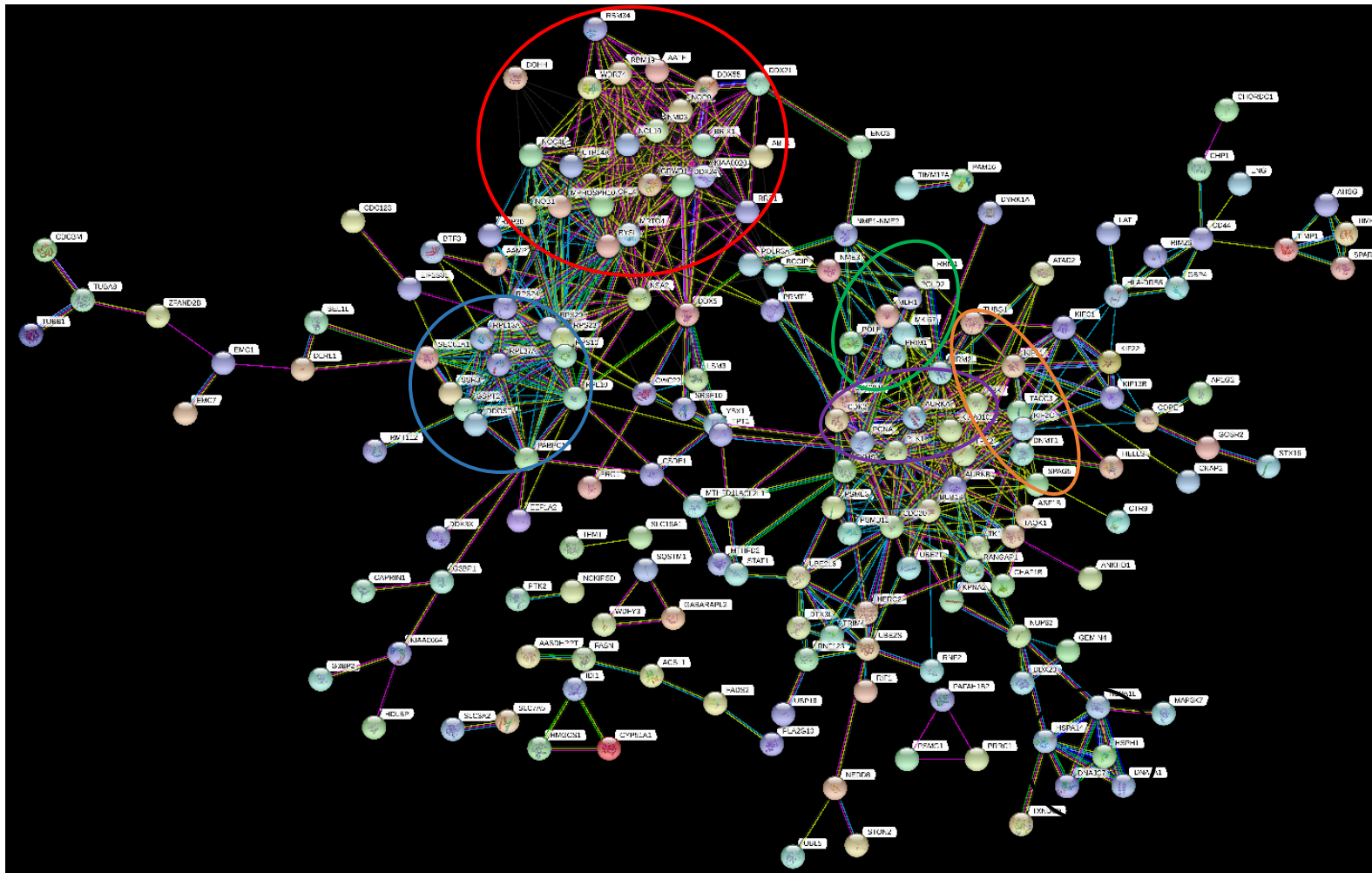


Figure 12: Protein network showing the proteins significantly downregulated (fold change <0.667) in response to 1 μ M RUX in SET2 cells cultured for 24 hours and detected by SWATH-MS analysis. Proteins were mapped using STRING database at high confidence. 305 UNIPROT identification numbers of significantly downregulated proteins were input into the database. Due to slight discrepancies between the two databases (UNIPROT and STRING), 3 proteins could not be identified leaving a network of 302 proteins. From this network, the medium interaction score parameter was set to high confidence (0.7000) and at this point, nodes with no interactions were removed from the protein network, leaving a total of 118 nodes within the protein map. Protein clusters indicated: Red = ribosome biogenesis, blue = translation control, green = DNA replication, purple = mitosis and cell cycle progression, orange = microtubule formation, black = polypeptide folding.

Figure 12 shows the protein map generated by STRING, with nodes indicating proteins that were downregulated in SET2 cells upon 1 μ M RUX treatment for 24 hours. Lines indicate relationships between proteins with similar structures and functions. Clustering of nodes shows proteins with strong relationships. Of the proteins identified through SWATH-MS, clusters of proteins involved in cell cycle progression and DNA replication were shown to be significantly downregulated by RUX treatment, along with proteins involved in post-translational processing and ribosome biogenesis.

STRING-DB results indicate that RUX has a significant effect on the overall survival of SET2 cells by affecting all pathways involved in the central dogma of biology, starting from the conversion of the genetic DNA code into an RNA sequence and eventually into fully folded proteins with specific cellular functions. The largest cluster of downregulated proteins were shown to be involved in ribosome biogenesis (red cluster) which subsequently affects RNA translation (blue cluster) and cell cycle progression. Many proteins involved in the initiation and control of mitosis (purple cluster) were also significantly downregulated upon RUX treatment, including DNA replication and microtubule formation (green and orange clusters), both of which are vital during the M phase of the cell cycle.

Analysis was then performed on significantly upregulated proteins, of which there were 129. A comprehensive list of all significantly upregulated proteins, as determined by Welch's T-test, is displayed below in Table VI.

Table VI: List of significantly upregulated proteins in SET2 cells upon 1 μ M RUX treatment for 24 hours, detected by SWATH-MS. Details of all significantly upregulated proteins in SET2 cells in response to 24hr RUX treatment. Information on the protein and associated UniProt ID, function (as described within the UniProt database), fold change and p-values comparing treated cells to untreated cells, as determined by Welch's T-test, are included.

Uniprot ID	Protein Identity	Protein Name	Function	p-value	Fold Change
Q05469	LIPS	Hormone-sensitive lipase	Converts cholesteryl esters to free cholesterol for steroid production in steroidogenic tissues	0.00791	3.91
P12259	FA5	Coagulation factor V	Central regulator of haemostasis that is an essential co-factor for factor Xa prothrombinase activity, resulting in the activation of prothrombin to thrombin	0.0126	3.84
Q9H4L5	OSBL3	Oxysterol-binding protein-related protein 3	Phosphoinositide-binding protein that has a role in regulation of the actin cytoskeleton, cell polarity and cell adhesion	0.03865	3.63
O00291	HIP1	Huntingtin-interacting protein 1	Involved in clathrin-mediated endocytosis and trafficking. May also induce cell death and promote apoptosis through the intrinsic apoptosis pathway	0.04194	3.23
P51687	SUOX	Sulphite oxidase, mitochondrial	Involved in sulphur metabolism	0.00021	3.19
Q8IUH4	ZDH13	Palmitoyltransferase ZDHHC13	May play a role in Mg ²⁺ transport	0.04297	3.12
Q13541	4EBP1	Eukaryotic translation initiation factor 4E-binding protein 1	Prevents EIF4E assembly into the eIF4F complex. The hypophosphorylated form of this protein competes with EIF4G1 and EIF4G3 and strongly binds to EIF4E, resulting in translation repression	2.27E-05	3.05
O43294	TGFI1	Transforming growth factor beta-1-induced transcript 1 protein	Regulates the Wnt and TGFB signalling pathways and also coordinates multiple protein-protein interactions at the focal adhesion complex and in the nucleus	0.00954	2.9
Q99988	GDF15	Growth/differentiation factor 15	Regulates food intake, energy expenditure and body weight in response to metabolic and toxin-induced stresses	0.03523	2.79
Q3V6T2	GRDN	Girdin	Involved in PI3K phosphorylation and downstream signalling. Regulates DNA replication and cell proliferation through phosphorylation of AKT1/PKB. Also required for maintenance of actin cytoskeleton integrity and cell migration	0.0492	2.49
O14907	TX1B3	Tax1-binding protein 3	May regulate several protein-protein interactions by competing for PDZ domain binding sites	0.00475	2.45

Q53EL6	PDCD4	Programmed cell death protein 4	Tumour suppressor protein that plays a role in apoptosis. Down-regulates the expression of MAP4K1, thus inhibiting events important in invasion	1.68E-11	2.42
P13224	GP1BB	Platelet glycoprotein Ib beta chain	Involved in the production of platelet plugs by binding to von Willebrand factor	0.01271	2.39
Q9H7N4	SFR19	Splicing factor, arginine/serine-rich 19	May function in pre-mRNA splicing	0.01033	2.37
Q13885	TBB2A	Tubulin beta-2A chain	The major constituent of microtubules	0.00242	2.24
Q96AQ6	PBIP1	Pre-B-cell leukaemia transcription factor-interacting protein 1	Regulates the function of pre-B-cell leukaemia transcription factors (BPXs). Inhibits PBX1-HOX complex binding to DNA and blocks the transcriptional activity of E2A-PBX1	0.00128	2.22
Q9H7C9	AAMDC	Mth938 domain-containing protein	May play a role in preadipocyte differentiation and adipogenesis	0.00061	2.21
O95372	LYPA2	Acyl-protein thioesterase 2	Has lysophospholipase activity. Hydrolyses fatty acids from S-acylated cysteine residues in proteins such as trimeric G alpha proteins	0.03141	2.19
P28289	TMOD1	Tropomodulin-1	Inhibits the elongation and depolymerization of the actin filaments at the pointed end. Forms a complex with TM (Tmod/TM) to assist in the formation of the short actin protofilament	0.03973	2.17
Q9UJW2	TINAG	Tubulointerstitial nephritis antigen	Mediates adhesion of proximal tubule epithelial cells via integrins alpha3-beta1 and alphaV-beta3	0.02484	2.14
P42126	ECI1	Enoyl-CoA delta isomerase 1, mitochondrial	Involved in lipid metabolism, specifically fatty acid beta-oxidation.	0.03583	2.14
P62877	RBX1	E3 ubiquitin-protein ligase RBX1	Mediates the ubiquitination and degradation of target proteins, including proteins involved in cell cycle progression, signal transduction, transcription and transcription-coupled nucleotide excision repair	0.03774	2.14
P35612	ADDB	Beta-adducin	Associated with the membrane cytoskeleton to promote the assembly of the spectrin-actin network	4.79E-06	2.13
Q8WUZ0	BCL7C	B-cell CLL/lymphoma 7 protein family member C	May play an anti-apoptotic role	0.04815	2.12
P07711	CATL1	Cathepsin L1	Important for the overall degradation of proteins in lysosomes	1.38E-06	2.11

Q96TC7	RMD3	Regulator of microtubule dynamics protein 3	Involved in cellular calcium homeostasis regulation. Thought to be involved in the differentiation and apoptosis of keratinocytes	0.0024	2.06
Q9H4Z3	PCIF1	Phosphorylated CTD-interacting factor 1	Associates with the phosphorylated C-terminal domain of the largest subunit of RNAPII to assist in transcription elongation and coupling transcription to pre-mRNA processing	0.01038	2.03
P28676	GRAN	Grancalcin	Calcium-binding protein that assists in the adhesion of neutrophils to fibronectin. May also assist in the formation of focal adhesions	0.00017	2.01
O43924	PDE6D	Retinal rod rhodopsin-sensitive cGMP 3',5'-cyclic phosphodiesterase subunit delta	Regulates the subcellular location and activity of prenylated or palmitoylated Ras family members by releasing them from the cell membrane.	0.0162	2
Q9H9E3	COG4	Conserved oligomeric Golgi complex subunit 4	Required for normal Golgi function. Plays a role in SNARE-pin assembly and Golgi-to-ER retrograde transport via its interaction with SCFD1	0.05399	1.99
P08567	PLEK	Pleckstrin	Major protein kinase C substrate of platelets	0.00208	1.98
Q9NZC2	TREM2	Triggering receptor expressed on myeloid cells 2	Triggers immune activation of macrophages and dendritic cells by forming a receptor signalling complex with TYROBP. May also instigate chronic inflammation and production of constitutive chemokines and cytokines	0.02976	1.97
Q05823	RN5A	2-5A-dependent ribonuclease	Endoribonuclease involved in the interferon antiviral response by cleavage of single-stranded viral RNAs. Also induces apoptosis and inhibits protein synthesis through degradation of rRNA	0.03265	1.97
P61764	STXB1	Syntaxin-binding protein 1	Interacts with GTP-binding proteins to help regulate synaptic vesicle docking and fusion	0.01496	1.95
Q92747	ARC1A	Actin-related protein 2/3 complex subunit 1A	Probably functions as component of the Arp2/3 complex which is involved in regulation of actin polymerization and together with an activating nucleation-promoting factor (NPF) mediates the formation of branched actin networks	0.02987	1.94
P55060	XPO2	Exportin-2	Mediates the export of importin-alpha from the nucleus to the cytoplasm after cargo proteins have been released into the nucleoplasm	0.03491	1.93
Q92506	DHB8	Oestradiol 17-beta-dehydrogenase 8	Involved in oestrogen biosynthesis	0.00025	1.92

Q9NWB6	ARGL1	Arginine and glutamate-rich protein 1	Required for the oestrogen-dependent expression of ESR1 target genes. Can act in cooperation with MED1	0.03753	1.92
Q9H479	FN3K	Fructosamine-3-kinase	May initiate a process leading to the deglycation of fructoselysine and of glycosylated proteins	6.93E-06	1.9
P45954	ACDSB	Short/branched chain specific acyl-CoA dehydrogenase, mitochondrial	Involved in lipid metabolism, specifically mitochondrial fatty acid beta-oxidation	0.00018	1.89
P42338	PK3CB	Phosphatidylinositol 4,5-bisphosphate 3-kinase catalytic subunit beta isoform	Activates signalling cascades involved in cell growth, survival, proliferation, motility and morphology by recruiting PH domain-containing proteins, such as AKT1 and PDK1, to the membrane	0.00013	1.88
Q05707	COEA1	Collagen alpha-1(XIV) chain	Plays an adhesive role by integrating collagen bundles	0.0002	1.88
Q13620	CUL4B	Cullin-4B	Involved in the mediation of ubiquitination and subsequent proteasomal degradation of target proteins as it is a core component of multiple cullin-RING-based E3 ubiquitin-protein ligase complexes	7.72E-05	1.87
Q9UL33	TPC2L	Trafficking protein particle complex subunit 2-like protein	May play a role in vesicular transport from endoplasmic reticulum to Golgi	0.02152	1.87
Q96ME7	ZN512	Zinc finger protein 512	May be involved in transcriptional regulation	0.00014	1.85
Q9P0U4	CXXC1	CXXC-type zinc finger protein 1	Transcriptional activator that exhibits a unique DNA binding specificity for CpG unmethylated motifs with a preference for CpGG	0.00566	1.85
Q9Y5U9	IR3IP	Immediate early response 3-interacting protein 1	May be implicated in the regulation of apoptosis. May be involved in protein transport between endoplasmic reticulum and Golgi apparatus	0.01369	1.85
P09871	C1S	Complement C1s subcomponent	Serine protease that forms complexes with C1q and C1r to form C1, forming the first component of the classical pathway of the complement system	0.03051	1.85
Q9Y4F5	C170B	Centrosomal protein of 170 kDa protein B	Plays a role in microtubule organization	0.04564	1.85

Q13469	NFAC2	Nuclear factor of activated T-cells, cytoplasmic 2	Induces the expression of cytokine genes in T-cells, such as IL-2, IL-3, IL-4, TNF-alpha or GM-CSF	0.02516	1.84
Q15477	SKIV2	Helicase SKI2W	Involved in exosome-mediated RNA decay through forming part of the SKI complex	0.01723	1.8
Q9NUB1	ACS2L	Acetyl-coenzyme A synthetase 2-like, mitochondrial	Converts acetate to acetyl-CoA so that it can be used for oxidation in ketogenic conditions through the tricarboxylic cycle	5.72E-07	1.79
P20962	PTMS	Parathymosin	Blocks the effects of prothymosin alpha which confers resistance to certain opportunistic infections	0.00192	1.79
Q5JTJ3	COA6	Cytochrome c oxidase assembly factor 6 homolog	Involved in the maturation of the mitochondrial respiratory chain complex IV subunit MT-CO2/COX2. This complex is part of the respiratory chain that catalyses the transfer of electrons from intermembrane space to molecular oxygen in the matrix and contributes to the proton gradient in ATP synthesis	0.0046	1.79
O75323	NIPS2	Protein NipSnap homolog 2	May act as a positive regulator of L-type calcium channels	0.00659	1.78
Q2T9J0	TYSD1	Peroxisomal leader peptide-processing protease	Catalyses the processing of PTS1-proteins involved in the peroxisomal beta-oxidation of fatty acids	0.03505	1.77
P04179	SODM	Superoxide dismutase [Mn], mitochondrial	Destroys toxic superoxide anion radicals normally produced within the cells	0.00071	1.76
P28799	GRN	Granulins	Thought to have cytokine-like activity and thus are potentially are involved in inflammation, wound repair, and tissue remodelling	0.00735	1.75
O14617	AP3D1	AP-3 complex subunit delta-1	Facilitates the budding of vesicles from the Golgi membrane as part of the AP-3 adaptor-related complex.	0.01847	1.74
Q7Z4V5	HDGR2	Hepatoma-derived growth factor-related protein 2	Involved in cellular growth control through the regulation of cyclin D1 expression	0.03126	1.73
Q9Y624	JAM1	Junctional adhesion molecule A	Involved in the early stages of epithelial tight junction formation	0.00032	1.72
Q15853	USF2	Upstream stimulatory factor 2	Functions as a transcription factor that binds to a symmetrical DNA sequence (E-boxes) (5'-CACGTG-3') found in several viral and cellular promoter sequences	0.01757	1.72

O75208	COQ9	Ubiquinone biosynthesis protein COQ9, mitochondrial	Involved in the biosynthesis of coenzyme Q, a lipid-soluble electron transporter for aerobic cellular respiration	0.00436	1.69
P07305	H10	Histone H1.0	Assists in condensing nucleosome chains into higher-order structures. Found in cells in terminal stages of differentiation or with low cell division rates	2.49E-06	1.68
Q12959	DLG1	Disks large homolog 1	Recruits channels, receptors and signalling molecules to discrete plasma membrane domains in polarized cells. As such, this protein is involved in a number of cellular processes such as adheren junction assembly, signal transduction, cell proliferation, synaptogenesis and lymphocyte activation	0.04402	1.68
Q9Y5K8	VATD	V-type proton ATPase subunit D	Acidifies a variety of intracellular compartments in eukaryotic cells to provide energy for transport processes in the vacuolar system	0.00132	1.66
Q9BZ29	DOCK9	Dedicator of cytokinesis protein 9	Activates CDC42 by exchanging bound GDP for free GTP due to its role as a guanine nucleotide-exchange factor	0.00729	1.66
Q4G176	ACSF3	Acyl-CoA synthetase family member 3, mitochondrial	Activates malonate and methylmalonate into their respective CoA thioester during the first step of intramitochondrial fatty acid synthesis	4.20E-05	1.65
Q14643	ITPR1	Inositol 1,4,5-trisphosphate receptor type 1	Regulates epithelial secretion of electrolytes and fluid by influencing calcium release from the ER following stimulation by inositol 1,4,5-trisphosphate	0.03223	1.65
P13716	HEM2	Delta-aminolevulinic acid dehydratase	Catalyses an early step in the biosynthesis of tetrapyrroles	0.00274	1.64
P22830	HEMH	Ferrocyclase, mitochondrial	Catalyses the ferrous insertion into protoporphyrin IX	0.00016	1.63
Q9HAN9	NMNA1	Nicotinamide/nicotinic acid mononucleotide adenylyltransferase 1	Works with PARP1, PARG and NUDT5 to synthesise ATP in the nucleus, essential for extensive chromatin remodelling events	0.00349	1.63
P80365	DHI2	Corticosteroid 11-beta-dehydrogenase isozyme 2	Catalyses the conversion of cortisol to the inactive metabolite cortisone. Modulates intracellular glucocorticoid levels	0.0283	1.63
P31323	KAP3	cAMP-dependent protein kinase type II-beta regulatory subunit	Involved in cAMP signalling	0.04013	1.63

Q96Q05	TPPC9	Trafficking protein particle complex subunit 9	Functions as an activator of NF-kappa-B through increased phosphorylation of the IKK complex	0.00518	1.61
P50336	PPOX	Protoporphyrinogen oxidase	Catalyses the 6-electron oxidation of protoporphyrinogen-IX to form protoporphyrin-IX	0.00689	1.61
O94927	HAUS5	HAUS augmin-like complex subunit 5	Involved in mitotic spindle assembly, cytokinesis and centrosome integrity maintenance	0.02284	1.61
P06703	S10A6	Protein S100-A6	May function as calcium sensor and modulator. Indirectly plays a role in many physiological processes such as the reorganization of the actin cytoskeleton and in cell motility	0.00194	1.6
Q9Y6M7	S4A7	Sodium bicarbonate cotransporter 3	Functions as an electroneutral sodium- and bicarbonate-dependent cotransporter to regulate the intracellular pH	0.00791	1.6
Q15018	F175B	BRISC complex subunit Abro1	Involved in a number of cellular processes including: regulation of the onset of apoptosis via modulation of Lys-63-linked ubiquitination of target proteins; required for normal mitotic spindle assembly and microtubule attachment to kinetochores via deubiquitinating NUMA1; acts as a central scaffold protein in the BRISK complex of protein degradation	0.0096	1.6
Q9UH99	SUN2	SUN domain-containing protein 2	Involved in the connection between the nuclear lamina and the cytoskeleton (part of the LINC complex)	0.01153	1.6
Q92620	PRP16	Pre-mRNA-splicing factor ATP-dependent RNA helicase PRP16	Probable ATP-binding RNA helicase involved in pre-mRNA splicing	0.01522	1.6
Q05209	PTN12	Tyrosine-protein phosphatase non-receptor type 12	Dephosphorylates a range of proteins, and thereby regulates cellular signalling cascades via ERBB2 and PTK2B/PYK2	0.02853	1.6
Q5VVQ6	OTU1	Ubiquitin thioesterase OTU1	Removes conjugated ubiquitin from misfolded luminal proteins in the endoplasmic reticulum-associated degradation (ERAD) via its hydrolase activity	0.03342	1.6
Q02252	MMSA	Methylmalonate-semialdehyde dehydrogenase [acylating], mitochondrial	Plays a role in valine and pyrimidine metabolism. Binds fatty acyl-CoA	1.59E-05	1.59

P17900	SAP3	Ganglioside GM2 activator	Binds gangliosides and stimulates ganglioside GM2 degradation	0.001	1.59
Q99541	PLIN2	Perilipin-2	May be involved in development and maintenance of adipose tissue	0.00532	1.59
P49902	5NTC	Cytosolic purine 5'-nucleotidase	Co-operates with other nucleotidases to maintain a constant composition of purine/pyrimidine nucleotides within the cell	0.02014	1.59
P07858	CATB	Cathepsin B	Believed to participate in intracellular degradation and turnover of proteins. Has also been implicated in tumour invasion and metastasis	3.09E-05	1.58
Q9UEY8	ADDG	Gamma-adducin	Promotes the assembly of the spectrin-actin network and promotes actin filament capping by associating with the membrane cytoskeleton	0.00566	1.57
O14497	ARI1A	AT-rich interactive domain-containing protein 1A	Involved in transcriptional activation and repression of select genes by chromatin remodelling (alteration of DNA-nucleosome topology)	0.04257	1.57
Q9UIJ7	KAD3	GTP:AMP phosphotransferase AK3, mitochondrial	Involved in maintaining the homeostasis of cellular nucleotides by catalysing the interconversion of nucleoside phosphates	9.94E-05	1.56
P69905	HBA	Haemoglobin subunit alpha	Involved in oxygen transport from the lung to the various peripheral tissues	0.00047	1.56
O00115	DNS2A	Deoxyribonuclease-2-alpha	Involved in the degradation of nuclear DNA in cellular apoptosis during development and hydrolyses DNA under acidic conditions	0.00025	1.55
Q9H9H4	VP37B	Vacuolar protein sorting-associated protein 37B	Regulates vesicular trafficking and sorting of endocytic ubiquitinated cargos in multivesicular bodies as part of the ESCRT-I complex. May also be involved in cell growth and differentiation	0.00026	1.54
P10909	CLUS	Clusterin	Acts as an extracellular chaperone, preventing aggregation of non-native proteins and blood plasma protein aggregation induced by cellular stress. Also maintains partially unfolded proteins in a state of subsequent refolding by other chaperonins	0.02161	1.54
POCG12	CTF8A	Chromosome transmission fidelity protein 8 homolog isoform 2	Potential tumour suppressor	0.04628	1.54
Q7Z434	MAVS	Mitochondrial antiviral-signalling protein	May protect cells from apoptosis. Required for innate immune defence against viruses	0.00029	1.53

P35611	ADDA	Alpha-adducin	Membrane-cytoskeleton-associated protein that promotes the assembly of the spectrin-actin network	0.00045	1.53
P07108	ACBP	Acyl-CoA-binding protein	Binds and carries medium- and long-chain acyl-CoA esters (binds with very high affinity).	0.00176	1.53
P60468	SC61B	Protein transport protein Sec61 subunit beta	Necessary for protein translocation in the endoplasmic reticulum	0.00245	1.53
Q8IWS0	PHF6	PHD finger protein 6	Transcriptional regulator that suppresses rRNA transcription through associations with rRNA promoters	0.00373	1.53
P07942	LAMB1	Laminin subunit beta-1	Thought to mediate the attachment, migration and organization of cells into tissues during embryonic development by interacting with other extracellular matrix components	0.05486	1.53
Q96RQ3	MCCA	Methylcrotonoyl-CoA carboxylase subunit alpha, mitochondrial	Biotin-attachment subunit of the 3-methylcrotonyl-CoA carboxylase involved in leucine and isovaleric acid catabolism.	0.00106	1.52
P15144	AMPN	Aminopeptidase N	Broad specificity aminopeptidase which may be involved the cleavage of peptides bound to major histocompatibility complex class II molecules of antigen presenting cells	0.00175	1.52
O95182	NDUA7	NADH dehydrogenase [ubiquinone] 1 alpha subcomplex subunit 7	Accessory subunit of the mitochondrial membrane respiratory chain NADH dehydrogenase (Complex 1) which transfers electrons from NADH to the respiratory chain	0.00361	1.52
Q86UV5	UBP48	Ubiquitin carboxyl-terminal hydrolase 48	Involved in processing poly-ubiquitin precursors and ubiquitinated proteins by recognising and hydrolysing the peptide bond at the C-terminal Gly of ubiquitin	0.00463	1.52
P02008	HBAZ	Haemoglobin subunit zeta	An alpha-type chain of mammalian embryonic haemoglobin	0.03035	1.52
Q5SSJ5	HP1B3	Heterochromatin protein 1-binding protein 3	Maintains heterochromatin integrity during G1/S progression. Also regulates the duration of G1 phase to critically influence the cell's proliferative capacity	4.13E-07	1.51
P29590	PML	Protein PML	Associates with PML-nuclear bodies (PML-NBs) in various intracellular processes such as tumour suppression, transcriptional regulation, apoptosis, senescence and DNA damage response	0.00025	1.51

P32019	I5P2	Type II inositol 1,4,5-trisphosphate 5-phosphatase	Modulates cellular signalling events by hydrolysing phosphatidylinositol 4,5-bisphosphate (PtIns(4,5)P2) and phosphatidylinositol 1,4,5-trisphosphate (PtIns(1,4,5)P3)	0.0306	1.51
Q8IXM2	BAP18	Chromatin complexes subunit BAP18	Component of chromatin complexes such as the MLL1/MLL and NURF complexes	0.00065	1.5
P35914	HMGCL	Hydroxymethylglutaryl-CoA lyase, mitochondrial	Key enzyme in ketogenesis. Also involved in the terminal step of leucine catabolism	0.01721	1.5
Q9BUT1	BDH2	3-hydroxybutyrate dehydrogenase type 2	Plays a key role in iron homeostasis and transport by mediating the formation of 2,5-dihydrobenzoic acid	0.02237	1.5
Q9UKL0	RCOR1	REST corepressor 1	Controls hematopoietic differentiation and suppresses several genes involved in multilineage blood cell development by recruiting histone deacetylases (HDAC)	0.03752	1.5

As in Figure 12, all significantly upregulated proteins were also mapped using STRING-DB and are shown in Figure 13.

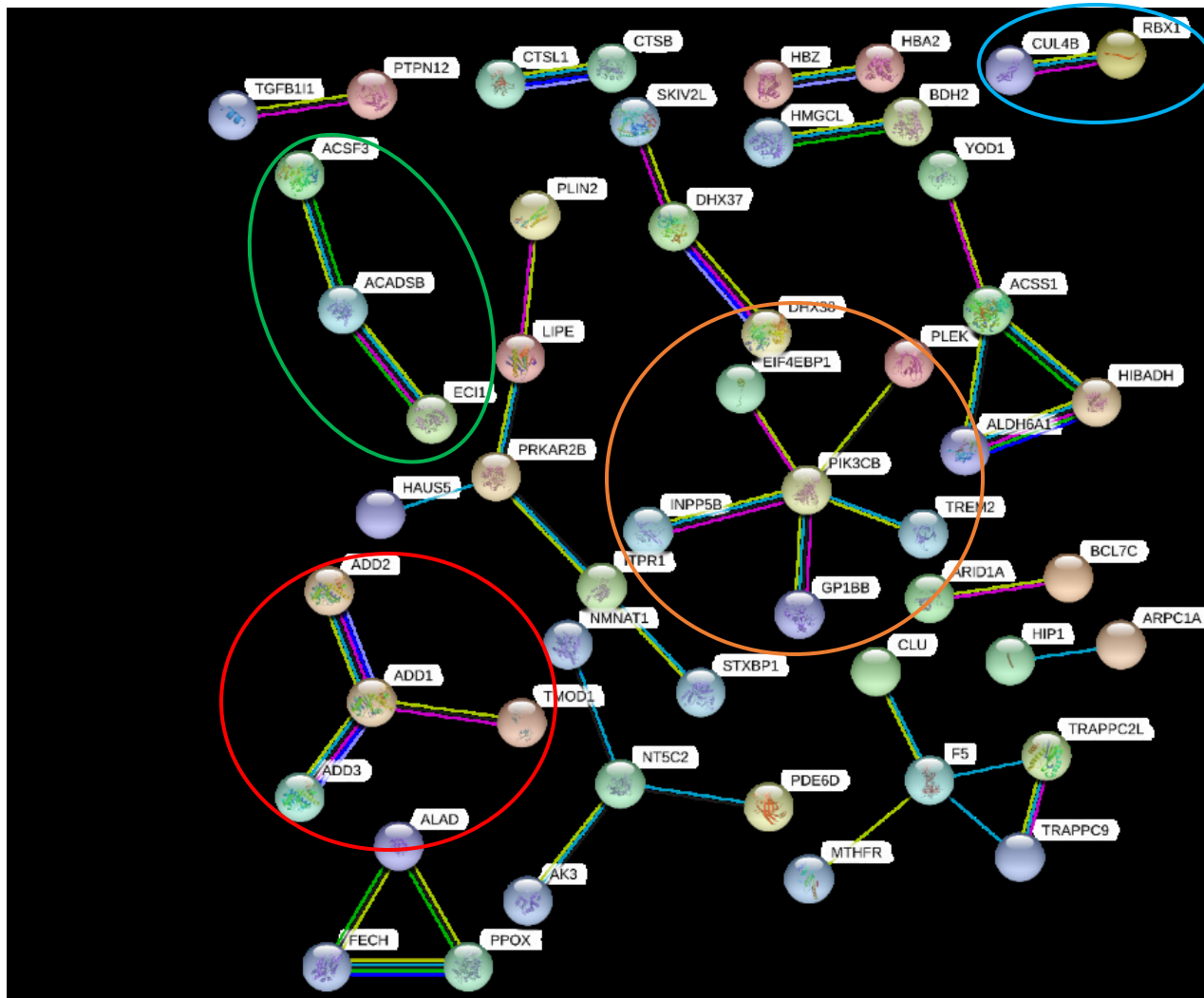


Figure 13: Protein network showing the proteins significantly upregulated (fold change >1.5) in response to 1 μ M RUX in SET2 cells cultured for 24 hours and detected by SWATH-MS analysis. Proteins were mapped using STRING database at high confidence. 129 UNIPROT identification numbers of significantly downregulated proteins were input into the database. From this network, the medium interaction score parameter was set to high confidence (0.7000) and at this point, nodes with no interactions were removed from the protein network, leaving a total of 52 nodes within the protein map. Protein clusters indicated: Red = cytoskeleton proteins, blue = ubiquitination, green = fatty acid synthesis, orange = platelet activation

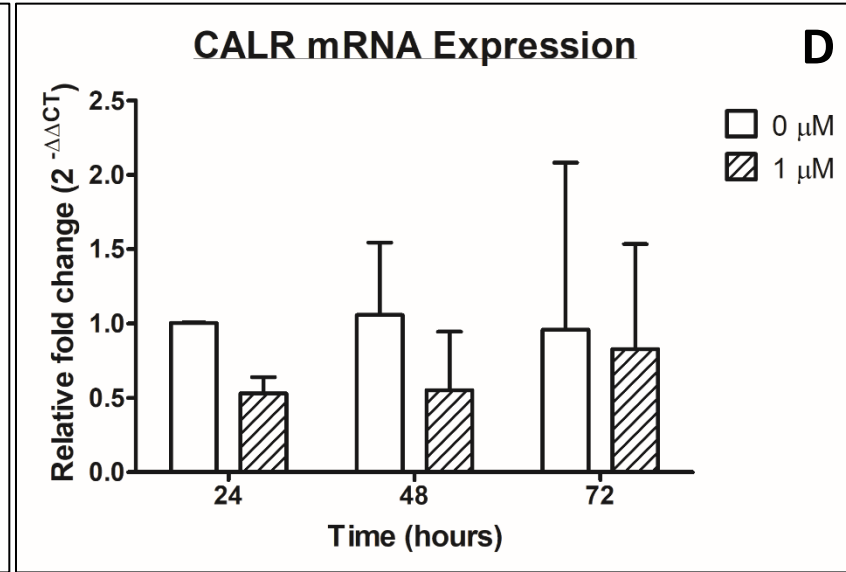
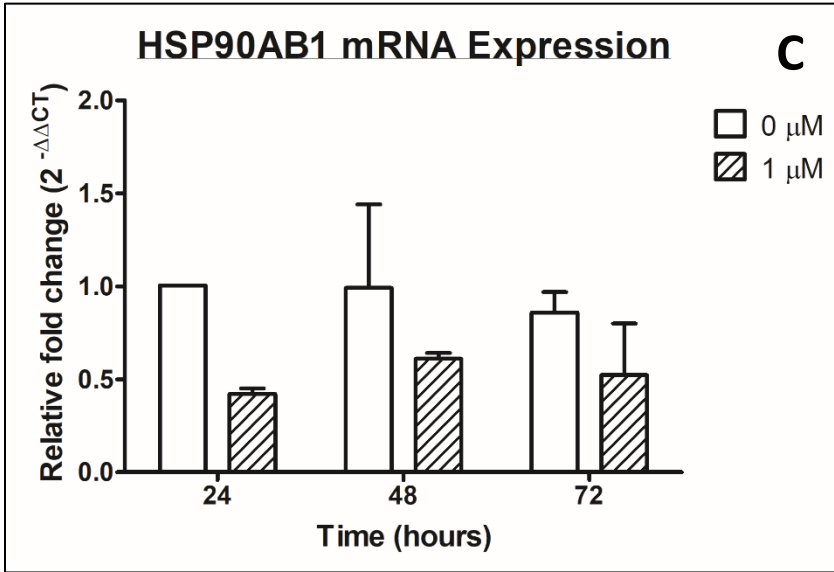
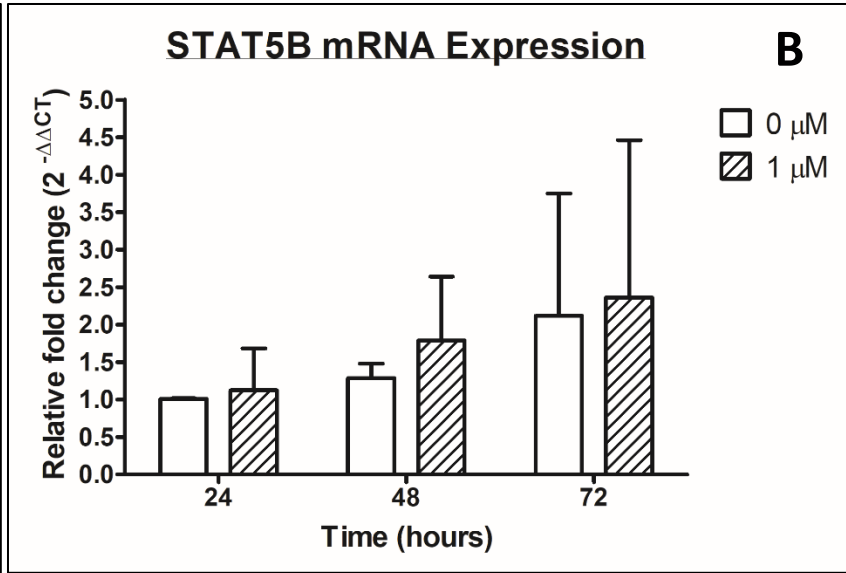
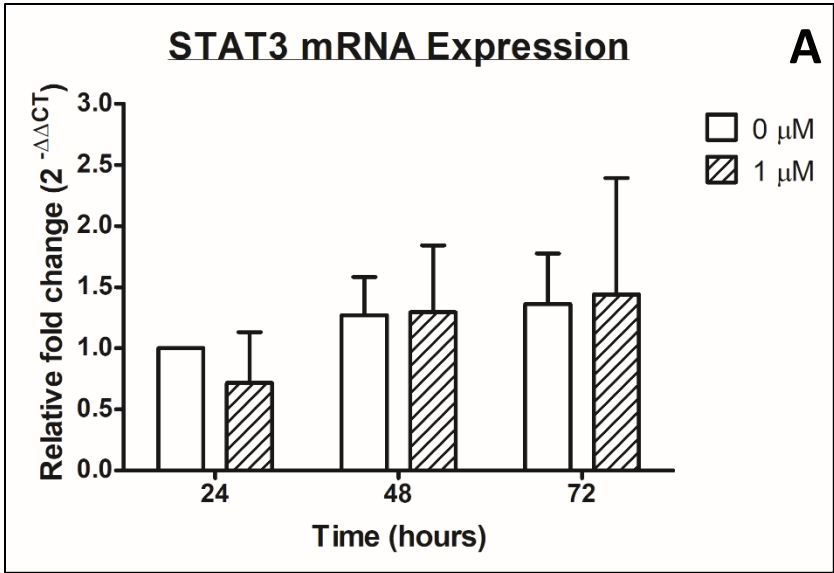
The protein map shown in Figure 13 shows clusters of upregulated proteins involved in several cellular pathways including: platelet aggregation, lipid metabolism, lysosomal proteins, intrinsic apoptotic signalling, negative regulation of calcium-mediated signalling.

STRING-DB uses many different techniques to assess the interactions between proteins, be that physical or functional associations, and each one gives a relative observation of protein interactions. Amending the confidence settings on the STRING-DB resulted in over half of the significantly upregulated proteins identified through SWATH-MS to be discounted from the final figure, indicating that there is a low probability that the interactions between these proteins exist. Proteins lost during analysis therefore may not have any relation to other proteins identified during SWATH and therefore are not associated with any clustering of protein families with similar structures and biological functions. The results in Figure 13 show that RUX significantly affects platelet activation and aggregation (orange cluster), which compliments the overall activation of the immune response. Membrane integrity is also affected by RUX treatment (red cluster), which could be because of intracellular stress or decreases transcription of membrane-associated proteins. Conversely, there was a significant increase in the expression of proteins involved in fatty acid synthesis (green cluster). Translation of ubiquitinating proteins was also significantly upregulated in response to 24-hour treatment with 1 μ M RUX (blue cluster), leading to an increase in ubiquitination and subsequent degradation of intracellular molecules.

Once proteins of interest had been identified through SWATH-MS and through evaluation of the current literature, conformational studies using Q-RT-PCR and Western Blots were performed to support previous findings and elucidate the functional significance of these target molecules and how they support the role of aberrant JAK2 signalling in the pathogenesis of ET.

3.3. The effect of 1 μ M ruxolitinib on target gene transcription in ET

Mass spectrum analysis results from Section 3.2 and a review of the current literature has highlighted various downstream JAK/STAT targets thought to be differentially expressed in ET, including STAT and SOCS proteins, molecular chaperones and members of the antigen presentation pathway. Analysis of these gene transcripts by Q-RT-PCR was performed in SET2 cells cultured in the presence and absence of 1 μ M RUX throughout a 72-hour period.



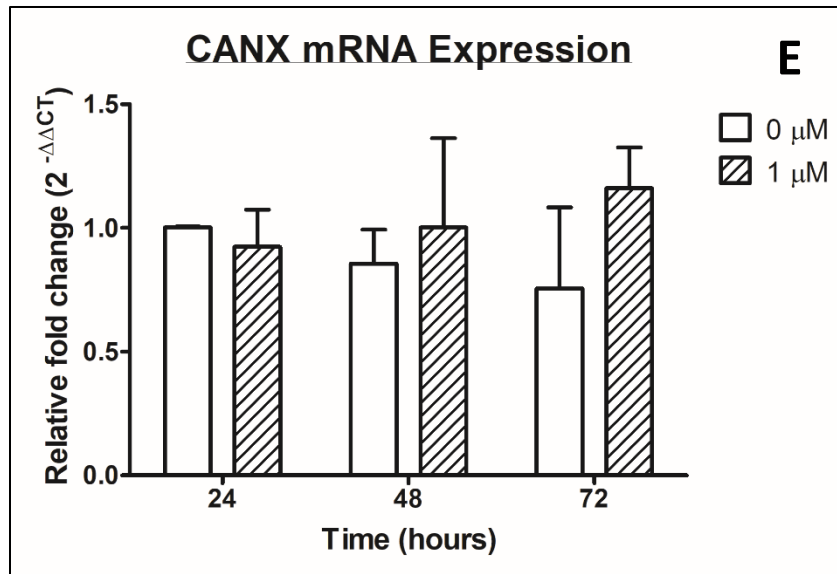
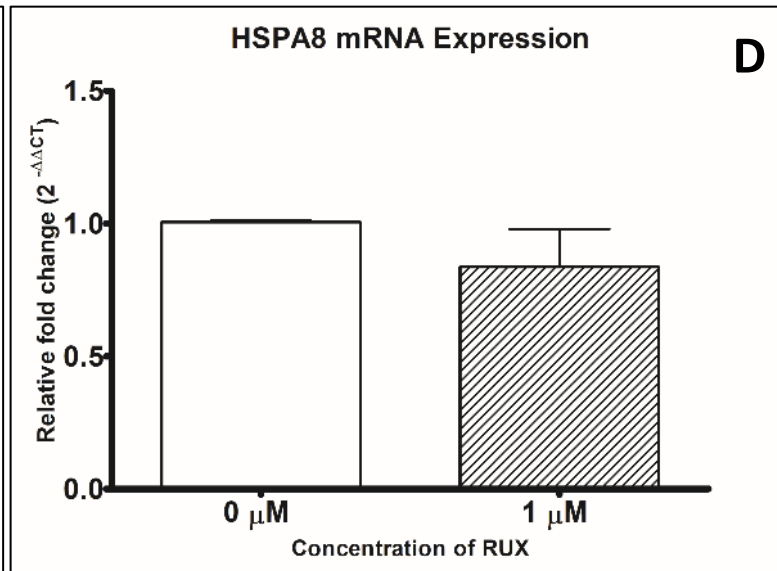
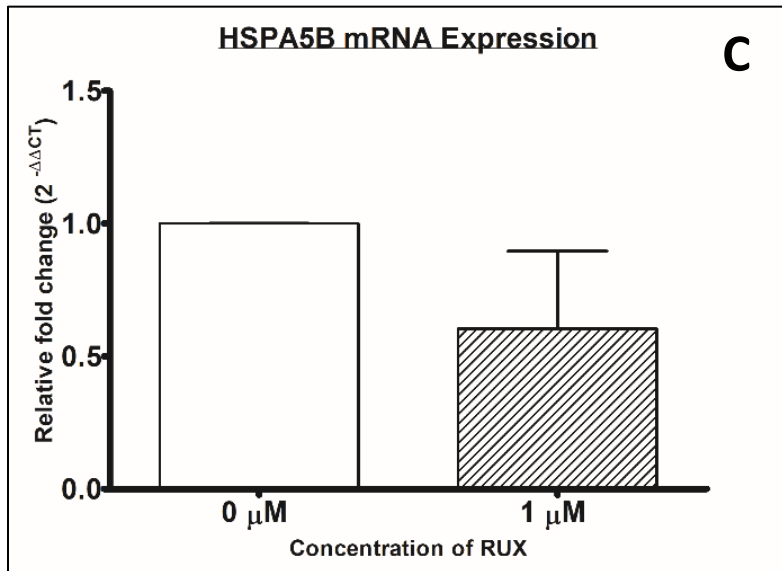
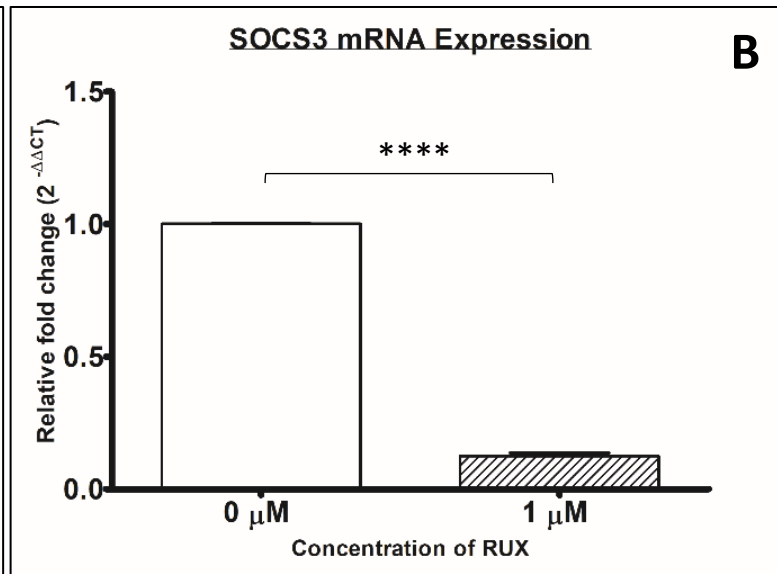
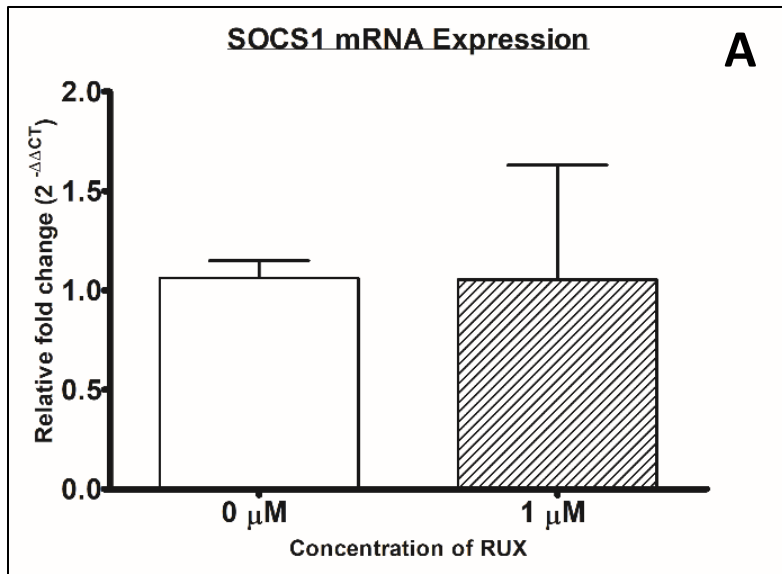


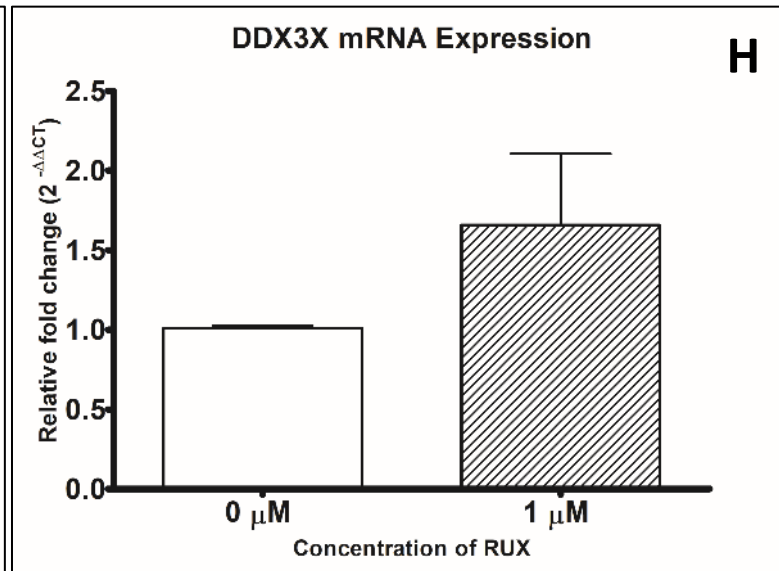
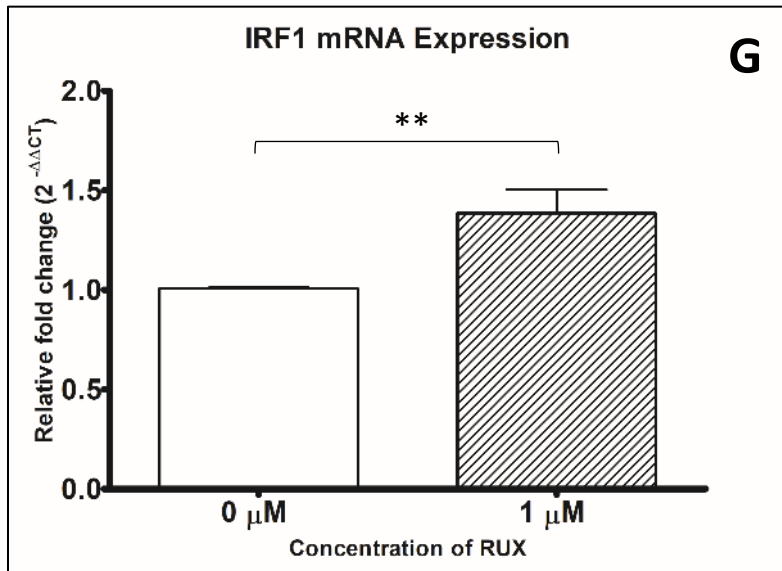
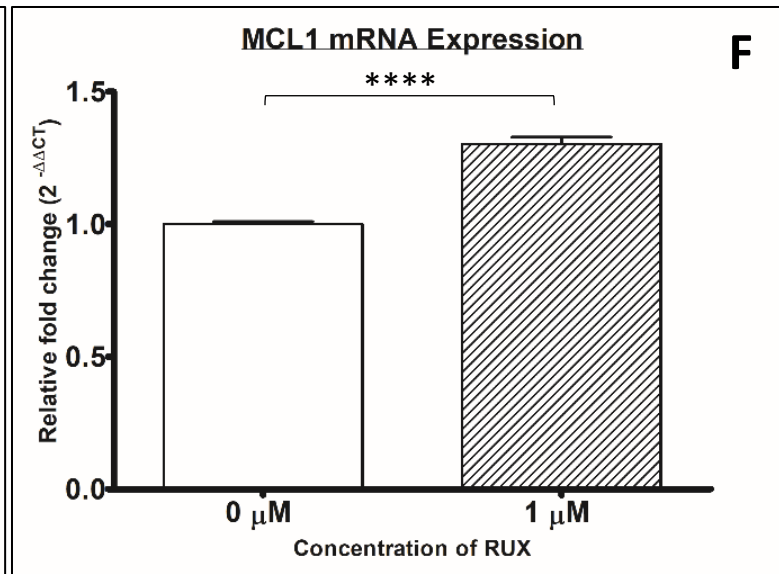
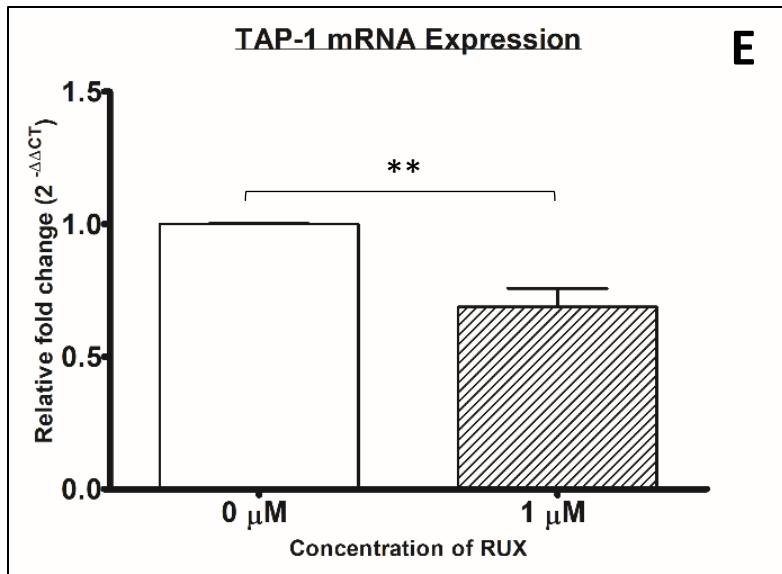
Figure 14: Relative gene expression of selected downstream JAK2/STAT targets in SET2 cells upon treatment with 1 μM RUX for 24, 48 and 72 hours, with fold change relative to untreated cells at 24 hours. STAT3, STAT5B, CALR (n=3). HSP90AB1, CANX, (n=2). Each bar and point represent the mean of the biological repeats with error bars indicating the standard deviation. Two-way ANOVA: STAT3 p=0.7074, STAT5B p=0.4566, HSP90AB1 p=0.1066, CALR p=0.1947, CANX p=0.4999.

Gene expression of selected downstream JAK2 targets upon treatment with RUX for up to 72 hours was determined by Q-RT-PCR. Two-way ANOVA analysis was performed to determine the statistical significance of results using GraphPad Prism. With respect to signal transducers, *STAT3* (Figure 14A) and *STAT5B* (14B) show differing responses to RUX in SET2 cells. *STAT3* mRNA expression is downregulated after 24 hours and gradually increases over time to a similar level as untreated cells at 48 and 72 hours.

In contrast, the expression of *STAT5B* is slightly upregulated in response to RUX at all 3 time-points, with a gradual increase in expression over time. Chaperone proteins *HSP90AB1* (Figure 14C) and *CALR* (14D) are both consistently downregulated in response to 1 μ M RUX at all time points assessed. *CANX* mRNA expression (Figure 14E) showed the same pattern of expression as *STAT3* and appeared to be downregulated in response to RUX after 24 hours and a gradual increase in expression up to 72 hours can be seen. None of the downstream JAK2/STAT targets investigated in SET2 cells showed any significant changes in RNA expression upon treatment with ruxolitinib, as analysed by two-way ANOVA. The absence of significant statistical results may be due to large error bars within the biological repeats analysed and significance may have been reached had the number of biological samples been increased.

In addition, Q-RT-PCR analysis has been performed on SET2 cells cultured in 1 μ M RUX for 24 hours only. 48 and 72hr mRNA expression was not investigated in the following genes shown below in Figure 15.





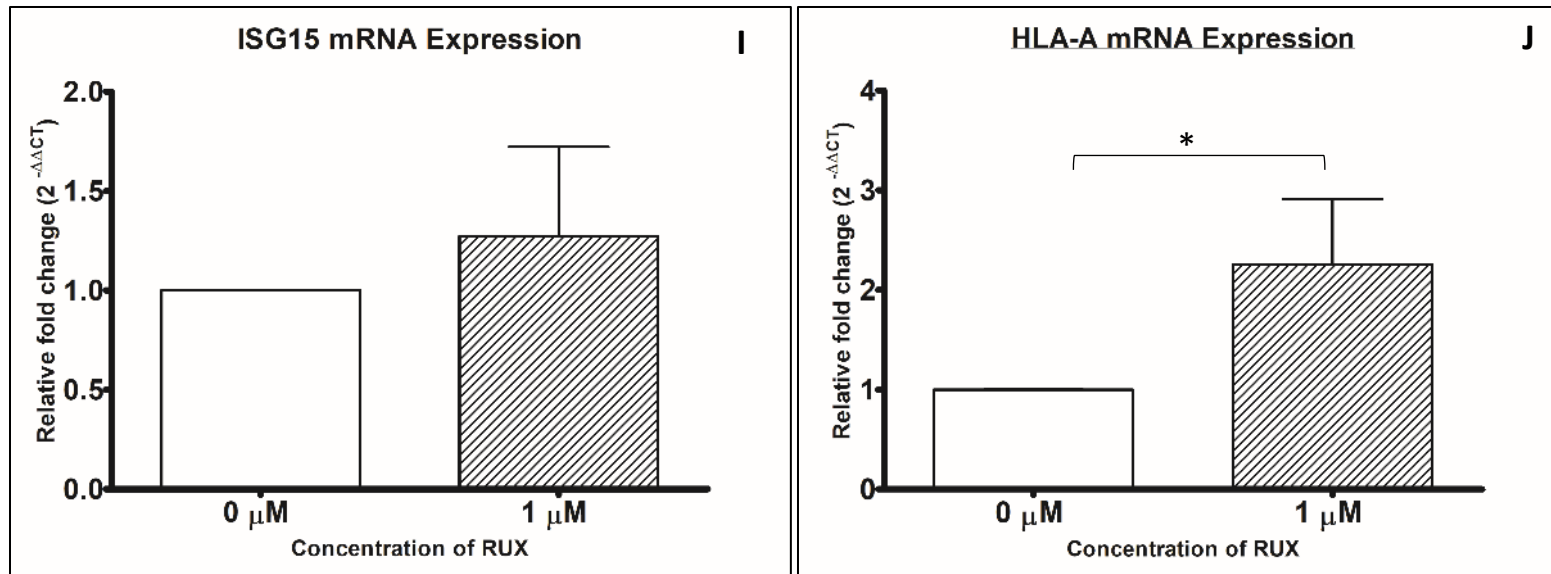


Figure 15: Relative gene expression of selected downstream JAK2/STAT targets in SET2 cells upon treatment with 1 μM RUX for 24 hours, with fold change relative to untreated cells (n=3). Each bar and point represent the mean of the biological repeats with error bars indicating the standard deviation. Unpaired T-test; *SOCS1* $p=0.9820$. *SOCS3* $p<0.0001$, *HSPA5B* $p=0.0783$, *HSPA8* $p=0.1101$, *TAP1* $p=0.0014$, *MCL1* $p<0.0001$, *IRF1* $p=0.0052$, *DDX3X* $p=0.0660$, *ISG15* $p=0.3516$, *HLA-A* $p=0.0302$.

Figure 15 shows the gene expression of selected downstream JAK2 targets upon treatment with RUX for 24 hours, as determined by Q-RT-PCR. Unpaired T-Tests were performed to determine the statistical significance of results using GraphPad Prism. Considering suppressors of cytokine signals, there was a significant decrease in the expression of *SOCS3* after 24-hour RUX treatment (Figure 15B, $p<0.0001$) while there was no change in *SOCS1* expression (15A). *HSPA5* and *HSPA8* transcription was decreased upon RUX treatment but not significantly (Figure 15C and 15D). *TAP-1* (Figure 15E) mRNA was significantly decreased in cells treated with 1 μM RUX compared to untreated cells ($p=0.0014$ respectively). In contrast, *MCL1*, *IRF1* and *HLA-A* (Figure 15F, 15GF and 15J respectively) were all significantly upregulated in RUX-treated SET2 cells ($p<0.0001$, $p=0.0052$ $p=0.0302$ respectively). Transcription of *DDX3X* (Figure 15H) and *ISG15* (15I) was also upregulated upon RUX treatment in SET2 cells.

3.4. The effect of 1 μ M ruxolitinib on target protein translation in ET

Heat shock proteins are members of the chaperone family and can be constitutively expressed or induced upon cellular stress (Jindal, 1996). Their expression has been shown to be upregulated in various malignancies (Lancet, et al., 2010) (Rajan, et al., 2011). Consequently, HSP70 translational expression was investigated in this report.

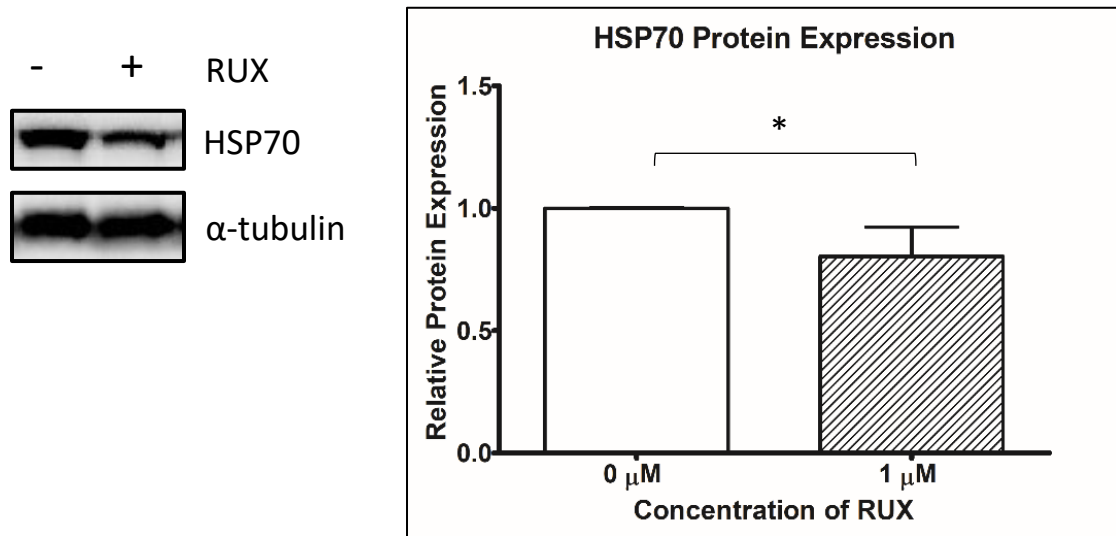


Figure 16: A) Western Blot images for HSP70 protein expression in SET2 cells grown in the presence or absence of 1 μ M RUX for 24 hours (n=3). Western blot analysis of HSP70 (70 kDa) and α -tubulin (50 kDa) proteins in SET2 cells cultured in the presence or absence of 1 μ M RUX (n=3). For this report, only one blot has been shown which is representative of all 3 biological repeats. **B) Densitometry of HSP70 protein expression in SET2 cells treated with 1 μ M RUX for 24 hours, showing fold change against respective control cells (n=3).** Relative protein expression of HSP70 upon 24-hour treatment with 1 μ M RUX in SET2 cells, relative to untreated control. All samples were normalized to expression levels of α -tubulin (loading control) and analysis performed using ImageLab software. Each bar represents the mean of three biological repeats with error bars indicating the standard deviation between replicates. Unpaired T-test: p=0.0467

Figure 16A shows nitrocellulose Western Blot membranes incubated with primary antibodies against HSP70 and α -tubulin housekeeping (for loading control). The blot images show a qualitative decrease in the expression of HSP70. Quantitative analysis using ImageLab allowed for densitometry to determine if any statistical significance in HSP70 protein expression was observed between treated and untreated SET2 cells after 24 hours. Figure 16B shows the quantitative expression of HSP70 within SET2 cells grown in the presence or absence of RUX for 24 hours. Densitometry analysis indicates the expression of HSP70 was significantly decreased upon ruxolitinib treatment.

Previous literature describes a critical role of STAT5 in the development of a PV-like phenotype in mice models and explains how loss of STAT5 prevents the development of *JAK2V617F* MPNs (Yan, et al., 2012). STAT5 phosphorylation is strongly associated with JAK2 activation and signal transduction therefore the expression of STAT5 was explored in SET2 cells treated with RUX. Figure 10 shows Western Blot membranes incubated with primary antibodies against STAT5 and α -tubulin housekeeping (for loading control) in SET2 cells treated with 1 M RUX for 24 hours.

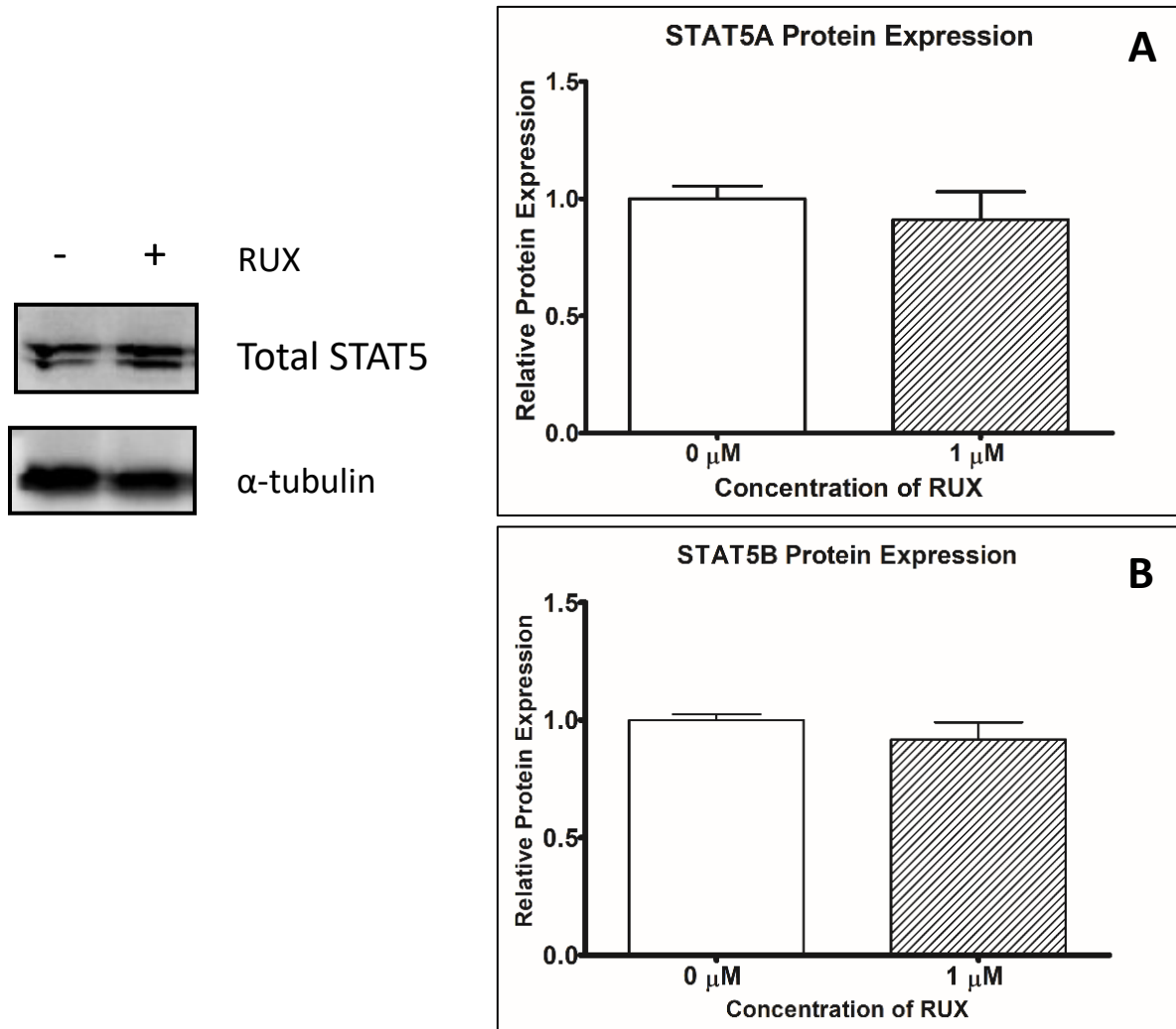


Figure 17: A) Western Blot images for STAT5 protein expression in SET2 cells grown in the presence or absence of 1 μ M RUX for 24 hours (n=3). Western blot analysis of STAT5 (90 kDa) and α -tubulin (50 kDa) proteins in SET2 cells cultured in the presence or absence of 1 μ M RUX (n=3). For this report, only one blot has been shown which is representative of all 3 biological repeats. **B) Densitometry of STAT5A and STAT5B protein expression in SET2 cells treated with 1 μ M RUX for 24 hours, showing fold change against respective control cells (n=3).** Relative protein expression of STAT5A and STAT5B upon 24-hour treatment with 1 μ M RUX in SET2 cells, relative to untreated control. All samples were normalized to expression levels of α -tubulin (loading control) and analysis performed using ImageLab software. Each bar represents the mean of three biological repeats with error bars indicating the standard deviation between replicates. Unpaired T-test: STAT5A p=0.3026. STAT5B p=0.1381.

Use of the STAT5 antibody detected two bands around 90kDa (Figure 10). From the molecular weights of both isoforms, it was understood that the heavier molecular weight band indicated STAT5A while the lighter molecular band was STAT5B (MW = 90.6 kDa and 89.9 kDa respectively). Densitometry analysis was also performed to obtain a quantitative evaluation of protein expression. For quantitative densitometry analysis, both isoforms were analysed separately. Figure 17 shows the densitometry analysis of STAT5A and STAT5B in response to 1 μ M RUX after 24 hours, with results normalized to the expression in untreated cells. Unpaired T-test analysis shows no difference in the expression of either isoform in response to RUX.

3.5. The effect of 1 μ M RUX on STAT1 expression in ET and PV

Since STAT1 is thought to be the driver of the ET phenotype (Chen, et al., 2010), its expression was investigated on a transcriptional and translational level using mass spectrometry, Western Blotting and Q-RT-PCR. Mass spectrometry results demonstrated a significant downregulation of STAT1 upon 24-hour ruxolitinib treatment in SET2 cells, with a fold change of 0.582. Expression of STAT1 and phosphorylated STAT1 (pSTAT1) protein was investigated along with the effect of short and long-term treatment with 1 μ M RUX on STAT1 mRNA expression. Figure 18 shows the relative protein expression of STAT1 and pSTAT1 via Western Blot analysis in SET2 and HEL cells 24-hours post-treatment with ruxolitinib.

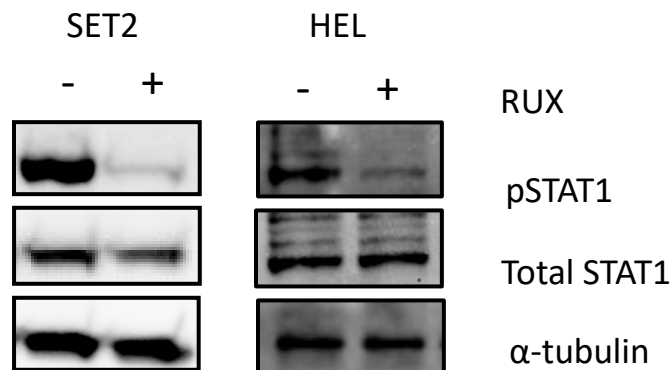


Figure 18: Western Blot images of STAT1 and pSTAT1 target proteins expressed in SET2 and HEL cells grown in the presence or absence of 1 μ M RUX for 24 hours (n=3 and n=2 respectively). Western blot analysis of total STAT1 and phosphorylated STAT1 (91 kDa), and α -tubulin (50 kDa) proteins in SET2 and HEL cells cultured in the presence or absence of 1 μ M RUX. For this report, only one blot has been shown which is representative of all biological repeats in each cell line.

Figure 18 shows western blot nitrocellulose membranes incubated with antibodies against STAT1, phosphorylated STAT1 and the housekeeping protein α -tubulin, for loading control purposes. A

qualitative decrease in expression of both total STAT1 and phosphorylated STAT1 (pSTAT1) protein can be seen in SET2 cells in response to 1 μ M RUX after 24 hours. Densitometry analysis was also performed to obtain a quantitative evaluation of protein expression, as shown below.

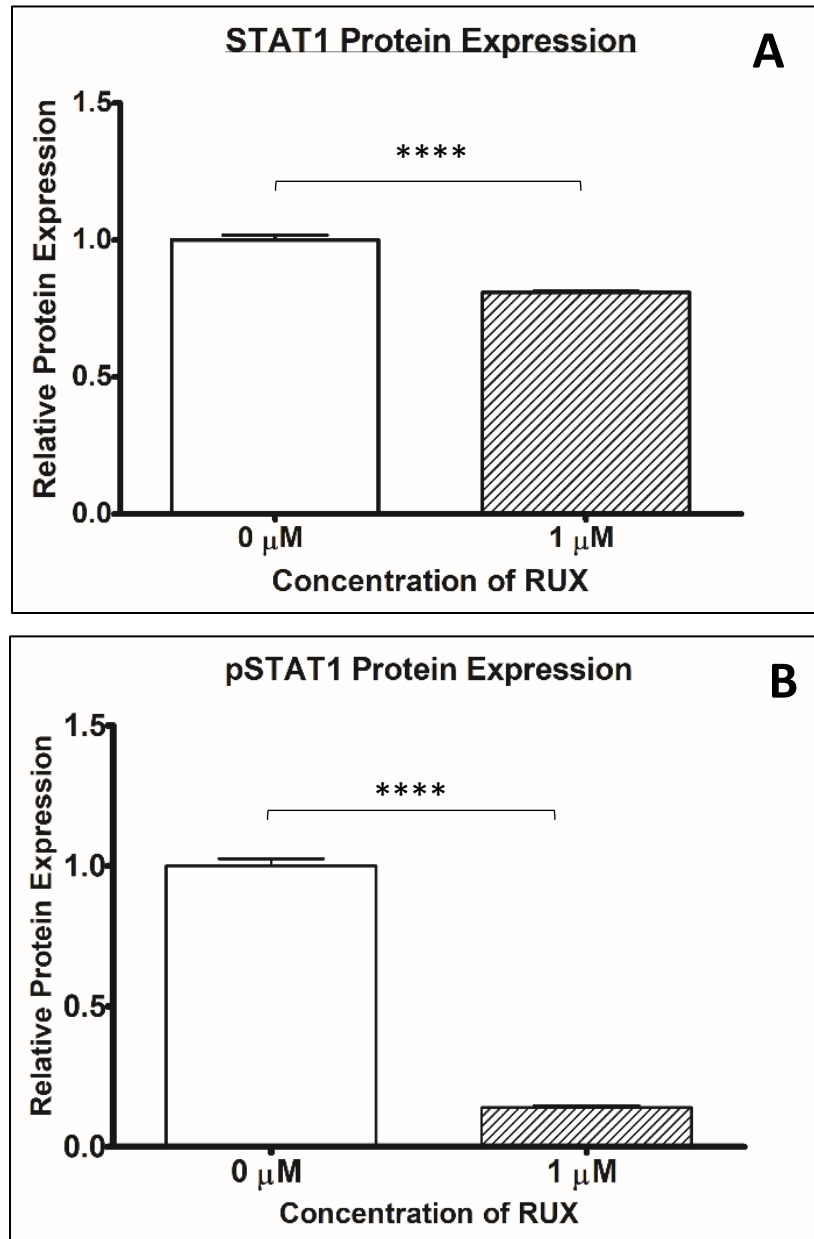


Figure 19: Densitometry of STAT1 and pSTAT1 protein expression in SET2 cells upon 24-hour treatment with 1 μ M RUX, showing fold change against respective control cells (n=3). Relative protein expression of A) STAT1 and B) pSTAT1 upon 24-hour treatment with 1 μ M RUX in SET2 cells, relative to untreated control. All samples were normalized to expression levels of α -tubulin (loading control) and analysis performed using ImageLab software. Each bar represents the mean of three biological repeats with error bars indicating the standard deviation between replicates. Unpaired T-test: STAT1: $p < 0.0001$. pSTAT1 $p < 0.0001$.

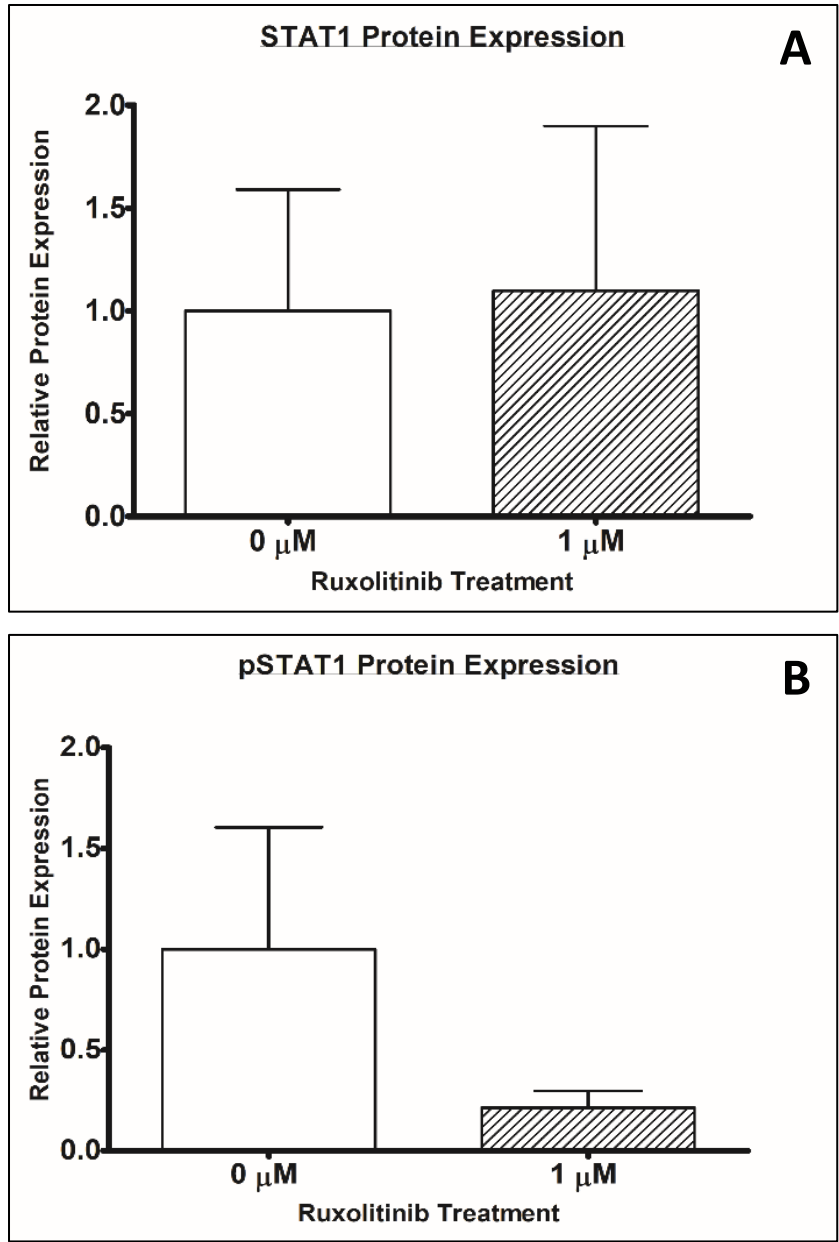


Figure 20: Densitometry of STAT1 and pSTAT1 protein expression in HEL cells upon 24-hour treatment with 1 μM RUX, showing fold change against respective control cells (n=2). Relative protein expression of A) STAT1 and B) pSTAT1 upon 24-hour treatment with 1 μM RUX in HEL cells, relative to untreated controls. All samples were normalized to expression levels of α -tubulin (loading control) and analysis performed using ImageLab software. Each bar represents the mean of two biological repeats with error bars indicating the standard deviation between replicates. Unpaired T-test: STAT1 $p=0.0001$, pSTAT1 $p=0.0001$).

Densitometry analysis displayed in Figure 19 shows the protein expression of total STAT1 (Figure 19A) and pSTAT1 (Figure 19B) and indicates a significant decreased expression of both active and inactive STAT1 after 24-hour treatment of SET2 cells with 1 μ M RUX (unpaired T-test: STAT1 $p=0.0001$, pSTAT1 $p=0.0001$). In contrast, HEL cell densitometry analysis shown in Figure 20 indicates the protein expression of total STAT1 (Figure 20A) and pSTAT1 (Figure 20B) is not significant altered after 1 μ M RUX treatment after 24 hours.

To further confirm that the expression of STAT1 protein is downregulated in SET2 cells upon RUX treatment, results from the mass spectrometry analysis explained in Section 3.2 were further analysed to look specifically at the expression of STAT1 (Uniprot ID: P42224). The resulting box plot was drawn illustrating the intensity of STAT1 ions detected in untreated SET2 cells and cells treated with 1 μ M RUX for 24 hours.

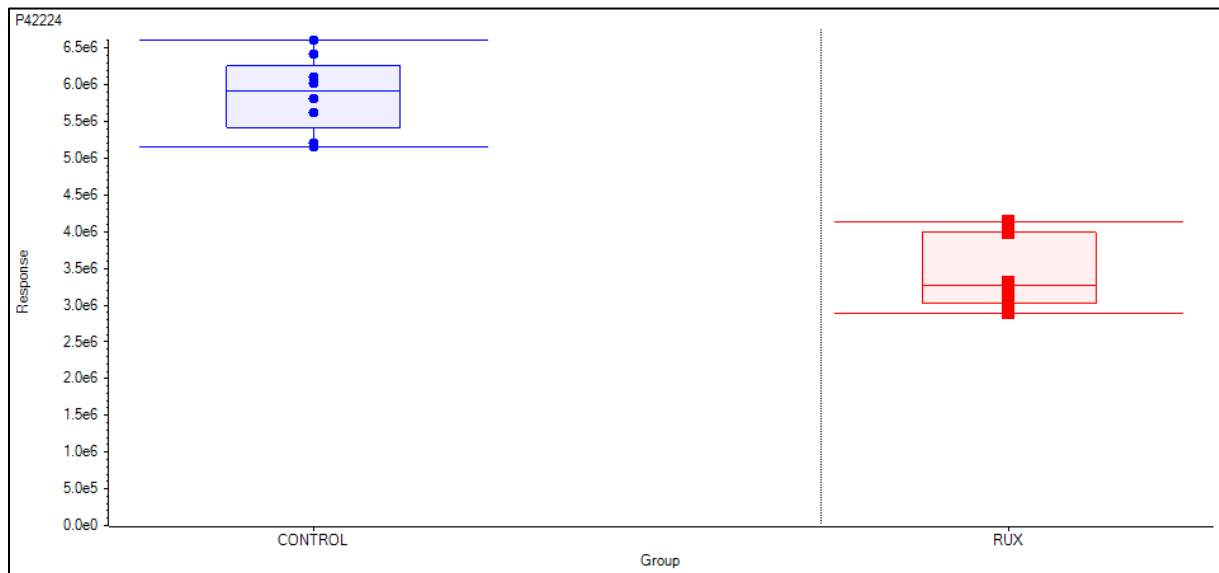


Figure 21: Box plot of STAT1 protein expression in RUX-treated and untreated SET2 cells, as determined by mass spectrometry. Each point indicates the expression of STAT1 protein in each sample injection ($n=3$ biological repeats, $n=3$ injections per sample). Box ends are indicative of Q1 (25th percentile) and Q3 (75th percentile) while the band inside the box indicates the Q2 (median) value. Whiskers represent the minimum and maximum values of the sample sets. Welch's T-test $p=7.359 \times 10^{-8}$

The box plot in Figure 21 shows the expression of STAT1 protein in SET2 cells is significantly downregulated in response to 24-hour RUX treatment, as detected by mass spectrometry analysis. A Welch's t-test was performed and showed that the expression of STAT1 protein is significantly downregulated in response to 1 μ M RUX ($p=7.359 \times 10^{-8}$).

To investigate the short and long-term effects of RUX on *STAT1* mRNA expression in ET, SET2 cells were cultured with RUX for up to 6 hours and harvested every 2 hours. Another experiment investigated the effect of RUX at 24-hour intervals for up to 72 hours. Isolated mRNA was converted to cDNA and Q-RT-PCR performed on the samples to examine the expression of STAT1. Figure 22 shows the expression of *STAT1* in treated SET2 cells, relative to the mRNA expression in untreated cells.

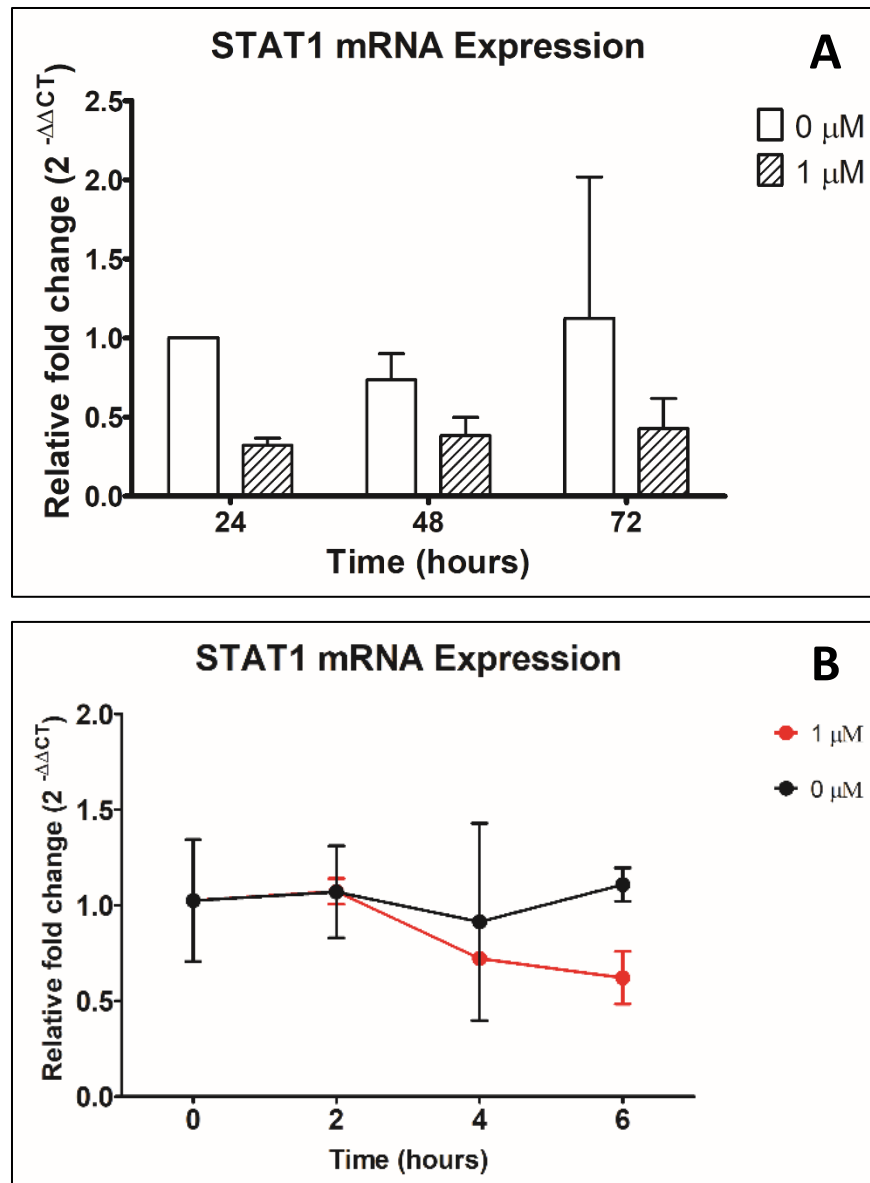


Figure 22: Relative gene expression of STAT1 upon treatment with 1 μM RUX in SET2 cells. A) 1 μM RUX treatment of SET2 cells for up to 72 hours, with cells harvested every 24 hours (n=3). B) SET2 cells treated with 1 μM RUX for a total of 6 hours, with cells harvested at 2-hour time points (n=2). Each bar in A) and point in B) represents the mean of the biological repeats with error bars indicating standard deviation. In A), fold change plotted against untreated cells at 24 hours. Two-way ANOVA: $p=0.0076$. In B), fold change plotted relative to untreated cells at 0hr time point. Two-way ANOVA: $p=0.2759$.

The results in Figure 22A indicate the relative expression of STAT1 mRNA after 24, 48 and 72 hours in SET2 cells cultured in the presence and absence of 1 μM RUX, with two-way ANOVA performed for

significance between treated and untreated samples over 72 hours. The graph shows a significant decrease in *STAT1* expression in treated SET2 cells compared to untreated cells ($p=0.0076$).

In comparison, Figure 22B shows the relative fold change of *STAT1* expression in SET2 cells upon RUX treatment, compared to *STAT1* levels within untreated cells harvested at 0hrs. Two-way ANOVA analysis of Figure 14A shows that *STAT1* expression in SET2 cells upon treatment with 1 μM RUX was not significantly affected within the first 6 hours post-treatment ($p=0.2759$). A trend of decreasing expression can be seen however, more biological repeats of this experiment may be needed, and time point extended to observe at what point a significant decrease in *STAT1* expression in SET2 cells is reached.

3.6. The effect of 1 μM ruxolitinib and 1 $\mu\text{g}/\text{ml}$ IFN- α on proliferation in ET and PV

To investigate the role of *STAT1* in the pathogenesis of PV and ET, both cell lines were treated with RUX, IFN- α (a *STAT1* activator) and a combination of the two drugs. For growth curves involving a combination of RUX and IFN- α , cells were seeded at a density of 5×10^4 cells/ml. Cells were treated with 1 μM RUX and/or 1 $\mu\text{g}/\text{ml}$ IFN- α and cultured at 37°C 5% CO_2 for a total of 72 hours. At 24-hour intervals, a single cell suspension was made and 50 μL cell suspension was removed. Cells were counted, and Trypan Blue exclusion assay performed as per Section 2.1.3.

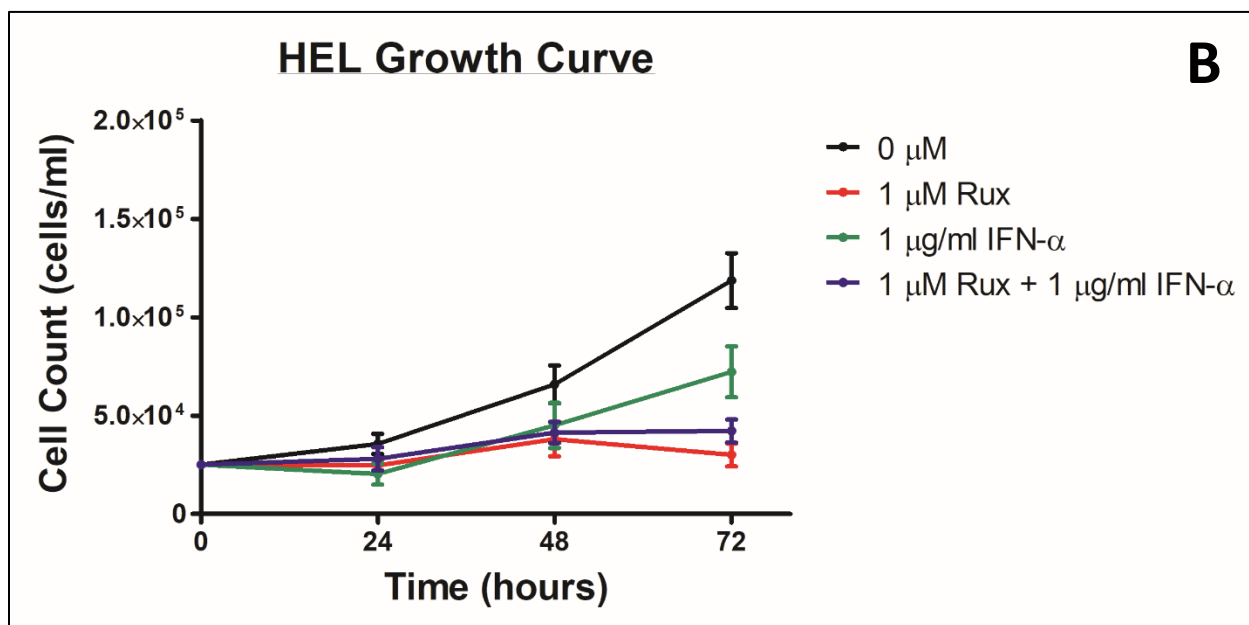
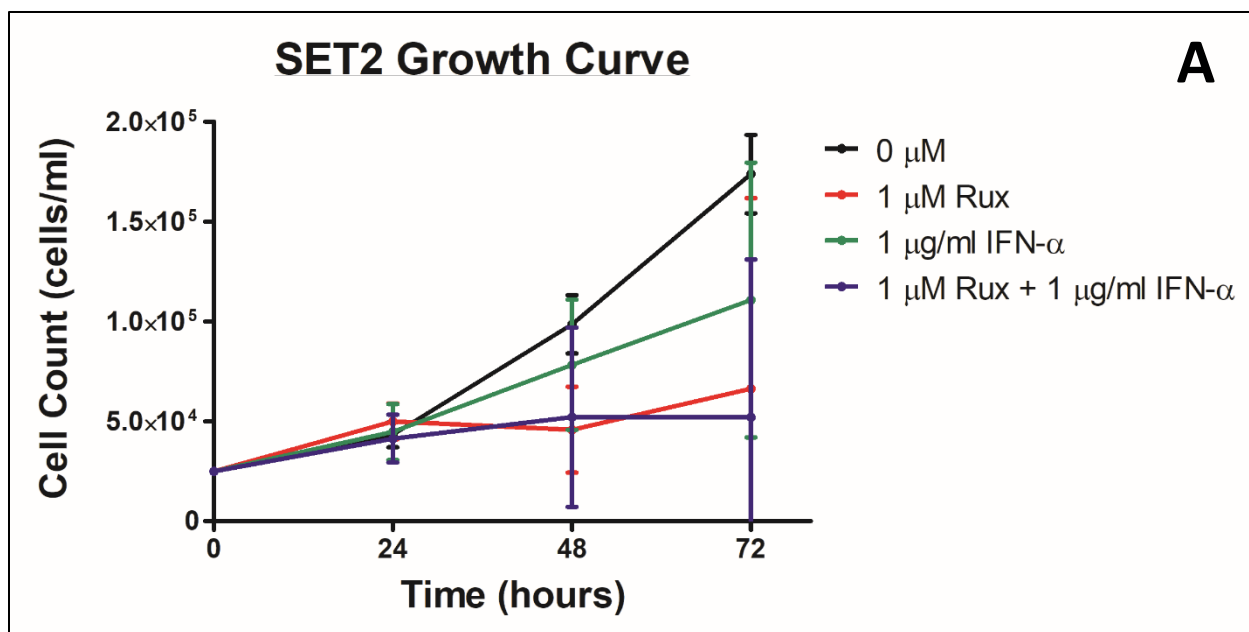


Figure 23: 72-hour growth curve of A) SET2 and B) HEL cells treated with 1 μ M RUX, 1 μ g/ml IFN α or a combination of the two treatments, with cells counted every 24 hours (n=3). Each point represents the mean of the biological repeats with error bars indicating the standard deviation. Two-way ANOVA results: SET2 p=0.2037. HEL p<0.0001.

Figure 23 shows the density of SET2 and HEL cells every 24 hours for a total of 72 hours when treated with 1 μ M RUX, 1 μ g/ μ L IFN- α , a combination of RUX and IFN- α , or VC (DMSO). The graphs illustrate that cellular proliferation is negatively affected by IFN- α and RUX as single agents and in combination as a

dual treatment after 72 hours in both cell lines. Figure 23A shows the greatest effect on SET2 cell proliferation was seen in cells subject to a combination of RUX and IFN- α treatment after 72 hours. Two-way ANOVA repeated measures analysis shows no overall significant difference in cell proliferation between the 3 treatment sets ($p=0.2037$). Bonferroni multiple comparisons analysis showed that the significant differences observed were after 72 hours when comparing untreated SET2 cells to cells treated 1 μ M RUX ($p<0.05$) and with a combination of 1 μ M RUX and 1 μ g/ml IFN- α ($p<0.05$).

In the HEL cell line shown in Figure 23B, two-way ANOVA repeated measures analysis indicated a significant difference in cellular proliferation across the different treatment options ($p=0.0001$). Bonferroni multiple comparisons analysis indicated a significant difference in proliferation in RUX-treated cells at 48 and 72 hours compared to untreated control cells ($p<0.01$ and $p<0.0001$ respectively). When comparing control cells to IFN- α treatment, a significant decrease in proliferation was observed at 48 and 72 hours ($p<0.05$ and $p<0.0001$ respectively). The combination of RUX and IFN- α showed a similar pattern with respect to decreasing proliferative capacity as the HEL cells treated with RUX alone as significance was observed at 48- and 72- hours post-treatment ($p<0.01$ and $p<0.0001$). Comparison of IFN- α and RUX as single therapeutic agents showed a significant difference in proliferation after 72 hours ($p<0.0001$) while comparison of IFN- α with the dual treatment (RUX + IFN- α) showed a significant difference in these two treatments at 72 hours ($p<0.001$). There was no significant difference in proliferative capacity in HEL cells treated with RUX alone compared to cells treated with a combined therapy of RUX and IFN- α over the 72 hours observed.

During cell counts in the production of growth curves shown in Figure 16, cell viability was also assessed by Trypan Blue exclusion assay. The Trypan Blue assay data shown below in Figure 24 is associated with samples taken for growth curve analysis in Figure 23.

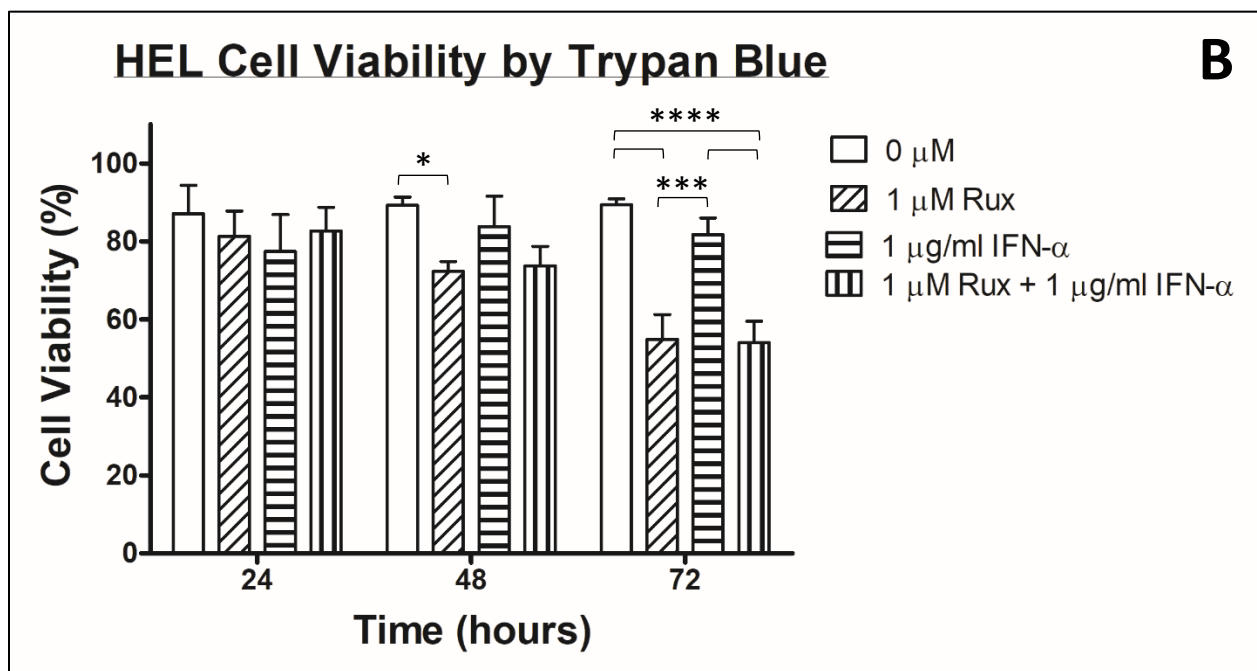
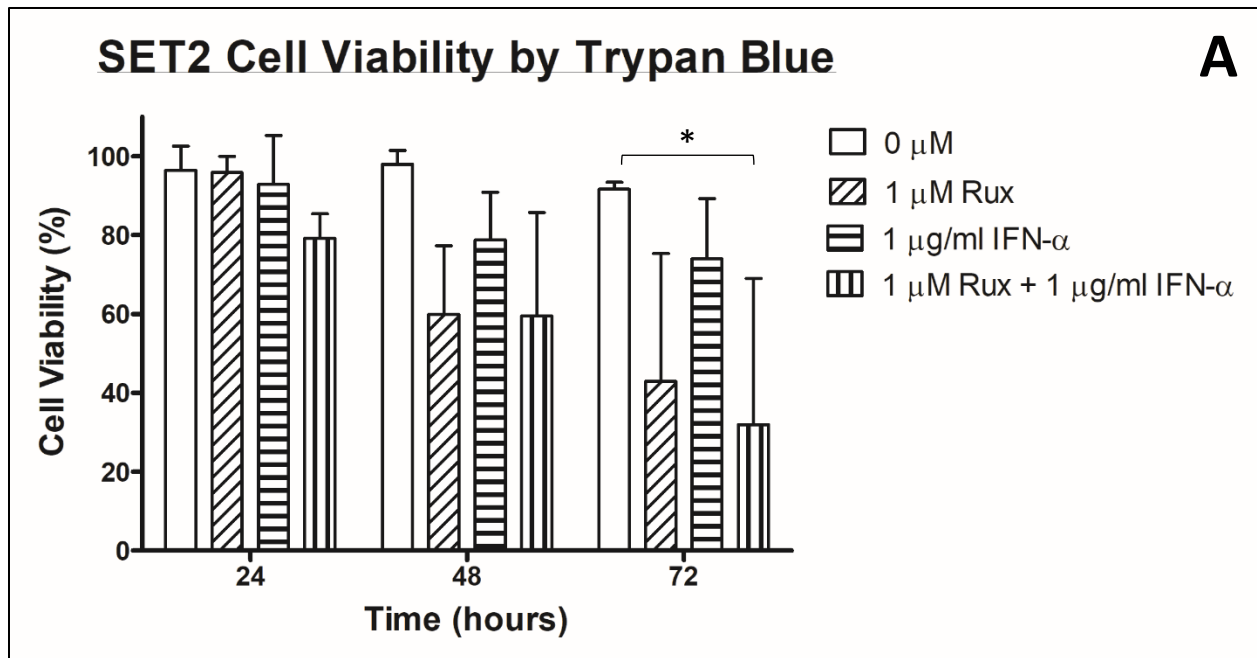


Figure 24: A) SET2 and B) HEL cells grown in the presence or absence of 1 μ M RUX, 1 μ g/ml IFN- α or a combination of the two treatments. Cell viability was assessed over 72 hours and determined by Trypan Blue every 24 hours (n=3). Each bar represents the mean of the biological repeats with error bars indicating the standard deviation. Two-way ANOVA: SET2 $p=0.0009$. HEL $p=0.0002$.

Figure 24 shows the assessment of cell viability by Trypan Blue exclusion assay in SET2 and HEL cells assessed every 24 hours for a total of 72 hours. Cells were treated with 1 μ M RUX, 1 μ g/ml IFN- α or a

combination of these two treatments. SET2 cell viability over 72 hours is shown in Figure 24A and demonstrates how all treatments negatively affect the viability of SET2 cells in comparison to untreated cells. Two-way ANOVA repeated measures and Bonferroni multiple comparisons analysis showed no significant decrease in cell viability in RUX-treated cells at any time point. With respect to IFN- α treatment, no significant difference in viability was seen over the 72-hour period observed when compared to untreated cells. This may be due to large error bars in the RUX and IFN single treatment groups. Dual treatment with RUX and IFN- α showed a significant difference in viability only after 72 hours ($p < 0.05$). There was also no significant difference observed when comparing RUX-treated cells to IFN- α alone or cells treated with a combination of RUX and IFN- α .

Treatment of HEL cells with RUX, IFN- α or a combination of the two show a different pattern to the SET2 cells (Figure 24B). Bonferroni multiple comparisons analysis showed a significant difference in RUX-treated cells compared to control cells after 48 and 72 hours ($p < 0.05$ and $p < 0.0001$). Dual treatment with RUX and IFN- α showed significant decrease compared to control cells after 72 hours ($p < 0.0001$) while IFN- α treatment did not affect cell viability across the 72 hours observed in comparison to untreated cells. There was a significant difference in HEL cell viability when comparing RUX and IFN- α as single treatments at 72 hours ($p < 0.001$) and when comparing IFN- α single treatment to the combined treatment of RUX and IFN- α ($p < 0.0001$).

Cellular proliferation was also assessed by MTS assay. As described previously, 1×10^4 cells were grown in a 96-well plate in the presence or absence of $1 \mu\text{M}$ RUX and cultured for 72 hours at 37°C $5\% \text{CO}_2$.

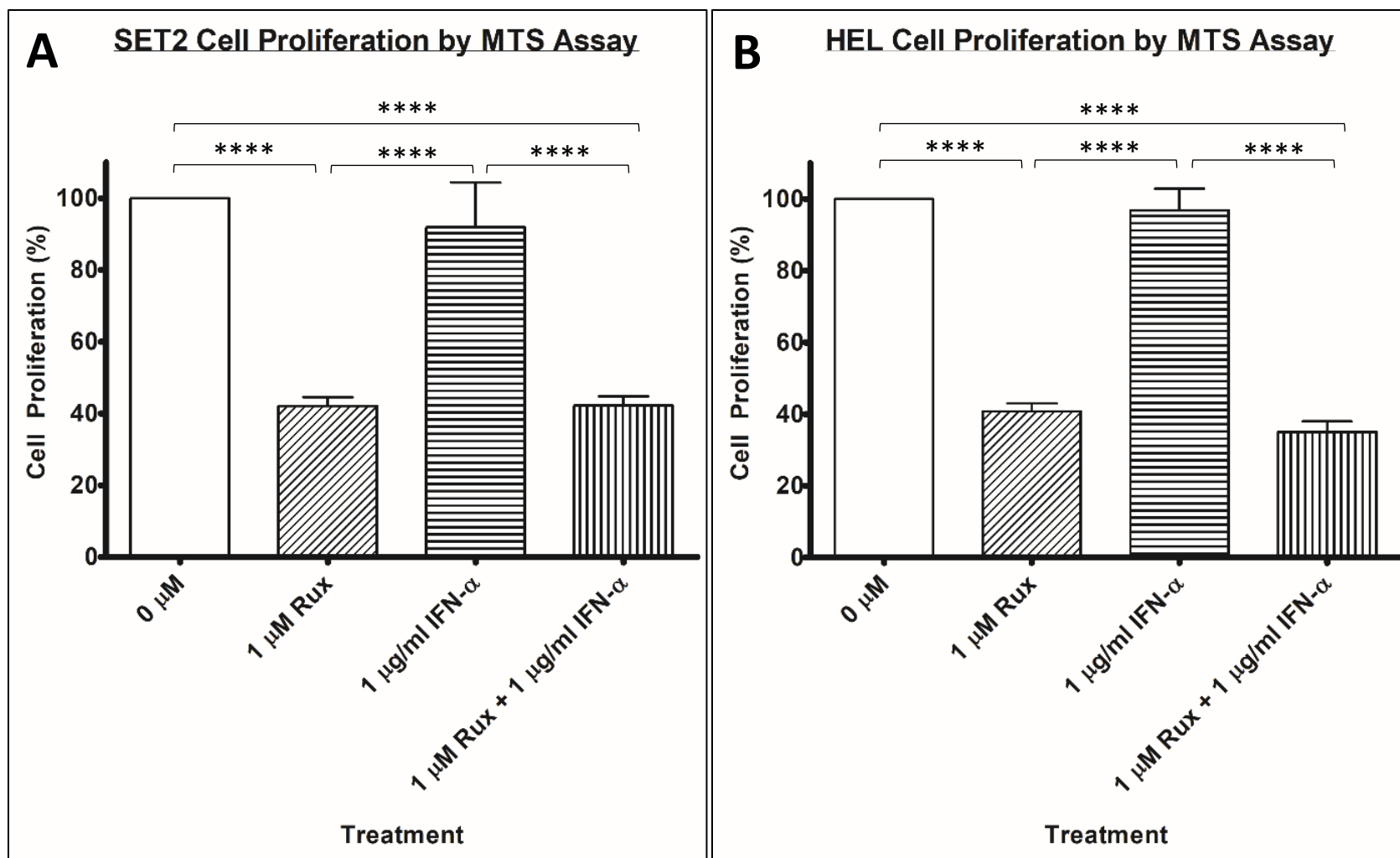


Figure 25: Cell proliferation in A) SET2 and B) HEL cells determined by MTS assay 72 hours post-treatment with 1 μM RUX, 1 $\mu\text{g/ml}$ IFN- α or a combination of the two drugs for 72 hours, normalised to untreated control cells ($n=3$ and $n=4$ respectively). Each bar represents the mean of the biological repeats with error bars indicating the standard deviation. One-way ANOVA: SET2 $p<0.0001$. HEL $p<0.0001$.

The results of the MTS assay in Figure 25 show the percentage proliferation of SET2 and HEL cells treated with 1 μ M RUX, 1 μ g/ml IFN- α , a combination of the two treatments or VC (DMSO), with results normalized to the VC. One-way ANOVA shows that for both cell lines, there is a significant difference in the proliferation of both SET2 and HEL cell lines when cultured with all treatment options ($p < 0.0001$). This experiment shows that cellular proliferation is negatively affected by RUX and IFN- α treatment in both SET2 and HEL cells after 72 hours. Tukey's multiple comparisons test was performed to compare between treatment groups. In SET2 cells, shown in Figure 25A, the proliferation of cells treated with RUX was significantly decreased compared to untreated cells 72 hours post-treatment ($p < 0.0001$). This effect was the same when comparing untreated cells to cells treated with a combination of RUX and IFN- α ($p < 0.0001$). There was also a significant difference in proliferation in cells treated with IFN- α as a single agent compared to both other treatments containing RUX (single and dual agent with IFN- α ($p < 0.0001$)). No significant difference was seen when comparing untreated cells to those treated with IFN- α alone. There was also no significant difference in response comparing RUX alone to the combination of RUX and IFN- α . This pattern was mirrored in HEL cells, as Figure 25B shows the MTS assay results of HEL cells treated with RUX and IFN- α or a combination of the two drugs.

3.7. The effect of 1 μ M ruxolitinib and 5 or 10 μ M fludarabine on proliferation

Fludarabine, a selective STAT1 inhibitor, was also used as a single and dual treatment to investigate the role of STAT1 in the pathogenesis of PV and ET. For growth curves involving a combination of RUX and FLU, cells were seeded at a density of 5×10^4 cells/ml. Cells were treated with 1 μ M RUX and/or 5 μ M or 10 μ M FLU and cultured at 37°C 5% CO₂ for a total of 72 hours. At 24-hour intervals, a single cell suspension was made and 50 μ L cell suspension was removed. Cells were counted, and Trypan Blue exclusion assay performed as per Section 2.1.3.

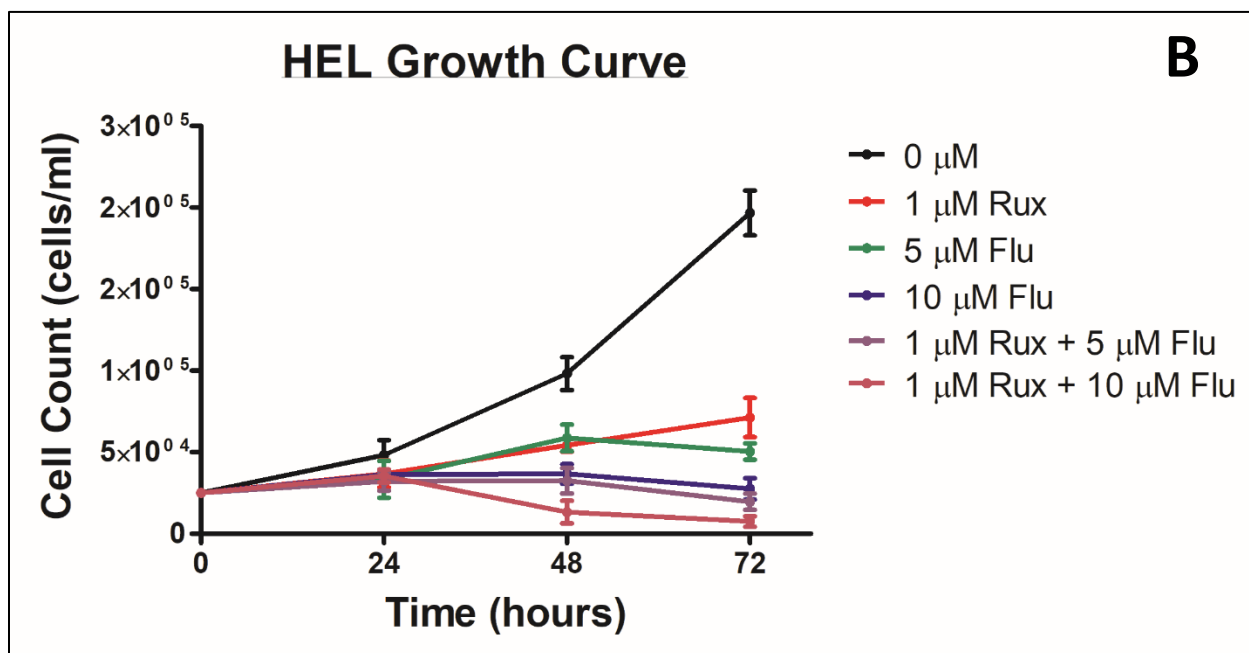
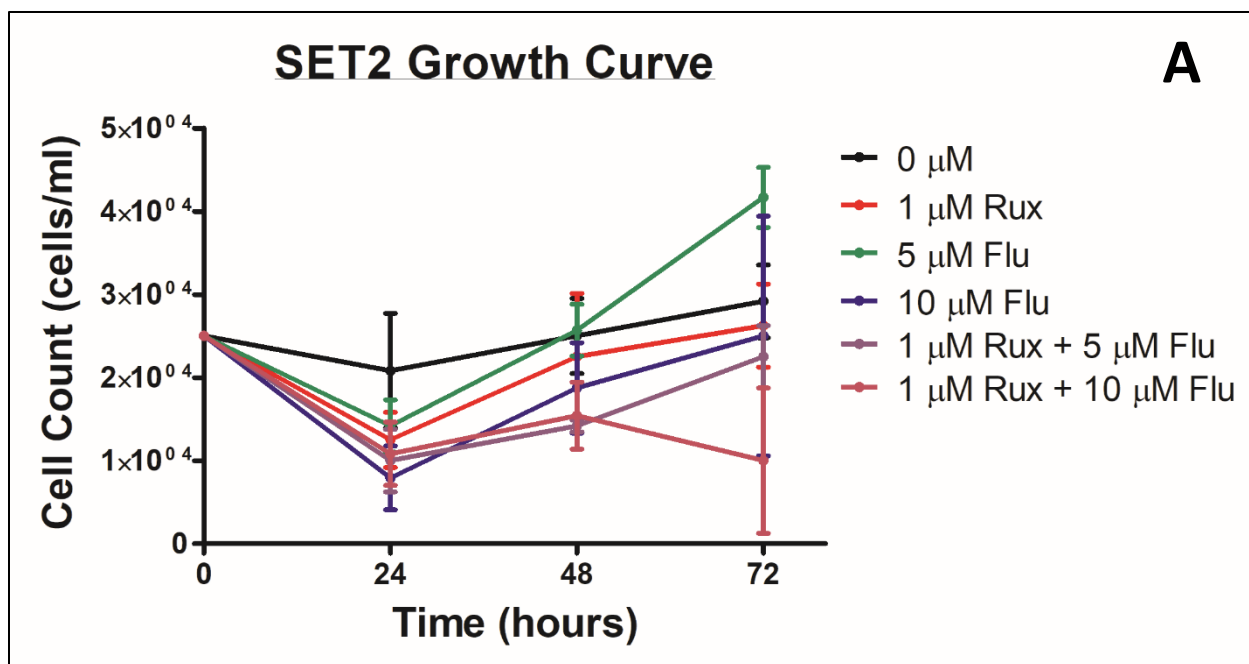


Figure 26: 72-hour growth curve of A) SET2 and B) HEL cells treated with 1 μM RUX, 5 or 10 μM FLU or a combination of the treatments, with cells counted every 24 hours (n=3). Each point represents the mean of the biological repeats with error bars indicating the standard deviation. Two-way ANOVA: SET2 $p < 0.0001$. HEL $p < 0.0001$.

Two-way ANOVA and Bonferroni multiple comparisons tests were performed to investigate the effect of different single and dual treatments on the proliferation of both SET2 and HEL cells over a period of 72

hours. In the SET2 cell line shown in Figure 26A, Bonferroni multiple comparisons test showed no significant difference in cellular proliferation when comparing untreated cells to any of the treatment options except when untreated cells were compared to cells under RUX + 10 μ M FLU treatment after 72 hours ($p < 0.01$). When comparing RUX alone to 5 μ M FLU, a significant increase in expression was seen after 72 hours ($p < 0.05$). No significance was seen at any time point when comparing RUX alone to 10 μ M FLU. With the combination therapies, a significant decrease in proliferation was only seen when comparing RUX alone to RUX + 10 μ M FLU ($p < 0.05$).

With respect to HEL cells in Figure 26B, Bonferroni comparisons following two-way ANOVA analysis shows that there was a significant decrease in cellular proliferation in HEL cells under any treatment condition after 48 and 72 hours ($p < 0.0001$ for both) but not at the 24-hour time point. Significance was achieved after 72 hours when comparing RUX and both concentrations of FLU (RUX vs 5 μ M FLU $p < 0.05$; RUX vs 10 μ M FLU $p < 0.0001$). When using a combination of RUX and FLU, significance was achieved at 48 hours and continued to 72 hours with both concentrations of FLU when compared to RUX treatment alone (RUX vs RUX + 5 μ M FLU: 48hr $p < 0.05$, 72hr $p < 0.0001$; RUX vs RUX + 10 μ M FLU: 48 and 72hr $p < 0.0001$).

During cell counts in the production of growth curves shown in Figure 20, cell viability was also assessed by Trypan Blue exclusion assay. The Trypan Blue assay data shown below in Figure 27 is associated with samples taken for growth curve analysis in Figure 26.

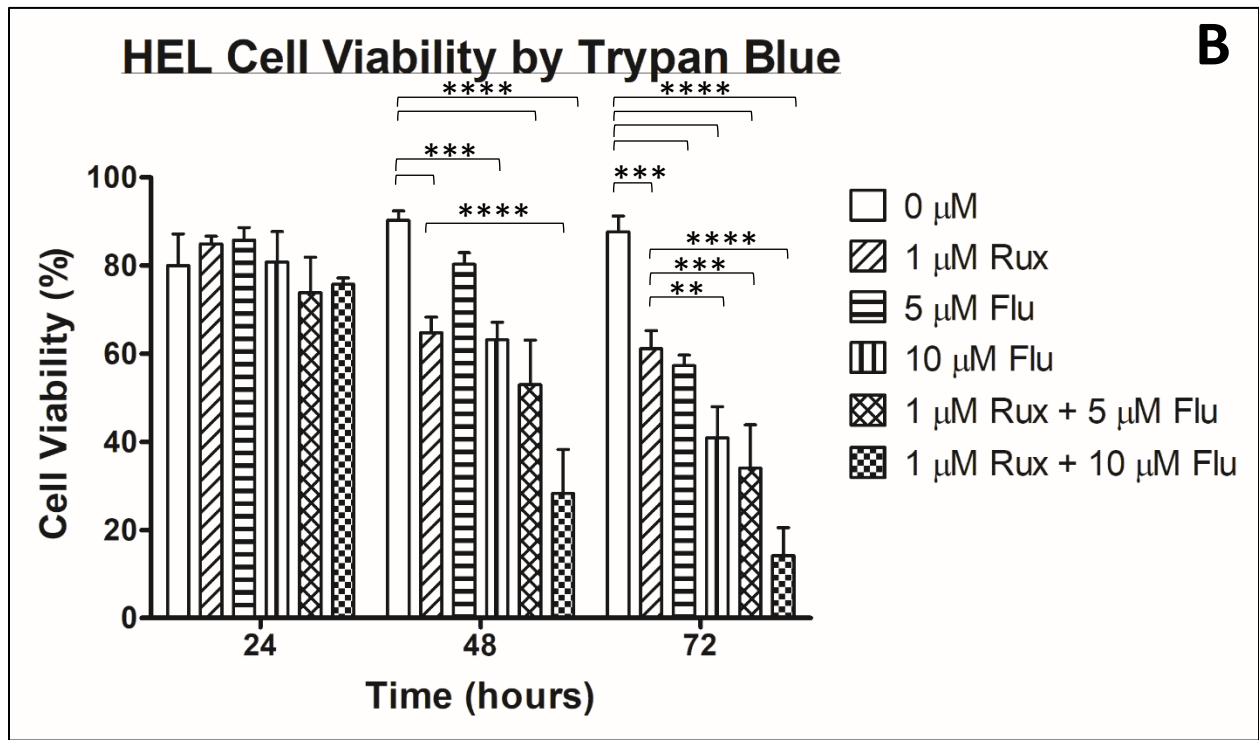
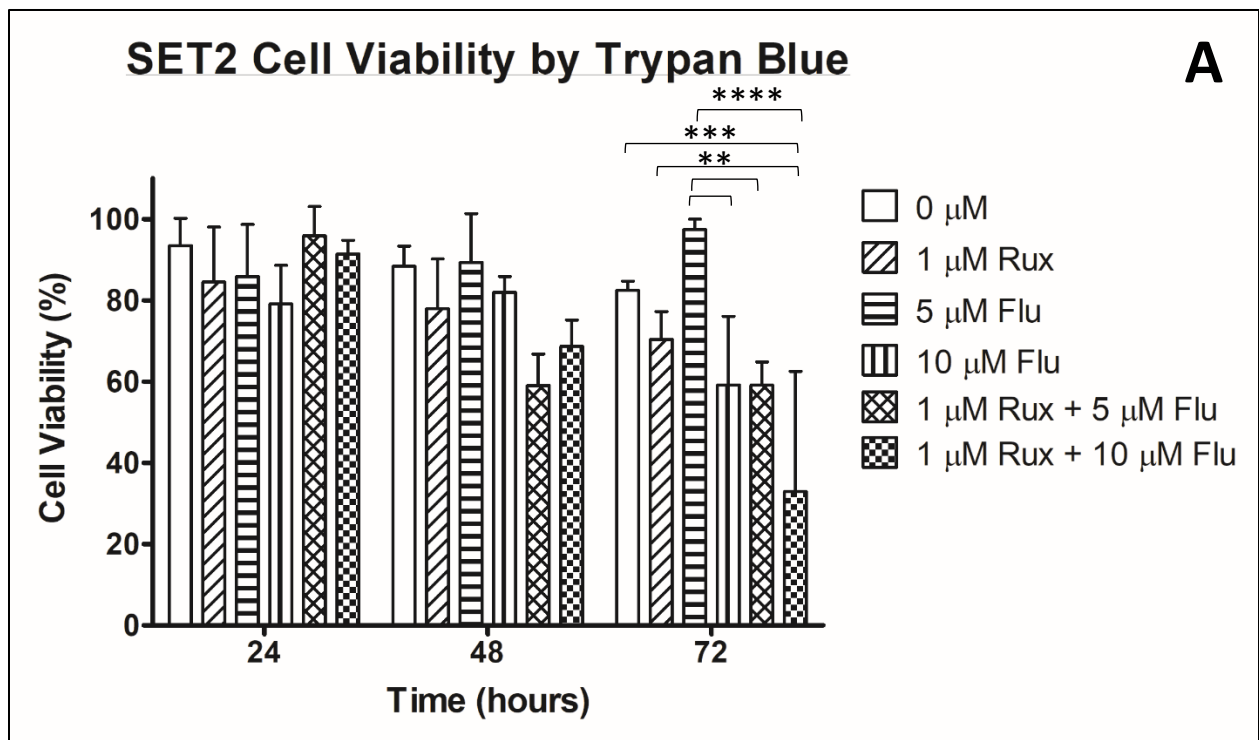


Figure 27: A) SET2 and B) HEL cells grown in the presence or absence of 1 μM RUX, 5 or 10 μM FLU or a combination of the treatments. Cell viability was assessed over 72 hours and determined by Trypan Blue every 24 hours (n=3). Each bar represents the mean of the biological repeats with error bars indicating the standard deviation. Two-way ANOVA: SET $p < 0.0001$. HEL $p < 0.0001$

As before in Figure 26, two-way ANOVA and Bonferroni multiple comparisons tests were performed on the treatments in each cell line. With respect to SET2 cells in Figure 27A, no significant decrease in cell viability was seen in any of the single treatments or in the combination treatment with a low FLU concentration. In the cells treated with RUX + 10 μ M FLU, a significant decrease in viability was only seen at the 72-hour time point ($p < 0.001$). When comparing treatments to RUX-treated cells, the only significant difference in cell viability was seen when compared against the RUX + 10 μ M FLU group after 72 hours ($p < 0.01$).

In the HEL cell line shown in Figure 27B, there was a significant decrease in cell viability in RUX-treated cells after 48 and 72 hours compared to untreated cells ($p < 0.001$ for both). Single agent treatment with 5 μ M FLU resulted in a significant drop in viability after 72 hours ($p < 0.0001$) and in the 10 μ M FLU treatment group, cell viability was decreased significantly after 48 hours and further decreased after 72 hours ($p < 0.001$ and $p < 0.0001$ respectively). Both dual treatment groups (RUX + 5 μ M FLU and RUX + 10 μ M FLU) resulted in the same significant decrease in cell viability after 48 and 72 hours when compared to the control group ($p < 0.0001$). In comparison to RUX treatment alone, no significant difference was seen when comparing cell viability within the 5 μ M FLU treatment group. At 10 μ M FLU, a significant difference in cell viability was seen after 72 hours ($p < 0.01$). Cell viability levels with the dual treatment of RUX + 5 μ M FLU was statistically significant at 72 hours when compared to RUX alone ($p < 0.001$). There was also a significant difference in viability by Trypan Blue assay when comparing RUX alone and RUX + 10 μ M FLU 48-hours and 72-hours post-treatment ($p < 0.0001$ for both).

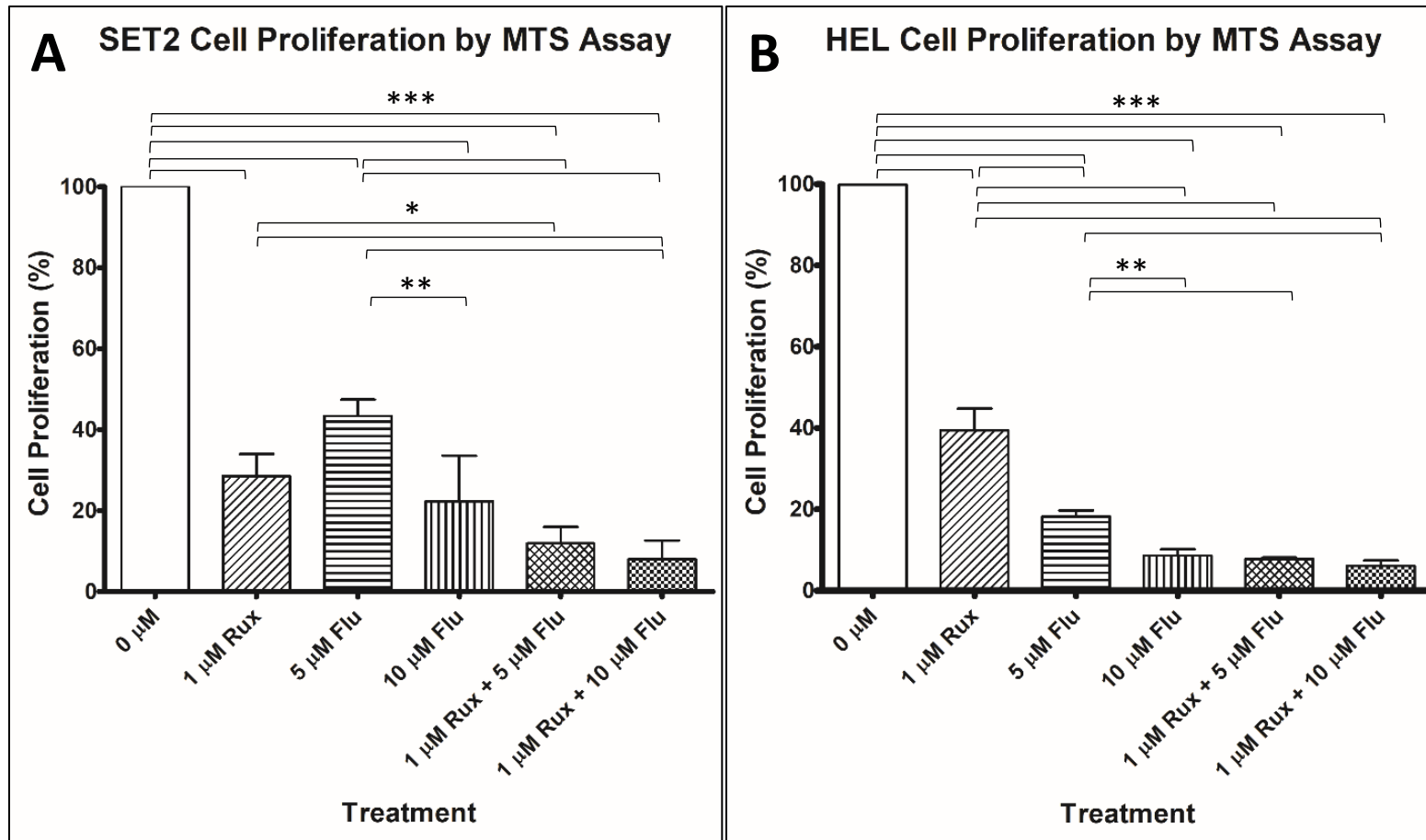


Figure 28: Cell proliferation in A) SET2 and B) HEL cells determined by MTS assay 072 hours post-treatment with 1 μM RUX, 1 $\mu\text{g/ml}$ IFN- α or a combination of the two drugs for 72 hours, normalised to untreated control cells ($n=3$ and $n=4$ respectively). Each bar represents the mean of the biological repeats with error bars indicating the standard deviation. One-way ANOVA: SET2 $p<0.0001$. HEL $p<0.0001$.

The MTS assay in Figure 28 shows that the percentage proliferation of SET2 (28A) and HEL (28B) cells treated with 1 μ M RUX, 5 μ M and 10 μ M FLU and a combination of the treatments or VC (DMSO), with results normalized to the VC. One-way ANOVA shows that there is a significant difference in cell viability with each of the single and combinations of treatments in both cell lines ($p < 0.0001$). Bonferroni post-hoc test shows that cellular proliferation is significantly negatively affected by RUX and FLU treatment in both SET2 and HEL cells after 72 hours, and a combination of the two treatments at both concentrations of FLU when compared to untreated cells ($p < 0.001$). There is a significant difference in the effect of ruxolitinib alone compared to the combination of RUX and 5 μ M FLU and with RUX and 10 μ M FLU in both cell lines ($p < 0.05$ for SET2 and $p < 0.01$ for HEL cells). There is also a significant difference in cellular viability when comparing 5 μ M and 10 μ M FLU as single agents, as 10 μ M performs better at decreasing viability in both cell lines ($p < 0.01$).

By looking at the trend of the two graphs, FLU treatment appears to have more of a negative affect HEL cells compared to SET2 cells, as RUX treatment alone has a greater effect on cell viability in SET2 cells whereas 5 μ M FLU treatment is more effective than RUX treatment alone in HEL cells.

4. Discussion

4.1. Ruxolitinib significantly decreases proliferation and viability of SET2 and HEL cells

Previous studies have shown that the introduction of ruxolitinib into cell culture medium decreases cellular proliferation in HEL and SET2 cells (Xu, et al., 2016) (Liang, et al., 2016) (Quintás-Cardama, et al., 2010) (Szymańska, et al., 2015) and this is also reflected in the ability of ruxolitinib to reduce the haematocrit and platelet count in PV and ET patients respectively (Verstovsek, et al., 2014) (Verstovsek, et al., 2014). The results in this report align with current literature and show a significant decrease in cell proliferation in both SET2 and HEL cells upon treatment with 1 μ M ruxolitinib after 72 hours. Considering growth curve patterns, no significant effect on proliferative capacity was seen after 24 hours in either cell line but significance was achieved at 48 hours and maintained at 72 hours. Furthermore, RUX is known to be cytotoxic to JAK-STAT activated cells (Wen, et al., 2015) (Quintás-Cardama, et al., 2010).

Cell viability upon treatment with ruxolitinib was investigated and shown to be significantly decreased over the 72-hour period, confirmed by Trypan Blue assay. Statistical analysis showed that HEL cell proliferation was significantly affected by RUX after 24 hours, whereas a significant reduction in viability in SET2 cells was observed after 48 hours, suggesting that the HEL cell line may be more sensitive to JAK2 inhibition by ruxolitinib. Previous researchers have demonstrated a dose-dependent reduction in viability in HEL cells treated with RUX 48-hours post treatment. The group report that HEL proliferation was not completely inhibited by RUX at 4 nM in comparison to BA/F3 cells expressing *JAK2V617F* that exhibited complete inhibition of proliferation, suggesting that proliferation in HEL cells is not entirely *JAK2V617F*-dependent (Quintás-Cardama, et al., 2010). It is worth noting that the study used a much lower concentration of RUX than the concentration used in this report which may explain the differences in results. In contrast, after 72 hours, both cell lines showed a similar level of reduced proliferative capability upon treatment with ruxolitinib, as determined by Trypan Blue exclusion assay. In relation to MTS results, both cell lines treated with ruxolitinib showed the same reduced proliferative capacity after 72 hours, with the same statistical significance. Overall, a similar pattern was described in both SET2 and HEL cells with respect to cell proliferation and viability, suggesting both cell types have a similar dependence on JAK2 signalling to maintain their hyperproliferative disease state.

In this study, both Trypan Blue exclusion assay and MTS assay were used to assess cell viability and proliferation. Trypan blue is a negatively-charged azo dye that is routinely used to assess cell viability by exclusively staining dead cells with a blue dye. Trypan blue exclusion method is one of the earliest and simplest viability assays and is based on the principle that live cells possess an intact cell membrane of which the impermeable dye cannot penetrate. In contrast, dead cells have a porous cell membrane and therefore the dye is able to enter the cytoplasm and stain the cells a blue colour which can be visualised under a microscope (Tran, et al., 2011). For the purpose of this study, use of trypan blue exclusion assay to determine cell viability was convenient as it can be performed using a light microscope and haemocytometer, so does not need particularly specialised equipment, and can determine cell viability quickly and accurately.

MTT assay is commonly used as colorimetric assay to investigate cell viability and proliferation based on detecting cellular metabolic activity. The assay uses a yellow tetrazolium salt known as 3-(4,5-dimethylthiazol-2-yl)-2,5-diphenyltetrazolium bromide (MTT), which is positively charged and readily penetrates cells. Viable cells with active metabolism use mitochondrial dehydrogenases to reduce MTT to an insoluble purple formazan product (Liu, et al., 1997). This product is then trapped inside living cells and can be detected by spectrophotometric analysis. The absorbance at 570nm correlates to the amount of formazan within the cells which subsequently correlates to the metabolic activity within the cells, as determined by the activity of mitochondrial dehydrogenase enzymes. Dead cells have lost their ability to convert MTT to a formazan and therefore, the purple colour formed is an indicator of the metabolic activity in viable cells.

In this study, the MTS assay is used. This assay was developed after the MTT assay but uses the same general principle of conversion of a tetrazolium salt into a coloured formazan product. Unlike MTT, MTS (3-(4,5-dimethylthiazol-2-yl)-5-(3-carboxymethoxyphenyl)-2-(4-sulfophenyl)-2*H*-tetrazolium inner salt) is negatively charged and does not readily penetrate cells. This compound uses an intermediate electron acceptor, known as PMF (phenazine methosulfate), to facilitate the reduction of the tetrazolium salt into the purple formazan product (Riss, et al., 2013). MTS assay is commonly described as a 'one-step MTT assay', as the reagent can be added straight to the cell culture without the intermittent steps required in the MTT assay needed to solubilize the formazan product. Furthermore, Alamar Blue uses

cellular metabolism to investigate cell proliferation and viability and is similar in principle to the MTT and MTS assays, in which a non-toxic permeable dye is reduced to a pink fluorescent product which is then measured by a spectrophotometer (Hamid, et al., 2004). Advantages of using Alamar Blue over MTS would be the nontoxic nature of the dye, allowing for the monitoring of cells in culture over time and providing somewhat more accurate information with respect to both proliferative rates and viability in comparison to MTT/MTS assays (O'Brien, et al., 2000).

One of the most informative viability assays available is named the live/dead assay, for its ability to present information relating to the number of viable cells, cellular morphology and cell distribution and metabolic activity. Instead of a traditional colour change assay as described above, this assay utilizes dual-colour fluorescent signals to discriminate between viable, proliferating cells and non-viable cells based on intracellular esterase activity (Periasamy, 2013). The two dyes present in this assay are calcein acetoxymethyl ester (AM) and ethidium homodimer. The former is a non-fluorescent based dye that enters both viable and non-viable cells by permeating the cell membrane. It is then hydrolysed by intracellular esterases and emits a green fluorescent signal, detectable under a fluorescent microscope which is used to determine the overall cell number and metabolic activity. In contrast, ethidium homodimer is a non-permeable red fluorescent dye that only penetrates compromised cell membranes, therefore entering non-viable cells and binding to DNA to emit red fluorescence (Maltaris, et al., 2006).

Cell enumeration and assessment of viability and proliferation in this study was important in providing information about drug efficacy and toxicity in cancerous cell lines. Through evaluation and consideration of different assays, it may have been more appropriate to use the Alamar Blue assay in this study for the investigation of cell viability over 72 hours in the long-term experiments, due to its non-toxicity in cell culture. Live/dead stain would have also been beneficial for investigating cell viability and proliferation over time and would provide a more accurate measure of viability and overall cell count due to its dual colour nature, however would require use of a fluorescent microscope and accompanying software, making this method more technically challenging but more reliable.

4.2. Ruxolitinib treatment decreases the expression of JAK2 downstream targets

Liquid-chromatography with tandem mass spectrometry (LC-MS/MS) is often the preferred method for identifying and quantifying proteins in a biological sample (Walther & Mann, 2010) (Han, et al., 2008). There are two main types of LC-MS/MS methods commonly used, both of which utilize proteolysis to convert proteins into peptides before separation by the LC system. The most widely used method is shotgun proteomics. In this method, the MS system is operated in a data-dependent acquisition method, where selected precursor ions from MS1 are selected for fragmentation in MS2 and the resulting fragment ion spectra is assigned to the corresponding peptide sequence by sequence database searching (Kapp & Schütz, 2007) (Nesvizhskii, 2007). The second method, targeted proteomics, uses the MS in a selected reaction monitoring (SRM) mode, whereby a sample is queried for the presence and quantity of a set of peptides specified prior to data acquisition. During this analysis, the acquisition of predefined pairs of precursor and product ion masses are analysed to detect peptides of interest in a biological sample as oppose to detecting targeted precursors, as in shotgun proteomics (Lange, et al., 2008). Both methods have their advantages and disadvantages: shotgun proteomics is superior for detecting the maximum number of proteins from one or few samples but suffers with irreproducible precursor ion selection and under-sampling with larger samples sets (Liu, et al., 2004) (Michalski, et al., 2011); targeted proteomics is more reproducible and accurate for the detection of sets of specific proteins in complex samples however this method cannot routinely quantify large peptide fractions (Kiyonami, et al., 2011).

To overcome these limitations, data independent acquisition (DIA) methods have been developed which consist of consecutive scans of fragment ion spectra of all precursors in predetermined isolation windows. SWATH-MS is a DIA method that combines targeted data extraction proteomics and the use of predetermined fragment ion spectra to obtain a complete record of all detectable peptide precursors in a sample. This data is then permanently stored and can be accessed at any time for cross-reference analysis. SWATH, as the name suggests, utilizes sequential isolation windows of a known m/z range of precursor ion spectra detected in MS1 and fractionates all peptides in that specific m/z window in MS2 (Ludwig, et al., 2018). SWATH-MS is now commonly used for the quantitative analysis of complex biological samples for the identification of potential biomarkers of disease (Guo, et al., 2018) (Harrison, et al., 2018) (Sajic, et al., 2018) (Miyachi, et al., 2018). In this report, SWATH-MS was used to investigate the effect of ruxolitinib on downstream JAK2 targets in SET2 cells, a cell line representative

of ET. The results show several pathways that were differentially affected by ruxolitinib treatment, with the most affected pathways being associated with cell cycle progression, apoptosis and post-translational processing.

Signal Transducers and Activators of Transcription (STATs)

STAT1 is thought to be the driver of the ET phenotype, with increased STAT1 activity promoting megakaryocytic development and producing an ET-like phenotype, whereas lower STAT1 activity produces a PV-like phenotype (Chen, et al., 2010) (Shi, et al., 2016) (Duek, et al., 2014). Aberrant signalling through STAT1 has also been documented in both acute and chronic leukaemia subtypes (Lin, et al., 2000) (Weber-Nordt, et al., 1996). It has been shown that decreases in STAT1 correlate with a defective ability to initiate an innate immune response to viral infection (Durbin, et al., 1996) and since JAK2 activity is strongly associated with STAT1 phosphorylation (Briscoe, et al., 1996), inhibition of STAT1 is likely to induce compromised immunity in ruxolitinib-treated patients. Gene expression via microarray study in CD34+ cells from MPN peripheral blood shows that *STAT1* is upregulated in *JAK2V617F*-positive ET patients (Čokić, et al., 2015). In this study, *STAT1* expression was significantly decreased at a transcriptional level with ruxolitinib treatment after 24 hours and was still significantly decreased 72 hours after treatment in SET2 cells. Q-RT-PCR results from pellets harvested within 6 hours post-RUX treatment show no initial significant change in *STAT1* expression, therefore indicating it may take over 6 hours for RUX to have a significant effect on *STAT1* expression in SET2 cells. More experimental repeats are needed to confirm these results and the time points extended to investigate at what time point ruxolitinib significantly decreases the mRNA expression of STAT1. STAT1 protein expression was also significantly decreased with 24-hour ruxolitinib treatment, as shown by Western Blot and mass spectrometry analysis. In addition, the expression of phosphorylated STAT1 protein was also shown to be significantly decreased in ruxolitinib-treated SET2 cells 24 hours after treatment. This finding supports previous literature where ruxolitinib was shown to inhibit the phosphorylation of STAT1 in SET2 cells (Nitulescu, et al., 2017). The decrease in STAT1 and phosphorylated STAT1 can be explained through direct inhibition of JAK2 via ruxolitinib, with inhibition of JAK2 leading to inactivation of JAK2 monomers and no recruitment of STAT proteins. In contrast, the protein expression of STAT1 and phosphorylated STAT1 in HEL cells was not significantly altered. This is most likely due to the large error bars, particularly in the case of phosphorylated STAT1 and more biological repeats may be necessary to indicate significance in this experiment.

MPN cells are known to rely on STAT3 and STAT5 for survival and proliferation (Yan, et al., 2012) (Friedbichler, et al., 2010) (Walz, et al., 2012) (Funakoshi-Tago, et al., 2010) (Jedidi, et al., 2009) (Röder, et al., 2001) (Kleppe, et al., 2015). Furthermore, STAT5 activation is necessary for tumourigenesis induced by the *JAK2V617F* and is a critical signalling molecule for *JAK2V617F* (Funakoshi-Tago, et al., 2010). Increased protein expression of STAT5 and phosphorylated STAT5 has previously been associated with *JAK2V617F*-positive cells (James, et al., 2005) however, studies have shown no significant difference in total STAT5 expression in *JAK2V617F*-positive cells upon treatment with ruxolitinib (Sahasrabudhe, et al., 2015) (Quintás-Cardama, et al., 2010) (Fridman, et al., 2007). In this report, the expression of both isomers of STAT5 were examined. STAT5A and STAT5B protein expression was not significantly altered in treated SET2 cells compared to untreated controls, as determined by Western Blot analysis. In previous studies, STAT5 phosphorylation was inhibited by ruxolitinib in *JAK2V617F* positive cells (Quintás-Cardama, et al., 2010) (Sahasrabudhe, et al., 2015) (Ma, et al., 2013) (Fridman, et al., 2007). To confirm the findings of these studies, phosphorylated STAT5 antibody must be examined via western blot analysis. With regards to mRNA expression, STAT5B was unaffected by ruxolitinib treatment in SET2 cells while STAT5A expression has not yet been determined.

There is additional evidence showing STAT3 expression is consistently upregulated in ET and this is independent of the presence of a *JAK2* mutation (Čokić, et al., 2015) (Hui, et al., 2013) (Senyuk, et al., 2009). STAT3 is activated through interferon and interleukin signals and is also activated through MAPK and c-src kinase (Silva, 2004) (Lim & Cao, 2006). Albeit a slight decrease in STAT3 protein expression was detected in SET2 cells treated with ruxolitinib after 24 hours, this change was not significant. STAT3 expression gradually increased over time in treated cells and was upregulated compared to untreated cells after 72 hours however RNA expression was never significantly affected by RUX. This could be explained by STAT3 activation occurring through an alternate pathway, such as MAPK or c-src. Alternatively, it has been reported that STAT3 has a role in tumour suppression, depending on the mutational background of tumour cells (de la Iglesia, et al., 2008) (Musteanu, et al., 2010). By this theory, an increase in transcription of STAT3 may be due to an increase in tumour suppression upon ruxolitinib treatment. Considering phosphorylation of STAT3, it is known that *JAK2*-specific inhibition blocks STAT3 phosphorylation (Colomiere, et al., 2009), so the expression of STAT3 protein may not alter significantly, but the phosphorylation status may change significantly under ruxolitinib treatment. The phosphorylation status of STAT3 should be investigated through western blot analysis.

Suppressors of Cytokine Signals (SOCS)

SOCS1 and SOCS3 are both powerful regulators of JAK2 signalling (Greenhalgh & Hilton, 2001) and directly inhibit the kinase activity of JAK2 through association with the JH1 catalytic domain (Ungureanu, et al., 2002) (Nicholson, et al., 1999). SOCS1 RNA expression is not significantly altered by ruxolitinib treatment in this study however, due to large error bars, PCR should be repeated. Purchase of a new primer set may be necessary due to melt curve analysis showing multiple curves (data not shown). SOCS3 is regulated by DNA methylation and was shown to be increased in MPN granulocytes independent of *JAK2* mutational status (Čokić, et al., 2015). SOCS3 mRNA expression was significantly downregulated after 24-hour treatment with ruxolitinib in SET2 cells. This is because SOCS3 is a known downstream target of JAK2/STAT signalling and constituent activation of JAK2/STAT through the *JAK2V617F* mutation activates SOCS3 through tyrosine phosphorylation. SOCS3 mRNA expression is significantly downregulated in response to 1 μ M ruxolitinib treatment due to decreased STAT signalling through JAK2 as a result of JAK2 inhibition. The decrease in STAT signalling subsequently decreases the transcription of the SOCS negative regulators of JAK-STAT signalling.

Cell Cycle Progression

P53 is a tumour suppressor protein involved in cell cycle regulation through growth arrest, DNA repair and apoptosis (Harris, 1996). PSME3 is a negative regulator of p53 and functions by promoting its nuclear export and targets cell cycle inhibitors for degradation in a ubiquitin-independent manner (Chen, et al., 2007). If the expression of PSME3 is downregulated, as it is in RUX-treated SET2 cells, the intracellular levels of p53 and other cell cycle inhibitors will increase, halting cell cycle progression. Conversely, cytoskeleton-associated protein 2 (CKAP2) is a p53 target gene which is known to enhance p53 activity (Tsuchihara, et al., 2005) and this protein is downregulated in SET2 cells treated with RUX, leading to the attenuation of p53. PLK1 is essential during the M-phase of the cell cycle, as it regulates centrosome maturation and segregation, and spindle assembly and orientation (van de Weerd & Medema, 2006). CDK2 is required for the transition between G1/S while M-phase inducer phosphatase 2 (MPIP2) allows G2/M progression (Elledge, 1996) (Sur & Agrawal, 2016). Both proteins are significantly decreased upon RUX treatment, as determined by mass spectrometry analysis, providing more evidence of cell cycle inhibition under RUX treatment.

Interferon Regulatory Factor 1, abbreviated to IRF1, is a transcription factor able to activate the expression of various cytokines such as IFN- β (Miyamoto, et al., 1988). Deletion of IRF-1 has been associated with the development of both solid tumours and leukaemia subtypes (Willman, et al., 1993) (Nozawa, et al., 1998) and has thus been associated with tumour suppressive functions. In addition, it has been reported that IRF1 assists in the activation of p53 cell cycle regulator by recruitment of p300 (Dornan, et al., 2004). Results of this report show that IRF1 mRNA expression is significantly upregulated in response to ruxolitinib in SET2 cells after 24 hours, suggesting that RUX treatment negatively affects the progression of the cell cycle and thus inhibits proliferation of SET2 cells. This is supported by previous growth curve results and examining cellular viability and proliferation. Conversely, DDX3X is a multifunctional ATP-dependent RNA helicase and is also involved in gene transcription, mRNA splicing, maturation and export (Leitão, et al., 2015) (Merz, et al., 2006) (Lai, et al., 2008). Increased expression of DDX3X has been associated with poor prognosis in both colorectal and breast carcinomas (Heerma van Voss, et al., 2017). DDX3X transcription was not significantly affected by treatment with ruxolitinib. ISG15 is a ubiquitin-like modifier known to have antiviral activity (Morales & Lenschow, 2013). Upregulation of ISG15 has been shown to decrease levels of oncogenic c-Myc which plays a role in cell cycle progression (Yoo, et al., 2018). ISG15 is upregulated, but not significantly, in RUX-treated SET2 cells, therefore aiding cell cycle arrest.

Heat Shock Proteins and other Molecular Chaperones

With respect to chaperone proteins, CALR is a ubiquitous calcium-binding protein chaperone that is responsible for the quality control of N-glycosylated protein and in calcium storage in the ER (Michalak, et al., 2009). Mutations within CALR are the second most prevalent mutation in ET patients following the *JAK2V617F* mutation, and have been identified in 15-25% of ET patients (Imai, et al., 2017) (Nangalia, et al., 2013) (Rotunno, et al., 2014). It has been previously shown that CALR mutants activate the thrombopoietin receptor (MPL) after binding to its N-glycosylated residues in the ER (Chachoua, et al., 2016) (Marty, et al., 2016). Moreover, MPL mutations have been identified in 3% of ET patients (Pardanani, et al., 2006), suggesting this chaperone may be of significance in ET. Expression of the CALR gene in treated cells increased over time up to 72 hours post-treatment. At 72 hours, expression of CALR had normalized to the levels observed in untreated cells but was not significantly affected by ruxolitinib treatment.

Heat shock proteins (HSP) are highly-conserved molecular chaperones that assist in the covalent folding or unfolding of newly synthesized polypeptides, the assembly/disassembly of macromolecular structures and transport of proteins across cellular membranes (Garrido, et al., 2001). Membrane-bound or extracellular HSPs are known to regulate apoptosis pathways (Gupta, et al., 2010) while intracellular HSPs show increased expression in the presence of cellular stress such as hypoxia, temperature changes, inflammation and infection (Jindal, 1996). HSPs are upregulated in a multitude of human cancers and are associated with increased proliferation and evasion of apoptosis (Lanneau, et al., 2008). Heat shock proteins are named according to their molecular weight, with HSP70 and HSP90 both being required for the differentiation of monocytes (Didelot, et al., 2008) (Jego, et al., 2014).

HSP90 chaperones are ATP-dependent and are involved in the activation and stabilisation of proteins in cellular signalling pathways, such as JAK2, and regulates the progression of the cell cycle (Reed, 1999) (Burrows, et al., 2004). HSP90 is a key signalling molecule in malignancies (Pearl, et al., 2008) and has been shown to be upregulated in AML and in several solid tumours (Lancet, et al., 2010) (Rajan, et al., 2011) (de Bono, et al., 2008). It has been shown that *JAK2V617F*-positive MPNs are dependent on HSP90, with enough evidence to develop HSP90 inhibitors for the treatment of *JAK2V617F*+ MPNs (Marubayashi, et al., 2010) (Fiskus, et al., 2011). In this study, HSP90 was downregulated in SET2 cells in response to 1 μ M ruxolitinib at a transcriptional level at 24, 48 and 72 hours, as determined by Q-RT-PCR. This decreased expression was not significant, possibly due to large statistical error. Co-chaperones of HSP90 were shown to be downregulated in response to RUX, as detected by mass spectrometry. CHRD1, DNJC7 and TTI1 were all shown to be downregulated after 24-hour RUX treatment.

HSP70 is an anti-apoptotic chaperone that regulates the function of NF κ B. HSP70 is essential for the differentiation of primary erythroblasts (Ribeil, et al., 2007) has been shown to have a significant role in the pathogenesis of PV (Gallardo, et al., 2013). CML patients also show elevated levels of HSP70 (Ray, et al., 2004). In this study, HSP70 protein expression was significantly downregulated upon introduction of ruxolitinib into SET2 cell culture medium, as determined by both Western Blot and mass spectrometry, indicating a decrease in the cell's anti-apoptotic mechanism required to prolong cell survival. HSPA8 is a constitutively expressed chaperone protein that forms part of the spliceosome and is required for the activation of a pre-mRNA splicing complex. HSPA8 is a member of the HSP70 family and is significantly

overexpressed in breast and endometrial cancer and is currently being investigated as a potential biomarker of disease (Hou, et al., 2016) (Shan, et al., 2016). CML patients also express high levels of HSPA8 and the upregulation of HSPA8 was partially dependent on STAT5-dependent transcriptional activation and results in cell cycle progression (José-Enériz, et al., 2008). In addition, HSPA5, also known as binding immunoglobulin protein (BiP), is also a highly-conserved member of the HSP70 chaperone protein family and is involved in the unfolded protein response (UPR), ER-associated degradation and calcium homeostasis (Wang, et al., 2017) and its overexpression has been noted in advanced breast cancer (Chen, et al., 2015) and even been the target of a new melanoma treatment (Cerezo & Rocchi, 2017). mRNA expression of both HSPA8 and HSPA5B was downregulated, but not significantly, in SET2 cells treated with 1 μ M ruxolitinib for 24 hours, suggesting that RUX affects post-transcriptional and post-translational patterns in cells through interfering with the spliceosome function and degradation of misfolded proteins.

Antigen Presentation

The progression of PV and ET to MF has been correlated with chronic inflammation (Hasselbalch, 2012) and an imbalance in the regulation of immune and inflammatory genes (Skov, et al., 2012) (Skov, et al., 2012). This is thought to impair the immune surveillance with respect to tumour cells and aid in the evasion of tumour cells from immune attack (Hasselbalch, 2012). It has been shown that defects in the expression of HLA class I on clonal myeloid cells may contribute to the aberrant tumour immune surveillance (Brodsky & Guagliardi, 1991) (Garrido, et al., 1997) (Garcia-Lora, et al., 2003) (Bukur, et al., 2012) (Seliger, 2012). Downregulation of antigen presentation genes may lead to defects in T-cell recognition of foreign antigens and therefore a dampened immune response to malignant cells. The dysregulation of HLA and associated genes within malignant cells has been previously investigated in many different tumour types and MPNs and reports show a significant downregulation of several HLA-related genes in MPN patients (Ferris, et al., 2006) (Meidenbauer, et al., 2004) (Seliger, et al., 2002) (Garrido, et al., 1997) (Pellagatti, et al., 2010) (Skov, et al., 2013). In addition, significant downregulation of members of the antigen presentation pathway have been demonstrated in CML progenitor cells, with antigen presentation pathway being the top downregulated pathway in CML (Tarafdar, et al., 2017).

MHC Class II downregulation has been associated with diffuse large B-cell lymphoma and is related to poor patient survival (Rimsza, et al., 2004). HLA-A was shown to be significantly downregulated in ET patients (Skov, et al., 2013). In this report, HLA-A was significantly upregulated in response to ruxolitinib treatment in the ET-representative SET2 cell line, suggesting an increased expression in antigen presentation genes. TAP-1 facilitates the transport of processed peptides to the ER (Nijenhuis & Hämmerling, 1996) before peptides associate with the MHC class I heavy chain and β 2-microglobulin to form a functional MCH complex on the cell surface (Satler & Creswell, 1986). Cells with TAP mutations have decreased MHC class I expression and defective antigen presentation (Townsend, et al., 1989). Downregulation of TAP has been noted in various malignancies (Ren, et al., 2014) (Vambutas, et al., 2000) (Ling, et al., 2017) while TAP-1 has also been shown to be significantly downregulated in MF patients (Skov, et al., 2013). The results show that TAP-1 was significantly decreased in ruxolitinib-treated SET2 cells. This may explain why patients treated with ruxolitinib experience an increased risk of opportunistic infections as a decrease in antigen presentation in response to RUX may lead to defective immune response to pathogens, despite an increase in HLA-A expression.

Regulation of Apoptosis

Apoptosis signalling in response to DNA damage was also significantly affected by RUX. This has been previously shown in a number of haematological cell lines, analysed by flow cytometry using Annexin V (Civallero, et al., 2017). This study also confirms the induction of caspase activation with ruxolitinib, which aligns with the findings in this report which show an upregulation of caspases under RUX treatment. In this report, BCL2-like protein 1 (B2CL1) and Ankyrin repeat and KH domain-containing protein 1 (ANKH1) are both significantly downregulated in response to RUX, as determined by mass spectrometry. Isoform 2 of ANKH1 has been shown to have anti-apoptotic effects by regulating caspase activation (Miles, et al., 2005) and its downregulation in RUX-treated SET2 cells suggests that RUX induces apoptosis. Similarly, the downregulation of B2CL1, which functions to inhibit caspase activation (Chao & Korsmeyer, 1988) also supports the role of RUX as an apoptosis-inducing compound. Other proteins involved in apoptosis inhibition were also significantly downregulated by SWATH-MS analysis, including DNAJA1 and PSME3. In contrast, some activators of apoptosis were also significantly downregulated in RUX-treated SET2 cells, such as DDX5, TPX2, NDK3 and FAK1. All these proteins contribute to the initiation and regulation of apoptosis but were seen to be downregulated in RUX-treated cells. This finding is controversial and more research into the function of these genes in SET2

cells may be required. Conversely, proteins involved in promoting apoptosis were shown to be significantly upregulated upon RUX treatment, such as DDND4, DNS2A, PML, F175B, IR3IPM, RN5A and HIP1. An increase in pro-apoptotic gene expression would be expected, as previous studies have confirmed the pro-apoptotic activity of RUX in JAK2-positive cell lines (Szymańska, et al., 2015).

MCL1 is an anti-apoptotic gene which is activated by STAT3 (Guo, et al., 2015). It has been shown that *JAK2V617F* increases MCL1 activation and inhibition of JAK2 by ruxolitinib reduces MCL1 expression in SET2 cells (Guo, et al., 2015). Since there was no significant change in the RNA expression of STAT3, it would be expected that the expression of MCL1 is also unaffected by RUX treatment. In this report, MCL1 expression was significantly upregulated in response to ruxolitinib. This result is contrary to current literature however, it has been previously reported that alternative splicing of the MCL1 gene results in two transcripts with opposing function. The longer transcript has been shown to have anti-apoptotic functions while the shorter transcript has pro-apoptotic properties (Bae, et al., 2000). Since it cannot be discerned which transcript is upregulated, the consequence of MCL1 upregulation in response to RUX cannot be fully elucidated.

As mentioned previously, HEL cell samples were not analysed by SWATH-MS due to problems with cell viability. Experiments were only conducted on cells with a viability of 90% or greater and during culture of HEL cells, viability when expanding cell numbers for proteomic and translational analysis never exceeded 90% so cells were not harvested for this purpose. In addition, the added time constraints for this study meant that this cell line could not be analysed to the same degree as the SET2 cell line. Furthermore, data on the differential changes in protein and RNA expression in SET2 and HEL cells 72-hours post-treatment would have complimented the analysis of growth curves and cell viability at these time points. Reflecting on these weaknesses within the study, the collection of both protein and RNA expression data by mass spectrometry and Q-RT-PCR for the both cell lines at multiple time points would have been exceptionally useful for a more extensive investigation into the molecular and genetic pathogenesis of each disease phenotype and the differentiating elements that define each of these hyperproliferative MPNs. Given more time, this analysis would have been performed and a more complete comparison between the effects of each treatment on the different phenotypes would have been conducted.

4.3. IFN- α and ruxolitinib dual treatment shows little synergy compared to ruxolitinib alone

The ability of IFN- α to reduce clonal burden and successfully initiate haematological and molecular responses makes this therapy attractive for combinational treatment in association with ruxolitinib. IFN- α treatment alone shows little effect on cell proliferation and viability in SET2 and HEL cells. This may be due to the absence of other immune cells in culture as one role of IFN- α is to stimulate immune cells which have a direct apoptotic effect on transformed cells, such as NK and T-cells. Still, a slight decrease in proliferation and viability is observed which could be explained by IFN- α 's intracellular pro-apoptotic mechanism, as mentioned previously. The combination of RUX and IFN- α has shown little synergy compared to RUX treatment alone, with respect to decreasing proliferation and viability of both MPN representative cell lines. Growth curves, Trypan Blue exclusion assay and MTS assay all show a similar pattern with respect to both RUX and IFN- α therapy, indicating that both cell types behave in a similar manner in response to JAK2 inhibition and IFN- α treatment.

4.4. Combination of fludarabine and ruxolitinib is more effective than ruxolitinib alone

The use of fludarabine in the treatment of MPNs has mainly been restricted to conditioning regimens in preparation for stem cell transplantation in myelofibrosis patients (idiopathic or post-PV or -ET MF) (Kerbaui, et al., 2007) (Slot, et al., 2015) (Ito, et al., 2012). This has been effective for decreasing splenomegaly and increasing success of graft transplantation. There is a very small pool of literature relating the use of fludarabine in PV and ET treatment. One small study noted its use in post-PV AML patients, comparing the use of fludarabine to cytarabine and cytarabine-plus-idarubicin. Results indicated all induction chemotherapies had no superiority to palliative care options and stem cell transplantation conferred the best survival outcome (Passamonti, et al., 2005).

This report illustrates that fludarabine is able to decrease cell viability to less than 50% over a 72-hour period (when used at 10 μ M). This finding compliments previous research that shows a decrease in cell viability of leukaemic cells with the use of fludarabine treatment (Opydo-Chanek, et al., 2012) (Bellosillo, et al., 1999). In these studies, 1 μ M fludarabine was able to decrease cell viability to between 60 and 10% over 48 hours, depending on the cell line treated. No studies to date have investigated the effects of a combination of ruxolitinib and fludarabine on the proliferation and viability of MPN cells. In this study, the combination of ruxolitinib and fludarabine was able to further decrease the viability of HEL

cells from 61% with ruxolitinib alone to 34% and 14% with the combination treatments at both 5 and 10 μM fludarabine respectively, 72-hours post-treatment. A similar pattern was seen in SET2 cells (1 μM RUX: 70%; 1 μM RUX + 5 μM FLU: 59%; 1 μM RUX + 10 μM FLU: 33%).

Proliferation is also negatively affected by a combination of ruxolitinib and fludarabine in both cell lines, with the greatest decrease in cellular proliferation seen after 72 hours in the combination group containing of 1 μM ruxolitinib and 10 μM fludarabine. MTS assay results show that HEL cell proliferation was more negatively affected by 10 μM fludarabine alone than 1 μM ruxolitinib alone, demonstrating that fludarabine may have a greater effect on HEL cells and that STAT1 inhibition in this cell line has a greater effect on cell survival. A similar pattern was observed when examining the effect of a combination of ruxolitinib and fludarabine on the proliferation of SET2 and HEL cells, again with a slightly greater decrease in proliferation seen in HEL cells (SET2: 1 μM RUX + 5 μM FLU: 11.9%. 1 μM RUX + 10 μM FLU: 8.0%. HEL: 1 μM RUX + 5 μM FLU: 7.9%. 1 μM RUX + 10 μM FLU: 6.2%). In the HEL growth curve, cellular proliferation is most negatively affected by a combination of ruxolitinib and 10 μM fludarabine after 72 hours, which correlates with the results of the MTS assay. Growth curve analysis for the SET2 cell line could be considered inaccurate due to the large error bars seen in all treatment groups. More experimental repeats are required to gain an accurate insight into the proliferative capacity of SET2 cells treated with a combination of ruxolitinib and fludarabine.

With respect to both cell proliferation and viability, fludarabine appears to affect HEL cells more than SET2 cells, indicating a preference of the combination therapy in the treatment of PV rather than ET. Nevertheless, it is important to note the large variation between experiments in the SET2 growth curve and Trypan Blue viability graphs may distort the experimental results of treating SET2 cells with a combination of ruxolitinib and fludarabine.

5. Conclusion

With respect to the hypotheses stated at the beginning of this report, the results show that ruxolitinib significantly affected the proliferative rate and viability of both SET2 and HEL cells over 72 hours as shown by growth curve analysis, Trypan Blue exclusion assay and MTS assays. Considering these results, the expression of a number of downstream JAK2 targets were also shown to be downregulated by ruxolitinib treatment in SET2 cells 24 hours post-treatment. The expression of downstream targets showed mixed results, with some known downstream targets, such as STAT5 and HSP90 shown to be not significantly altered by the presence of ruxolitinib in SET2 cells, whereas STAT1, SOCS3 and HSP70 are all significantly downregulated in response to ruxolitinib. In this case, the first null hypothesis, stating that ruxolitinib will have no effect on proliferation, viability and expression of downstream JAK2 targets, cannot be rejected completely due to the varying results with respect to expression of downstream targets. In addition, the analysis of JAK2/STAT targets was only investigated in SET2 cells and a more complete analysis, including examination of target expression in HEL cells, needs to be performed for this null hypothesis to be confidently rejected.

The second null hypothesis states that ruxolitinib in combination with IFN- α or fludarabine will have no effect on SET2 and HEL cells and changes with respect to cell proliferation and viability will not be superior to ruxolitinib treatment alone. This study found that, although ruxolitinib and the combination of ruxolitinib and IFN- α did significantly decrease proliferation and viability of SET2 and HEL cells, there was no significant difference in the extent to which this decrease was seen. Therefore, there was no synergistic effect on decreasing cell proliferation and viability when combining ruxolitinib with IFN- α . There is a failure to reject the null hypothesis in the case of ruxolitinib and IFN- α .

In contrast, there was a significant difference in response of SET2 and HEL cells to ruxolitinib alone compared to ruxolitinib combined with 10 μ M fludarabine with respect to cell proliferation in both cell lines after 72 hours. The same pattern was also seen with respect to cell viability as assessed by Trypan Blue assay, suggesting a synergistic effect is seen when ruxolitinib is combined with fludarabine. With respect to MTS assay, there was a significant difference in proliferative capacity of both cell lines under ruxolitinib treatment alone compared to ruxolitinib in combination with both 5 μ M and 10 μ M fludarabine. Reflecting on the results when combining ruxolitinib with fludarabine, the second null hypothesis can be rejected on the basis that a statistically significant difference was observed in both

cell lines when comparing both viability and proliferation of cells treated with ruxolitinib alone and in combination with fludarabine over a 72-hour period.

The final null hypothesis states that there will be no difference in responses between the two cell lines when investigating the effect of ruxolitinib or a combination of ruxolitinib and IFN- α or fludarabine on cell proliferation and viability. With respect to the effects of ruxolitinib treatment as a single agent on both cell lines, there seems to be no difference in response. Two-way ANOVA shows that both cell lines are significantly affected by 1 μ M ruxolitinib treatment however the p-value is smaller in SET2 cells ($p < 0.0001$) compared to HEL cells ($p = 0.0135$). In contrast, by Trypan Blue assay, HEL cells seem to be more sensitive to ruxolitinib as a significant decrease in cell viability is observed at 24 hours in HEL cells compared to significance reached at 48 hours in SET2 cells. Considering MTS assay, both cell lines show the same decrease in viability at 72 hours post-ruxolitinib treatment. In this case, there is a failure to reject the null hypothesis as both cell lines appear to respond in the same way in the presence of ruxolitinib alone.

In the case of ruxolitinib combined with IFN- α , two-way ANOVA of growth curve analysis shows HEL cells are significantly affected by ruxolitinib alone, IFN- α alone and the combination of the two at 48 and 72 hours. In contrast, the proliferation of the SET2 cell line is only significantly affected by ruxolitinib and the combination treatment after 72 hours. This difference between responses in each cell line could be due to the large error bars between biological repeats in the SET2 cell line. With respect to cell viability, both cell lines are significantly altered by the treatments, however the p-value for HEL cells is still smaller than the p-value for SET2 cells using two-way ANOVA. Since the growth curve analysis and Trypan Blue assay were performed on the same biological samples, the samples may still be providing a lot of variance as opposed to the treatment being the reasoning behind the differences seen in response between both cell lines. With respect to the MTS assay, the proliferation of both cell lines is decreased to the same extent, therefore the responses of each disease phenotype are similar and indistinguishable. Repeated analysis of SET2 cells for growth curve analysis and Trypan Blue exclusion assay should be performed to decrease variability between biological repeats and obtain a more accurate result of the effects of ruxolitinib on each cell line. In this case, the null hypothesis cannot be confidently rejected due to the presence of large error bars in the SET2 cell line.

Observing growth curve analysis of the combination of ruxolitinib and fludarabine, SET2 cell proliferation is only significantly affected after 72 hours by ruxolitinib and 10 μ M fludarabine. Conversely, HEL cells are affected by all treatment conditions after 48 and 72 hours. Trypan blue exclusion assay gives a similar pattern in SET2 cells as proliferation by growth curve analysis, with viability only being significantly affected after 72 hours and only by a combination of ruxolitinib and fludarabine. HEL cells also show a similar pattern to the growth curve analysis, as viability is significantly decreased in all treatments at 48 and 72 hours. As with the combination experiments with ruxolitinib and IFN- α , the large error bars in the SET2 cell line for growth curve analysis and Trypan Blue exclusion assay could explain the difference in response observed between SET2 and HEL cell lines and phenotypic differences may not actually be the reason behind the difference in responses. The SET2 growth curve and Trypan blue experiments should be repeated to decrease the variability between biological repeats. Only then can the potential difference in response of both cell lines to ruxolitinib and fludarabine be elucidated. On the contrary, the MTS assay illustrates that HEL cells may be more sensitive to the presence of fludarabine than SET2 cells, as fludarabine alone at 5 μ M decreases the proliferation of HEL cells more than 1 μ M ruxolitinib alone, whereas in SET2 cells, treatment with 1 μ M ruxolitinib decreases the proliferation more than 5 μ M fludarabine. Furthermore, fludarabine treatment at 5 and 10 μ M in HEL cells decreases the proliferation greater than fludarabine treatment in SET2 cells at 5 and 10 μ M.

JAK2 inhibition by ruxolitinib has shown great clinical potential for the alleviation of disease-related symptoms in Philadelphia-chromosome-negative MPNs and use of JAK2 inhibitors are able to support research into disease aetiology, drug discovery and personalized medicine. Ruxolitinib has shown great ability to decrease the proliferation and viability of PV and ET-representative cell lines *in vitro*, with no substantial difference in response to JAK2 inhibition between the two diseases. SWATH-MS analysis identified several proteins and associated signalling pathways significantly downregulated in response to JAK2 inhibition in ET however this work should be extended to include the PV-associated HEL cell line for a more comprehensive analysis of JAK2 signalling in each phenotype. Further conformational studies by Q-PCR and Western Blot highlighted potential novel therapeutic targets for the treatment of PV and ET. Dual treatment of SET2 and HEL cells with IFN- α and ruxolitinib does not seem to have a synergistic effect on decreasing cell proliferation and viability in SET2 and HEL cells, however a combination of ruxolitinib and 10 μ M fludarabine seems to have a greater effect on inhibiting cellular proliferation and decreasing cell viability in both cell lines compared to ruxolitinib alone. More experimental repeats may

be needed for growth curve analysis and Trypan Blue exclusion assay for the combination experiments including both IFN- α and fludarabine, as the biological repeats in this report show great variability in results. A more detailed investigation into the expression of proliferative genes and proteins is required to gain a more complete insight into whether IFN α or fludarabine therapy is a suitable complimentary agent for the treatment of PV and ET. Transcriptional and translational analysis by Q-RT-PCR and Western Blots should be performed to continue to investigate the changes in expression of anti-apoptotic, proliferative and antigen presentation genes in IFN- α - and fludarabine-supplemented treatments and results compared to ruxolitinib treatment alone, in hopes to ascertain the most effective treatment combination for Ph-MPNs that overcome some of limitations of current treatments.

In conclusion, ruxolitinib at 1 μ M concentration has shown great ability in decreasing the proliferation and viability of SET2 and HEL cells, representative of ET and PV, two hyperproliferative myeloproliferative neoplasms. Downstream targets of JAK2 are significantly affected by the presence of 1 μ M ruxolitinib in SET2 cells but further investigation is needed into the effect of ruxolitinib on downstream targets in HEL cells to distinguish different biological mechanisms involved in each disease phenotype. In addition, the combination of ruxolitinib and IFN- α does not seem to have a synergistic effect on decreasing cell viability or proliferation however, the combination of ruxolitinib and fludarabine has potential to be a synergistic combination of treatments, as demonstrated by their ability to further decrease the proliferation and viability of SET2 and HEL cells over 72 hours compared to ruxolitinib alone. Further exploration into the exact mechanisms underlying the pathogenesis of PV and ET could be facilitated by more experiments investigating the effects of ruxolitinib and fludarabine on mRNA and protein expression of downstream JAK2 targets, and on cell viability and proliferation in these cell lines.

6. References

- Aebersold, R. & Mann, M., 2003. Mass spectrometry-based proteomics.. *Nature*, 422(6928), pp. 198-207.
- Albu, R. & Constantinescu, S., 2011. Extracellular domain N-glycosylation controls human thrombopoietin receptor cell surface levels.. *Frontiers in Endocrinology*, 2(71).
- Argetsinger, L. et al., 2004. Autophosphorylation of JAK2 on tyrosines 221 and 570 regulates its activity.. *Molecular and Cellular Biology*, 24(11), pp. 4955-4967.
- Avramis, V. et al., 1998. Pharmacokinetic and pharmacodynamic studies of fludarabine and cytosine arabinoside administered as loading boluses followed by continuous infusions after a phase I/II study in pediatric patients with relapsed leukemias. The Children's Cancer Group.. *Clinical Cancer Research*, 4(1), pp. 45-52.
- Bacon, C. et al., 1995. Thrombopoietin (TPO) induces tyrosine phosphorylation and activation of STAT5 and STAT3.. *FEBS Letters*, 370(1-2), pp. 63-68.
- Bae, J., Leo, C., Hsu, S. & Hsueh, A., 2000. MCL-1S, a splicing variant of the antiapoptotic BCL-2 family member MCL-1, encodes a proapoptotic protein possessing only the BH3 domain.. *The Journal of Biological Chemistry*, 275(33), pp. 25255-25261.
- Baran-Marszak, F. et al., 2004. Differential roles of STAT1alpha and STAT1beta in fludarabine-induced cell cycle arrest and apoptosis in human B cells.. *Blood*, 104(8), pp. 2475-2483.
- Barbui, T. et al., 2011. Survival and disease progression in essential thrombocythemia are significantly influenced by accurate morphologic diagnosis: an international study.. *Journal of Clinical Oncology*, 29(23), pp. 3179-3184.
- Barosi, G. et al., 2009. Response criteria for essential thrombocythemia and polycythemia vera: result of a European LeukemiaNet consensus conference.. *Blood*, 113(20), pp. 4829-4833.
- Barosi, G. et al., 2010. A unified definition of clinical resistance and intolerance to hydroxycarbamide in polycythaemia vera and primary myelofibrosis: results of a European LeukemiaNet (ELN) consensus process.. *British Journal of Haematology*, 148(6), pp. 961-963.
- Barosi, G. et al., 2013. Revised response criteria for polycythemia vera and essential thrombocythemia: an ELN and IWG-MRT consensus project.. *Blood*, 121(23), pp. 4778-4781.
- Barrueco, J. et al., 1987. Proposed mechanism of therapeutic selectivity for 9-beta-D-arabinofuranosyl-2-fluoroadenine against murine leukemia based upon lower capacities for transport and phosphorylation in proliferative intestinal epithelium compared to tumor cells.. *Cancer Research*, 47(3), pp. 700-706.
- Baxter, E. et al., 2005. Acquired mutation of the tyrosine kinase JAK2 in human myeloproliferative disorders.. *Lancet*, 365(9464), pp. 1054-61.

- Bekisz, J. et al., 2010. Antiproliferative Properties of Type I and Type II Interferon.. *Pharmaceuticals (Basel, Switzerland)*, 3(4), pp. 994-1015.
- Bellosillo, B. et al., 1999. In vitro evaluation of fludarabine in combination with cyclophosphamide and/or mitoxantrone in B-cell chronic lymphocytic leukemia.. *Blood*, 94(8), pp. 2836-2843.
- Bellucci, S., Harousseau, J., Brice, P. & Tobelem, G., 1988. Treatment of essential thrombocythaemia by alpha 2a interferon. *Lancet*, Volume 2, pp. 960-961.
- Bellucci, S., Harousseau, J., Brice, P. & Tobelem, G., 1988. Treatment of essential thrombocythaemia by alpha 2a interferon.. *Lancet*, 2(8617), pp. 960-961.
- Birbrair, A. & Frenette, P., 2016. Niche heterogeneity in the bone marrow.. *Annals of the New York Academy of Science*, 1370(1), pp. 82-96.
- Biron, C., 2001. Interferons alpha and beta as immune regulators--a new look.. *Immunity*, 14(6), pp. 661-664.
- Björkholm, M. et al., 2011. Treatment-related risk factors for transformation to acute myeloid leukemia and myelodysplastic syndromes in myeloproliferative neoplasms. *Journal of Clinical Oncology*, 29(17), pp. 2410-5.
- Björkholm, M. et al., 2011. Treatment-related risk factors for transformation to acute myeloid leukemia and myelodysplastic syndromes in myeloproliferative neoplasms.. *Journal of Clinical Oncology*, 29(17), pp. 2410-2415.
- Bjørn, M. et al., 2013. Rapid Clearance Of JAK2 V617F Allele Burden In Patient With Advanced Polycythemia Vera (PV) During Combination Therapy With Ruxolitinib and Peg-Interferon Alpha-2a. *Blood*, 122(5241).
- Bjørn, M. et al., 2014. Combination therapy with interferon and JAK1-2 inhibitor is feasible: Proof of concept with rapid reduction in JAK2V617F-allele burden in polycythemia vera.. *Leukemia Research Reports*, 3(2), pp. 73-75.
- Bose, P. & Verstovsek, S., 2017. JAK2 inhibitors for myeloproliferative neoplasms: what is next?. *Blood*, 130(2), pp. 155-125.
- Briscoe, J. et al., 1996. Kinase-negative mutants of JAK1 can sustain interferon-gamma-inducible gene expression but not an antiviral state.. *EMBO Journal*, 15(4), pp. 799-809.
- Brockman, R., Schabel, F. J. & Montgomery, J., 1977. Biologic activity of 9-beta-D-arabinofuranosyl-2-fluoroadenine, a metabolically stable analog of 9-beta-D-arabinofuranosyladenine.. *Biochemical Pharmacology*, 26(22), pp. 2193-2196.
- Brodsky, F. & Guagliardi, L., 1991. The cell biology of antigen processing and presentation.. *Annual Review of Immunology*, Volume 9, pp. 707-744.
- Brooks, A. et al., 2014. Mechanism of activation of protein kinase JAK2 by the growth hormone receptor.. *Science*, 344(6185), p. 1249783.

- Buchdunger, E. et al., 1996. Inhibition of the Abl protein-tyrosine kinase in vitro and in vivo by a 2-phenylaminopyrimidine derivative. *Cancer Research*, 56(1), pp. 100-104.
- Bukur, J., Jasinski, S. & Seliger, B., 2012. The role of classical and non-classical HLA class I antigens in human tumors.. *Seminars in Cancer Biology*, 22(4), pp. 350-358.
- Burchert, A. et al., 2010. Sustained molecular response with interferon alfa maintenance after induction therapy with imatinib plus interferon alfa in patients with chronic myeloid leukemia.. *Journal of Clinical Oncology*, 28(8), pp. 1429-1435.
- Burchert, A. et al., 2015. Interferon alpha 2 maintenance therapy may enable high rates of treatment discontinuation in chronic myeloid leukemia.. *Leukemia*, 29(6), pp. 1331-1335.
- Burrows, F., Zhang, H. & Kamal, A., 2004. Hsp90 activation and cell cycle regulation.. *Cell Cycle*, 3(12), pp. 1530-1536.
- Catapano, C., Perrino, F. & Fernandes, D., 1993. Primer RNA chain termination induced by 9-beta-D-arabinofuranosyl-2-fluoroadenine 5'-triphosphate. A mechanism of DNA synthesis inhibition. *Journal of Biological Chemistry*, Volume 268, pp. 7179-7185.
- Cerezo, M. & Rocchi, S., 2017. New anti-cancer molecules targeting HSPA5/BIP to induce endoplasmic reticulum stress, autophagy and apoptosis.. *Autophagy*, 13(1), pp. 216-217.
- Chachoua, I. et al., 2016. Thrombopoietin receptor activation by myeloproliferative neoplasm associated calreticulin mutants.. *Blood*, 127(10), pp. 1325-1335.
- Chachoua, I. et al., 2016. Thrombopoietin receptor activation by myeloproliferative neoplasm associated calreticulin mutants.. *Blood*, 127(10), pp. 1325-1335.
- Chao, D. & Korsmeyer, S., 1988. BCL-2 family: regulators of cell death.. *Annual Review of Immunology*, Volume 16, pp. 395-419.
- Chawla-Sarkar, M. et al., 2003. Apoptosis and interferons: role of interferon-stimulated genes as mediators of apoptosis.. *Apoptosis*, 8(3), pp. 237-249.
- Chen, E. et al., 2010. Distinct clinical phenotypes associated with JAK2V617F reflect differential STAT1 signaling.. *Cancer Cell*, 18(5), pp. 524-535.
- Chen, E. & Mullally, A., 2014. How does JAK2V617F contribute to the pathogenesis of myeloproliferative neoplasms?. *American Society of Haematology*, Issue 1, pp. 268-76.
- Cheng, Q. et al., 2018. TREM2-activating antibodies abrogate the negative pleiotropic effects of the Alzheimer's disease variant Trem2R47H on murine myeloid cell function.. *The Journal of Biological Chemistry*, 293(32), pp. 12620-12633.
- Chen, H. et al., 2015. E1A-mediated inhibition of HSPA5 suppresses cell migration and invasion in triple-negative breast cancer.. *Annals of Surgical Oncology*, 22(3), pp. 889-898.
- Chen, X. et al., 2007. Ubiquitin-independent degradation of cell cycle inhibitors by the REGγ proteasome. *Molecular Cell*, 26(6), pp. 843-852.

Chun, H., Leyland-Jones, B. & Cheson, B., 1991. Fludarabine phosphate: a synthetic purine antimetabolite with significant activity against lymphoid malignancies.. *Journal of Clinical Oncology*, 9(1), pp. 175-188.

Cimino, R. et al., 1993. Recombinant interferon alpha-2b in the treatment of polycythemia vera.. *American Journal of Hematology*, 44(3), pp. 155-157.

Civallero, M., Cosenza, M., Pozzi, S. & Sacchi, S., 2017. Ruxolitinib combined with vorinostat suppresses tumor growth and alters metabolic phenotype in hematological diseases.. *Oncotarget*, 8(61), pp. 103797-103814.

Čokić, V. et al., 2015. Proinflammatory Cytokine IL-6 and JAK-STAT Signaling Pathway in Myeloproliferative Neoplasms.. *Mediators of Inflammation*, p. 453020.

Colomiere, M. et al., 2009. Cross talk of signals between EGFR and IL-6R through JAK2/STAT3 mediate epithelial-mesenchymal transition in ovarian carcinomas.. *British Journal of Cancer*, 100(1), pp. 134-144.

Constantinescu, S., 2014. *de Duve Institute: Receptor and JAK signaling and hematology*. [Online] Available at: <https://www.deduveinstitute.be/receptor-and-JAK-signaling-and-hematology>

Cortelazzo, S. et al., 1995. Hydroxyurea for patients with essential thrombocythemia and a high risk of thrombosis.. *New England Journal of Medicine*, 332(17), pp. 1132-1136.

Costa, M. et al., 2018. Pharmacokinetics comparison of two pegylated interferon alfa formulations in healthy volunteers.. *BMC Pharmacology and Toxicology*, 19(1), p. 1.

Dameshek, W., 1951. Some speculations on the myeloproliferative syndromes. *Blood*, 6(4), pp. 372-5.

Danhauser, L., Plunkett, W., Keating, M. & Cabanillas, F., 1986. 9-beta-D-arabinofuranosyl-2-fluoroadenine 5'-monophosphate pharmacokinetics in plasma and tumor cells of patients with relapsed leukemia and lymphoma.. *Cancer Chemotherapy and Pharmacology*, 18(2), pp. 145-152.

De Angelis, R. et al., 2014. Cancer survival in Europe 1999-2007 by country and age: results of EURO CARE--5-a population-based study.. *The Lancet. Oncology*, 15(1), pp. 23-34.

de Bono, J. et al., 2008. Phase I pharmacokinetic and pharmacodynamic study of LAQ824, a hydroxamate histone deacetylase inhibitor with a heat shock protein-90 inhibitory profile, in patients with advanced solid tumors.. *Clinical Cancer Research*, 14(20), pp. 6663-6673.

de la Iglesia, N. et al., 2008. Identification of a PTEN-regulated STAT3 brain tumor suppressor pathway.. *Genes & Development*, 22(4), pp. 449-462.

Delhommeau, F. et al., 2007. Evidence that the JAK2 G1849T (V617F) mutation occurs in a lymphomyeloid progenitor in polycythemia vera and idiopathic myelofibrosis. *Blood*, 109(1), pp. 71-7.

Deshpande, A. et al., 2012. Kinase domain mutations confer resistance to novel inhibitors targeting JAK2V617F in myeloproliferative neoplasms.. *Leukemia*, 26(4), pp. 708-715.

Didelot, C. et al., 2008. Interaction of heat-shock protein 90 beta isoform (HSP90 beta) with cellular inhibitor of apoptosis 1 (c-IAP1) is required for cell differentiation. *Cell Death and Differentiation*, 15(5), pp. 859-866.

- Ding, X. et al., 2008. Ocular toxicity of fludarabine: a purine analog.. *Expert review of ophthalmology*, 3(1), pp. 97-109.
- Doll, D. et al., 1989. Antineoplastic agents and pregnancy.. *Seminars in Oncology*, 16(5), pp. 337-346.
- Dornan, D. et al., 2004. Interferon Regulatory Factor 1 Binding to p300 Stimulates DNA-Dependent Acetylation of p53. *Molecular and Cellular Biology*, 24(22), pp. 10083-10098.
- Drachman, J., Griffin, J. & Kaushansky, K., 1995. The c-Mpl Ligand (Thrombopoietin) Stimulates Tyrosine Phosphorylation of Jak2, Shc, and c-Mpl. *Journal of Biological Chemistry*, Volume 270, pp. 4979-4982.
- Duek, A. et al., 2014. Loss of Stat1 decreases megakaryopoiesis and favors erythropoiesis in a JAK2-V617F-driven mouse model of MPNs.. *Blood*, 123(25), pp. 3943-3950.
- Durbin, J., Hackenmiller, R., Simon, M. & Levy, D., 1996. Targeted disruption of the mouse Stat1 gene results in compromised innate immunity to viral disease.. *Cell*, 84(3), pp. 443-450.
- Egle, A. et al., 2018. Fludarabine and rituximab with escalating doses of lenalidomide followed by lenalidomide/rituximab maintenance in previously untreated chronic lymphocytic leukaemia (CLL): the REVLIRIT CLL-5 AGMT phase I/II study.. *Annals of hematology*.
- Elledge, S., 1996. Cell cycle checkpoints: preventing an identity crisis.. *Science*, 274(5293), pp. 1664-1672.
- Falchi, L., Newberry, K. & Verstovsek, S., 2015. New Therapeutic Approaches in Polycythemia Vera.. *Clinical Lymphoma, Myeloma & Leukemia*, 15(Supplementary), pp. 27-33.
- Feng, J. et al., 1997. Activation of Jak2 catalytic activity requires phosphorylation of Y1007 in the kinase activation loop.. *Molecular and Cellular Biology*, 17(5), pp. 2497-2501.
- Ferris, R., Whiteside, T. & Ferrone, S., 2006. Immune escape associated with functional defects in antigen-processing machinery in head and neck cancer.. *Clinical Cancer Research*, 12(13), pp. 3890-3895.
- Fialkow, P. et al., 1981. Evidence for a multistep pathogenesis of chronic myelogenous leukemia. *Blood*, Volume 58, pp. 158-63.
- Fiskus, W. et al., 2011. Heat shock protein 90 inhibitor is synergistic with JAK2 inhibitor and overcomes resistance to JAK2-TKI in human myeloproliferative neoplasm cells. *Clinical Cancer Research*, 17(23), pp. 7347-7358.
- Foss, F. et al., 1994. Phase II trial of fludarabine phosphate and interferon alfa-2a in advanced mycosis fungoides/Sézary syndrome.. *Journal of Clinical Oncology*, 12(10), pp. 2051-2059.
- Frank, D., Mahajan, S. & Ritz, J., 1999. Fludarabine-induced immunosuppression is associated with inhibition of STAT1 signaling.. *Nature medicine*, 5(4), pp. 444-447.
- Frank, D. et al., 1999. Fludarabine-induced immunosuppression is associated with inhibition of STAT1 signaling.. *Nature medicine*, 5(4), pp. 444-447.

- Frantsve, J. et al., 2001. Socs-1 inhibits TEL-JAK2-mediated transformation of hematopoietic cells through inhibition of JAK2 kinase activity and induction of proteasome-mediated degradation.. *Molecular and Cellular Biology*, 21(10), pp. 3547-3557.
- Fridman, J. et al., 2007. Discovery and Preclinical Characterization of INCB018424, a Selective JAK2 Inhibitor for the Treatment of Myeloproliferative Disorders.. *Blood*, 110(11), p. 3538.
- Friedbichler, K. et al., 2010. Stat5a serine 725 and 779 phosphorylation is a prerequisite for hematopoietic transformation.. *Blood*, 116(9), pp. 1548-1558.
- Funakoshi-Tago, M. et al., 2010. STAT5 activation is critical for the transformation mediated by myeloproliferative disorder-associated JAK2 V617F mutant.. *Journal of Biological Chemistry*, 285(8), pp. 5296-5307.
- Gallardo, M. et al., 2013. Proteomic analysis reveals heat shock protein 70 has a key role in polycythemia Vera.. *Molecular Cancer*, 142(12).
- Gandhi, V. et al., 1998. Modulation of Ara-C Metabolism to Improve AML Response. In: W. Hiddemann, et al. eds. *Acute Leukemias VII: Experimental Approaches and Novel Therapies*. Berlin: Springer-Verlag Berlin Heidelberg, pp. 577-581.
- Gandhi, V. & Plunkett, W., 2002. Cellular and clinical pharmacology of fludarabine. *Clinical Pharmacokinetics*, 41(2), pp. 93-103.
- Gandhi, V. & Plunkett, W., 2002. Cellular and clinical pharmacology of fludarabine.. *Clinical pharmacokinetics*, 41(2), pp. 93-103.
- Garcia-Lora, A., Algarra, I. & Garrido, F., 2003. MHC class I antigens, immune surveillance, and tumor immune escape.. *Journal of Cellular Physiology*, 195(3), pp. 346-355.
- Garçon, L. et al., 2006. Constitutive activation of STAT5 and Bcl-xL overexpression can induce endogenous erythroid colony formation in human primary cells. *Blood*, 108(5), pp. 1551-1554.
- Garrido, C., Gurbuxani, S., Ravagnan, L. & Kroemer, G., 2001. Heat shock proteins: endogenous modulators of apoptotic cell death. *Biochemical and biophysical research communications*, 286(3), pp. 433-442.
- Garrido, F. et al., 1997. Implications for immunosurveillance of altered HLA class I phenotypes in human tumours.. *Immunology Today*, 18(2), pp. 89-95.
- Geddis, A. et al., 2001. Phosphatidylinositol 3-kinase is necessary but not sufficient for thrombopoietin-induced proliferation in engineered Mpl-bearing cell lines as well as in primary megakaryocytic progenitors.. *The Journal of Biological Chemistry*, 276(37), pp. 34473-34479.
- Geyer, H. & Mesa, R., 2014. Therapy for myeloproliferative neoplasms: when, which agent, and how?. *Blood*, 124(24), pp. 3529-3537.
- Giles, F. et al., 2003. Phase I and pharmacodynamic study of Triapine, a novel ribonucleotide reductase inhibitor, in patients with advanced leukemia.. *Leukemia Research*, 27(12), pp. 1077-1083.

- Gisslinger, H. et al., 2016. Final Results from PROUD-PV a Randomized Controlled Phase 3 Trial Comparing Ropoginterferon Alfa-2b to Hydroxyurea in Polycythemia Vera Patients. *Blood*, 128(475).
- Gisslinger, H. et al., 2015. Ropoginterferon alfa-2b, a novel IFN α -2b, induces high response rates with low toxicity in patients with polycythemia vera.. *Blood*, 126(15), pp. 1762-1769.
- Goptu, M. et al., 2018. A Comparison of the Myeloablative Conditioning Regimen Fludarabine/Busulfan with Cyclophosphamide/Total Body Irradiation, for Allogeneic Stem Cell Transplantation in the Modern Era: A Cohort Analysis.. *Journal of the American Society for Blood and Marrow Transplantation*, S1083-8791(18), pp. 30124-1.
- Gowin, K. et al., 2012. Experience with pegylated interferon α -2a in advanced myeloproliferative neoplasms in an international cohort of 118 patients.. *Haematologica*, 97(10), pp. 1570-1573.
- Greenhalgh, C. & Hilton, D., 2001. Negative regulation of cytokine signaling.. *Journal of Leukocyte Biology*, 70(3), pp. 348-356.
- Gugliotta, L. et al., 1989. In vivo and in vitro inhibitory effect of alpha-interferon on megakaryocyte colony growth in essential thrombocythaemia.. *British Journal of Haematology*, 71(2), pp. 177-181.
- Guo, J. et al., 2015. JAK2V617F drives Mcl-1 expression and sensitizes hematologic cell lines to dual inhibition of JAK2 and Bcl-xL.. *PLoS One*, 10(3), p. e0114363.
- Guo, T. et al., 2018. Multi-region proteome analysis quantifies spatial heterogeneity of prostate tissue biomarkers.. *Life Science Alliance*, 1(2).
- Gupta, S. et al., 2010. Heat shock proteins in toxicology: how close and how far?. *Life Sciences*, 86(11-12), pp. 377-384.
- Gupta, V. et al., 2016. Exploring the Potential of JAK1/2 Inhibitor Ruxolitinib with Reduced Intensity Hematopoietic Cell Transplantation (HCT) for Myelofibrosis: Stage I Results of a Prospective Trial Conducted through the Myeloproliferative Disorders - Research Consortium (MPD. *Blood*, 128(1126).
- Hamid, R. et al., 2004. Comparison of alamar blue and MTT assays for high through-put screening.. *Toxicology In Vitro*, 18(5), pp. 703-710.
- Hansen, I., Sørensen, A. & Hasselbalch, H., 2017. Second malignancies in hydroxyurea and interferon-treated Philadelphia-negative myeloproliferative neoplasms.. *European Journal of Haematology*, 98(1), pp. 75-84.
- Han, X., Aslanian, A. & Yates, J. 3., 2008. Mass spectrometry for proteomics. *Current Opinion in Chemical Biology*, 12(5), pp. 483-490.
- Harlow, E. & Lane, D., 1988. Table 18.3 Solutions for Preparing Resolving Gels for Tris glycine SDS-Polyacrylamide Gel Electrophoresis. In: E. Harlow & D. Lane, eds. *Antibodies: A Laboratory manual*. Cold Spring Harbour: Cold Spring Harbour Laboratory.
- Harris, C., 1996. Structure and function of the p53 tumor suppressor gene: clues for rational cancer therapeutic strategies.. *Journal of the National Cancer Institute*, 88(20), pp. 1442-1455.

- Harrison, C. et al., 2005. Hydroxyurea compared with anagrelide in high-risk essential thrombocythemia.. *New England Journal of Medicine*, 353(1), pp. 33-45.
- Harrison, C. et al., 2012. JAK inhibition with ruxolitinib versus best available therapy for myelofibrosis.. *New England Journal of Medicine*, 366(9), pp. 787-798.
- Harrison, C. et al., 2017. Ruxolitinib vs best available therapy for ET intolerant or resistant to hydroxycarbamide.. *Blood*, 130(17), pp. 1889-1897.
- Harrison, C. & Vannucchi, A., 2012. Ruxolitinib: a potent and selective Janus kinase 1 and 2 inhibitor in patients with myelofibrosis. An update for clinicians.. *Therapeutic Advances in Hematology*, 3(6), pp. 341-354.
- Harrison, C. et al., 2016. Long-term findings from COMFORT-II, a phase 3 study of ruxolitinib vs best available therapy for myelofibrosis.. *Leukemia*, 30(8), pp. 1701-1707.
- Harrison, O. et al., 2018. Candidate plasma biomarkers for predicting ascending aortic aneurysm in bicuspid aortic valve disease.. *Journal of Cardiothoracic Surgery*, 13(1).
- Hasselbalch, H., 2012. Perspectives on chronic inflammation in essential thrombocythemia, polycythemia vera, and myelofibrosis: is chronic inflammation a trigger and driver of clonal evolution and development of accelerated atherosclerosis and second cancer?. *Blood*, 119(14), pp. 3219-3225.
- Hasselbalch, H., 2013. Chronic inflammation as a promotor of mutagenesis in essential thrombocythemia, polycythemia vera and myelofibrosis. A human inflammation model for cancer development?. *Leukemia Research*, 37(2), pp. 214-220.
- Hasselbalch, H. et al., 2011. Interferon-alpha in the treatment of Philadelphia-negative chronic myeloproliferative neoplasms. Status and perspectives.. *Current Drug Targets*, 12(3), pp. 392-419.
- Hebenstreit, D., Horejs-Hoeck, J. & Duschl, A., 2005. JAK/STAT-dependent gene regulation by cytokines.. *Drug news & perspectives*, 18(4), pp. 243-249.
- Heerma van Voss, M. et al., 2017. Nuclear DDX3 expression predicts poor outcome in colorectal and breast cancer.. *Oncotargets and Therapy*, Volume 10, pp. 3501-3513.
- Heikkilä, K., Ebrahim, S. & Lawlor, D., 2008. Systematic review of the association between circulating interleukin-6 (IL-6) and cancer.. *European Journal of Cancer*, 44(7), pp. 937-945.
- Hoffman, R., 2017. *Randomized Trial of Pegylated Interferon Alfa-2a Versus Hydroxyurea in Polycythemia Vera (PV) and Essential Thrombocythemia (ET)*. *ClinicalTrials.gov Identifier: NCT01259856*, s.l.: clinicaltrials.gov.
- Hou, L. et al., 2016. Systematic analyses of key genes and pathways in the development of invasive breast cancer.. *Gene*, 593(1), pp. 1-12.
- Hsu, H. et al., 1999. Circulating levels of thrombopoietic and inflammatory cytokines in patients with clonal and reactive thrombocytosis.. *The Journal of Laboratory and Clinical Medicine*, 134(4), pp. 392-397.

- Huang, H., Lin, Y., Chen, C. & Chang, T., 2005. Simultaneous activation of JAK1 and JAK2 confers IL-3 independent growth on Ba/F3 pro-B cells.. *Journal of Cellular Biochemistry*, 96(2), pp. 361-375.
- Hui, W. et al., 2013. Aberrant expression of signaling proteins in essential thrombocythemia. *Annals of Hematology*, 92(9), pp. 1229-1238.
- Ihle, J. et al., 1995. Signaling through the hematopoietic cytokine receptors.. *Annual Review of Immunology*, Volume 13, pp. 369-398.
- Imai, M., Araki, M. & Komatsu, N., 2017. Somatic mutations of calreticulin in myeloproliferative neoplasms.. *International Journal of Hematology*, 105(6), pp. 743-747.
- Incyte, 2014. *Jakafi (ruxolitinib) tablets [prescribing information]*. [Online] Available at: <https://www.jakafi.com/hcp/safety-profile.aspx> [Accessed 26 June 2018].
- Ito, T. et al., 2012. Splenic irradiation as a component of a reduced-intensity conditioning regimen for hematopoietic stem cell transplantation in myelofibrosis with massive splenomegaly.. *The Tokohu Journal of Experimental Medicine*, 288(4), pp. 295-299.
- Ivashkiv, L. & Donlin, L., 2014. Regulation of type I interferon responses.. *Nature Reviews. Immunology*, 14(1), pp. 36-49.
- Iwasaki, H., Huang, P., Keating, M. & Plunkett, W., 1997. Differential incorporation of ara-C, gemcitabine, and fludarabine into replicating and repairing DNA in proliferating human leukemia cells.. *Blood*, 90(1), pp. 270-278.
- Jackson, G., 2004. Use of fludarabine in the treatment of acute myeloid leukemia.. *The Hematology Journal: The Official Journal of the European Hematology Association*, 5(S1), pp. S62-67.
- James, C. et al., 2005. A JAK2 mutation in myeloproliferative disorders: pathogenesis and therapeutic and scientific prospects. *Trends in molecular medicine*, 11(12), pp. 546-54.
- James, C. et al., 2005. A unique clonal JAK2 mutation leading to constitutive signalling causes polycythaemia vera.. *Nature*, 434(7037), pp. 1144-8.
- Jamieson, C. et al., 2006. The JAK2 V617F mutation occurs in hematopoietic stem cells in polycythemia vera and predisposes toward erythroid differentiation.. *Proceedings of the National Academy of Sciences of the United States of America*, 103(16), pp. 6224-6229.
- Jedidi, A. et al., 2009. Selective reduction of JAK2V617F-dependent cell growth by siRNA/shRNA and its reversal by cytokines.. *Blood*, 114(9), pp. 1842-1851.
- Jego, G. et al., 2014. Dual regulation of SPI1/PU.1 transcription factor by heat shock factor 1 (HSF1) during macrophage differentiation of monocytes. *Leukemia*, 28(8), pp. 1676-1686.
- Jen, J. et al., 2017. Oncoprotein ZNF322A transcriptionally deregulates alpha-adducin, cyclin D1 and p53 to promote tumor growth and metastasis in lung cancer.. *Oncogene*, 36(36).
- Jiang, S. et al., 1994. Cytokine production by primary bone marrow megakaryocytes.. *Blood*, 84(12), p. 4151.

- Jia, S. et al., 2008. Essential roles of PI(3)K-p110beta in cell growth, metabolism and tumorigenesis.. *Nature*, 454(7205), pp. 776-779.
- Jindal, S., 1996. Heat shock proteins: applications in health and disease. *Trends in Biotechnology*, 14(1), pp. 17-20.
- Joffe, E. et al., 2018. Outcomes of Second-Line Treatment After Fludarabine Cyclophosphamide and Rituximab in Patients with Chronic Lymphocytic Leukemia Outside Clinical Trials.. *European Journal of Haematology*.
- José-Enériz, E. et al., 2008. BCR-ABL1-induced expression of HSPA8 promotes cell survival in chronic myeloid leukaemia.. *British Journal of Haematology*, 142(2), pp. 571-582.
- Kano, Y. et al., 2001. In vitro cytotoxic effects of a tyrosine kinase inhibitor STI571 in combination with commonly used antileukemic agents.. *Blood*, 97(7), pp. 1999-2007.
- Kapp, E. & Schütz, F., 2007. Overview of tandem mass spectrometry (MS/MS) database search algorithms.. *Current Protocols in Protein Science*, Volume 25.
- Katayama, T. et al., 2007. Type I interferon prolongs cell cycle progression via p21WAF1/CIP1 induction in human colon cancer cells.. *International Journal of Oncology* , 31(3), pp. 613-620.
- Kaushansky, K., 1995. Thrombopoietin: the primary regulator of megakaryocyte and platelet production.. *Thrombosis and Haemostasis*, 74(1), pp. 521-525.
- Kawamura, M. et al., 1994. Molecular cloning of L-JAK, a Janus family protein-tyrosine kinase expressed in natural killer cells and activated leukocytes.. *Proceedings of the National Academy of Sciences of the United States of America*, 91(14), pp. 6374-6378.
- Kemena, A., Keating, M. & Plunkett, W., 1991. Plasma and cellular bioavailability of oral fludarabine [abstract].. *Blood*, 52a(78).
- Kerbaui, D. et al., 2007. Hematopoietic cell transplantation as curative therapy for idiopathic myelofibrosis, advanced polycythemia vera, and essential thrombocythemia.. *Biology of Blood and Marrow Transplantation*, 13(3), pp. 355-365.
- Khalil, M. et al., 2018. Fludarabine and busulfan plus low-dose TBI as reduced intensity conditioning in older patients undergoing allogeneic hematopoietic cell transplant for myeloid malignancies.. *Annals of hematology*, pp. s00277-018-3391-9.
- Kiladjian, J. et al., 2008. Pegylated interferon-alfa-2a induces complete hematologic and molecular responses with low toxicity in polycythemia vera.. *Blood*, 112(8), pp. 3065-3072.
- Kiladjian, J. et al., 2006. High molecular response rate of polycythemia vera patients treated with pegylated interferon alpha-2a.. *Blood*, 108(6), pp. 2037-3040.
- Kiladjian, J., Chomienne, C. & Fenau, P., 2008. Interferon-alpha therapy in bcr-abl-negative myeloproliferative neoplasms.. *Leukemia*, 22(11), pp. 1990-1998.
- Kiladjian, J. et al., 2018. Efficacy and safety of ruxolitinib after and versus interferon use in the RESPONSE studies.. *American Journal of Hematology*, p. Epub ahead of print.

- Kiladjian, J., Mesa, R. & Hoffman, R., 2011. The renaissance of interferon therapy for the treatment of myeloid malignancies.. *Blood*, 117(18), pp. 4706-4715.
- Kim, H. et al., 2013. Allelic expression imbalance of JAK2 V617F mutation in BCR-ABL negative myeloproliferative neoplasms.. *PLoS One*, 8(1), p. e52518.
- Kiyonami, R. et al., 2011. Increased selectivity, analytical precision, and throughput in targeted proteomics.. *Molecular & Cellular Proteomics: MCP*, 10(2).
- Kleppe, M. et al., 2015. JAK-STAT pathway activation in malignant and nonmalignant cells contributes to MPN pathogenesis and therapeutic response.. *Cancer Discovery*, 5(3), pp. 316-331.
- Klyuchnikov, E. et al., 2012. Donor lymphocyte infusions and second transplantation as salvage treatment for relapsed myelofibrosis after reduced-intensity allografting.. *British Journal of Haematology*, 159(2), pp. 172-181.
- Kondo, T. et al., 2008. Validation of the revised 2008 WHO diagnostic criteria in 75 suspected cases of myeloproliferative neoplasm.. *Leukemia & Lymphoma*, 49(9), pp. 1784-1791.
- Koppikar, P. et al., 2012. Heterodimeric JAK-STAT activation as a mechanism of persistence to JAK2 inhibitor therapy.. *Nature*, 489(7414), pp. 115-119.
- Kralovics, R. et al., 2005. A gain-of-function mutation of JAK2 in myeloproliferative disorders.. *The New England Journal of Medicine*, 352(17), pp. 1779-1990.
- Krebs, D. & Hilton, D., 2001. SOCS proteins: negative regulators of cytokine signaling.. *Stem Cells*, 19(5), pp. 378-387.
- Lacout, C. et al., 2006. JAK2V617F expression in murine hematopoietic cells leads to MPD mimicking human PV with secondary myelofibrosis.. *Blood*, 108(5), pp. 1652-1660.
- Lai, M., Lee, Y. & Tarn, W., 2008. The DEAD-box RNA helicase DDX3 associates with export messenger ribonucleoproteins as well as tip-associated protein and participates in translational control.. *Molecular Biology of the Cell*, 19(9), pp. 3847-3858.
- Lancet, J. et al., 2010. Phase I study of the heat shock protein 90 inhibitor alvespimycin (KOS-1022, 17-DMAG) administered intravenously twice weekly to patients with acute myeloid leukemia.. *Leukemia*, 24(4), pp. 699-705.
- Landgren, O. et al., 2008. Increased risks of polycythemia vera, essential thrombocythemia, and myelofibrosis among 24,577 first-degree relatives of 11,039 patients with myeloproliferative neoplasms in Sweden. *Blood*, 112(6), pp. 2199-2204.
- Lange, V., Picotti, P., Domon, B. & Aebersold, R., 2008. Selected reaction monitoring for quantitative proteomics: a tutorial. *Molecular Systems Biology*, 4(222).
- Lanneau, D. et al., 2008. Heat shock proteins: essential proteins for apoptosis regulation.. *Journal of Cellular and Molecular Medicine*, 12(3), pp. 743-761.

Leblond, V. et al., 2013. Results of a randomized trial of chlorambucil versus fludarabine for patients with untreated Waldenström macroglobulinemia, marginal zone lymphoma, or lymphoplasmacytic lymphoma.. *Journal of Clinical Oncology*, 31(3), pp. 301-307.

Lee, C. et al., 2006. Janus kinase-signal transducer and activator of transcription mediates phosphatidic acid-induced interleukin (IL)-1 β and IL-6 production.. *Molecular Pharmacology*, 69(3), pp. 1041-1047.

Leitão, A., Costa, M. & Enguita, F., 2015. Unzippers, resolvers and sensors: a structural and functional biochemistry tale of RNA helicases.. *International Journal of Molecular Sciences*, 16(2), pp. 2269-2293.

Leonard, W., 2001. Role of Jak kinases and STATs in cytokine signal transduction.. *International Journal of Hematology*, 73(3), pp. 271-277.

Levine, R. et al., 2005. The JAK2V617F activating mutation occurs in chronic myelomonocytic leukemia and acute myeloid leukemia, but not in acute lymphoblastic leukemia or chronic lymphocytic leukemia.. *Blood*, 106(10), pp. 3377-3379.

Levine, R. et al., 2005. Activating mutation in the tyrosine kinase JAK2 in polycythemia vera, essential thrombocythemia, and myeloid metaplasia with myelofibrosis.. *Cancer Cell*, 7(4), pp. 387-397.

Liang, X. et al., 2016. Design, Synthesis, and Antitumor Evaluation of 4-Amino-(1H)-pyrazole Derivatives as JAKs Inhibitors.. *ACS Medicinal Chemistry Letters*, 7(10), pp. 950-955.

Liang, Y. et al., 2017. Downregulated SOCS1 expression activates the JAK1/STAT1 pathway and promotes polarization of macrophages into M1 type.. *Molecular Medicine Reports*, 16(5), pp. 6405-6411.

Lim, C. & Cao, X., 2006. Structure, function, and regulation of STAT proteins.. *Molecular Biosystems*, 2(11), pp. 536-550.

Ling, A. et al., 2017. TAP1 down-regulation elicits immune escape and poor prognosis in colorectal cancer.. *Oncoimmunology*, 6(11), p. e1356143.

Lin, T., Mahajan, S. & Frank, D., 2000. STAT signaling in the pathogenesis and treatment of leukemias.. *Oncogene*, 19(21), pp. 2496-2504.

Liu, H., Sadygov, R. & Yates, J., 2004. A model for random sampling and estimation of relative protein abundance in shotgun proteomics. *Analytical Chemistry*, 76(14), pp. 4193-4201.

Liu, Y., Peterson, D., Kimura, H. & Schubert, D., 1997. Mechanism of cellular 3-(4,5-dimethylthiazol-2-yl)-2,5-diphenyltetrazolium bromide (MTT) reduction.. *Journal of Neurochemistry*, 69(2), pp. 581-593.

Liu, Y. & Ye, Y., 2012. Roles of p97-associated deubiquitinases in protein quality control at the endoplasmic reticulum.. *Current Protein & Peptide Science*, 13(5), pp. 436-446.

Looyenga, B. et al., 2012. STAT3 is activated by JAK2 independent of key oncogenic driver mutations in non-small cell lung carcinoma.. *PLoS One*, 7(2), p. 30820.

Ludwig, C. et al., 2018. Data-independent acquisition-based SWATH-MS for quantitative proteomics: a tutorial.. *Molecular Systems Biology*, 14(8), p. e8126.

- Ludwig, H. et al., 1985. Treatment with recombinant interferon-alpha-2C: multiple myeloma and thrombocythaemia in myeloproliferative diseases.. *Oncology*, 42(Suppl 1), pp. 19-25.
- Lynch, J. et al., 2002. Phase II study of fludarabine combined with interferon-alpha-2a followed by maintenance therapy with interferon-alpha-2a in patients with low-grade non-hodgkin's lymphoma.. *American Journal of Clinical Oncology*, 25(4), pp. 391-397.
- Ma, L. et al., 2013. Discovery and characterization of LY2784544, a small-molecule tyrosine kinase inhibitor of JAK2V617F.. *Blood Cancer Journal*, Volume 3, p. 109.
- Maltaris, T. et al., 2006. Comparison of xenografting in SCID mice and LIVE/DEAD assay as a predictor of the developmental potential of cryopreserved ovarian tissue.. *In Vivo*, 20(1), pp. 11-16.
- Manoukian, G. et al., 2010. Rituximab, fludarabine, mitoxantrone, and dexamethasone (R-FND) for patients with relapsed indolent B-cell lymphoma (RIL). *Journal of Clinical Oncology*.
- Marchioli, R. et al., 2005. Vascular and neoplastic risk in a large cohort of patients with polycythemia vera.. *Journal of Clinical Oncology*, 23(10), pp. 2224-2232.
- Marit, M. et al., 2012. Random mutagenesis reveals residues of JAK2 critical in evading inhibition by a tyrosine kinase inhibitor.. *PloS One*, 7(8), p. e43437.
- Martin, P. & Papayannopoulou, T., 1982. HEL cells: a new human erythroleukemia cell line with spontaneous and induced globin expression.. *Science*, 216(4551), pp. 1233-1235.
- Marty, C. et al., 2016. Calreticulin mutants in mice induce an MPL-dependent thrombocytosis with frequent progression to myelofibrosis.. *Blood*, 127(10), pp. 1317-1324.
- Marubayashi, S. et al., 2010. HSP90 is a therapeutic target in JAK2-dependent myeloproliferative neoplasms in mice and humans.. *Journal of Clinical Investigation*, 120(10), pp. 3578-3593.
- Masarova, L. et al., 2017. Pegylated interferon alfa-2a in patients with essential thrombocythaemia or polycythaemia vera: a post-hoc, median 83 month follow-up of an open-label, phase 2 trial.. *Lancet Haematology*, 4(4), pp. 165-175.
- Ma, S. et al., 2004. Fludarabine, mitoxantrone and dexamethasone in the treatment of indolent B- and T-cell lymphoid malignancies in Chinese patients.. *British Journal of Haematology*, 124(6), pp. 754-761.
- Mascarenhas, J., Mesa, R., Prchal, J. & Hoffman, R., 2014. Optimal therapy for polycythemia vera and essential thrombocythemia can only be determined by the completion of randomized clinical trials. *Haematologica*, 99(6), pp. 945-949.
- Mascarenhas, J. et al., 2016. Interim Analysis of the Myeloproliferative Disorders Research Consortium (MPD-RC) 112 Global Phase III Trial of Front Line Pegylated Interferon Alpha-2a Vs. Hydroxyurea in High Risk Polycythemia Vera and Essential Thrombocythemia. *Blood*, 128(479).
- Maserati, M. et al., 2011. Wdr74 Is Required for Blastocyst Formation in the Mouse. *PLoS One*, 6(7), p. e22516.

- Matsubara, E. et al., 2016. Usefulness of Low-Dose Splenic Irradiation prior to Reduced-Intensity Conditioning Regimen for Hematopoietic Stem Cell Transplantation in Elderly Patients with Myelofibrosis.. *Case Reports in Haematology*, p. 8751329.
- Matsuoka, Y., Li, X. & Bennett, V., 2000. Adducin: structure, function and regulation.. *Cellular and Molecular Life Sciences: CMLS*, 57(6), pp. 884-895.
- Mauro, F. et al., 2003. Fludarabine + prednisone +/- alpha-interferon followed or not by alpha-interferon maintenance therapy for previously untreated patients with chronic lymphocytic leukemia: long term results of a randomized study.. *Haematologica*, 88(12), pp. 1348-1357.
- Maxson, J. et al., 2013. Oncogenic CSF3R Mutations in Chronic Neutrophilic Leukemia and Atypical CML. *The New England Journal of Medicine*, Volume 368, pp. 1781-1790.
- Mazzacurati, L. et al., 2015. The PIM inhibitor AZD1208 synergizes with ruxolitinib to induce apoptosis of ruxolitinib sensitive and resistant JAK2-V617F-driven cells and inhibit colony formation of primary MPN cells. *Oncotarget*, 6(37), pp. 40141-40157.
- McLornan, D., Percy, M. & McMullin, M., 2006. JAK2 V617F: a single mutation in the myeloproliferative group of disorders.. *The Ulster Medical Journal*, 75(2), pp. 112-119.
- Meidenbauer, N. et al., 2004. High frequency of functionally active Melan-a-specific T cells in a patient with progressive immunoproteasome-deficient melanoma.. *Cancer Research*, 64(17), pp. 6319-6326.
- Merz, C., Urlaub, H., Will, C. & Lührmann, R., 2006. Protein composition of human mRNPs spliced in vitro and differential requirements for mRNP protein recruitment.. *RNA*, 13(1), pp. 116-128.
- Mesa, R. et al., 2017. NCCN Guidelines Insights: Myeloproliferative Neoplasms, Version 2.2018.. *Journal of the National Comprehensive Cancer Network (JNCCN)*, 15(10), pp. 1193-1207.
- Meyer, S. et al., 2015. CHZ868, a Type II JAK2 Inhibitor, Reverses Type I JAK Inhibitor Persistence and Demonstrates Efficacy in Myeloproliferative Neoplasms.. *Cancer Cell*, 28(1), pp. 15-28.
- Michalak, M. et al., 2009. Calreticulin, a multi-process calcium-buffering chaperone of the endoplasmic reticulum.. *The Biochemical Journal*, 417(3), pp. 651-666.
- Michalak, M. et al., 2009. Calreticulin, a multi-process calcium-buffering chaperone of the endoplasmic reticulum.. *The Biochemical Journal*, 417(3), pp. 651-666.
- Michalski, A., Cox, J. & Mann, M., 2011. More than 100,000 detectable peptide species elute in single shotgun proteomics runs but the majority is inaccessible to data-dependent LC-MS/MS.. *Journal of Proteome Research*, 10(4), pp. 1785-1793.
- Miles, M. et al., 2005. Molecular and functional characterization of a novel splice variant of ANKHD1 that lacks the KH domain and its role in cell survival and apoptosis.. *The FEBS Journal*, 272(16), pp. 4091-4102.
- Mirantes, C., Passequé, E. & Pietras, E., 2014. Pro-inflammatory cytokines: emerging players regulating HSC function in normal and diseased hematopoiesis.. *Experimental Cell Research*, 329(2), pp. 248-254.

- Miyamoto, M. et al., 1988. Regulated expression of a gene encoding a nuclear factor, IRF-1, that specifically binds to IFN-beta gene regulatory elements.. *Cell*, 54(6), pp. 903-913.
- Miyauchi, E. et al., 2018. Identification of blood biomarkers in glioblastoma by SWATH mass spectrometry and quantitative targeted absolute proteomics.. *PLoS One*, 13(3), p. e0193799.
- Molavi, O. et al., 2013. Gene methylation and silencing of SOCS3 in mantle cell lymphoma.. *British Journal of Haematology*, 161(3), pp. 348-356.
- Mondet, J. et al., 2015. Endogenous megakaryocytic colonies underline association between megakaryocytes and calreticulin mutations in essential thrombocythemia.. *Haematologica*, 100(5), pp. 176-178.
- Morales, D. & Lenschow, D., 2013. The antiviral activities of ISG15.. *Journal of Molecular Biology*, 425(24), pp. 4995-5008.
- Morris, G. et al., 2004. Phase II study of fludarabine and alpha-interferon in patients with low-grade non-Hodgkin's lymphoma.. *Haematologica*, 89(12), pp. 1484-1491.
- Mottok, A. et al., 2009. Inactivating SOCS1 mutations are caused by aberrant somatic hypermutation and restricted to a subset of B-cell lymphoma entities.. *Blood*, 114(20), pp. 4503-4506.
- Moulard, O. et al., 2014. Epidemiology of myelofibrosis, essential thrombocythemia, and polycythemia vera in the European Union. *European Journal of Haematology*, 92(4), pp. 289-97.
- Mullally, A. et al., 2013. Depletion of Jak2V617F myeloproliferative neoplasm-propagating stem cells by interferon- α in a murine model of polycythemia vera. *Blood*, 121(18), pp. 3692-3702.
- Müller, M. et al., 1993. The protein tyrosine kinase JAK1 complements defects in interferon- α/β and - γ signal transduction. *Nature*, 366(6451), pp. 129-135.
- Musteanu, M. et al., 2010. Stat3 is a negative regulator of intestinal tumor progression in Apc(Min) mice.. *Gastroenterology*, 138(3), pp. 1003-1011.
- Nangalia, J. et al., 2013. Somatic CALR mutations in myeloproliferative neoplasms with nonmutated JAK2.. *New England Journal of Medicine*, 369(25), pp. 2391-2405.
- Nesvizhskii, A., 2007. Protein identification by tandem mass spectrometry and sequence database searching.. *Methods in Molecular Biology*, Volume 367, pp. 87-119.
- Nicholson, S. et al., 1999. Mutational analyses of the SOCS proteins suggest a dual domain requirement but distinct mechanisms for inhibition of LIF and IL-6 signal transduction.. *The EMBO Journal*, 18(2), pp. 375-385.
- Nielsen, I. & Hasselbalch, H., 2003. Acute leukemia and myelodysplasia in patients with a Philadelphia chromosome negative chronic myeloproliferative disorder treated with hydroxyurea alone or with hydroxyurea after busulphan.. *American Journal of Hematology*, 74(1), pp. 26-31.
- Nijenhuis, M. & Hämmerling, G., 1996. Multiple regions of the transporter associated with antigen processing (TAP) contribute to its peptide binding site. *Journal of Immunology*, 157(12), pp. 5467-5477.

- Nitulescu, I. et al., 2017. Mediator Kinase Phosphorylation of STAT1 S727 Promotes Growth of Neoplasms With JAK-STAT Activation.. *EBioMedicine*, pp. 112-125.
- Nowell, P. & Hungerford, D., 1960. A minute chromosome in human chronic granulocytic leukaemia. *Science*, Volume 132, p. 1497.
- Nozawa, H. et al., 1998. Functionally inactivating point mutation in the tumor-suppressor IRF-1 gene identified in human gastric cancer.. *International Journal of Cancer*, 77(4), pp. 522-527.
- O'Brien, J., Wilson, I., Orton, T. & Pognan, F., 2000. Investigation of the Alamar Blue (resazurin) fluorescent dye for the assessment of mammalian cell cytotoxicity.. *European Journal of Biochemistry*, 267(17), pp. 5421-5426.
- Odenike, O., 2013. Beyond JAK inhibitor therapy in myelofibrosis.. *Hematology. American Society of Hematology*, 2013(1), pp. 545-552.
- Oncology, W. P., 1991. *Fludarabine approved for use in chronic lymphocytic leukemia*.. Willison Park, NY: Oncology.
- OpenStax College, 2013. 18.2 Production of the Formed Elements. In: *Anatomy & Physiology*. Houston, Texas: OpenStax College, Rice University, p. 126.
- Opydo-Chanek, M., Stokaj, M. & Mazur, L., 2012. In Vitro Response of Human Pathological Hematopoietic Cells to Fludarabine Phosphate. *ACTA Biologica Cracoviensia*, Volume 54, pp. 33-38.
- O'Reilly, S., Ciecchomska, M., Cant, R. & van Laar, J., 2014. Interleukin-6 (IL-6) trans signaling drives a STAT3-dependent pathway that leads to hyperactive transforming growth factor- β (TGF- β) signaling promoting SMAD3 activation and fibrosis via Gremlin protein.. *The Journal of Biological Chemistry*, 289(14), pp. 9952-9960.
- Orkin, S., 2000. Diversification of haematopoietic stem cells to specific lineages.. *Nature Reviews. Genetics*, 1(1), pp. 57-64.
- Ostojic, A., Vrhovac, R. & Verstovsek, S., 2012. Ruxolitinib for the treatment of myelofibrosis: its clinical potential. *Therapeutics and clinical risk management*, Volume 8, pp. 95-103.
- Panteli, K. et al., 2005. Serum interleukin (IL)-1, IL-2, sIL-2Ra, IL-6 and thrombopoietin levels in patients with chronic myeloproliferative diseases.. *British Journal of Hematology*, 130(5), pp. 709-715.
- Papadopoulos, C. et al., 2017. VCP/p97 cooperates with YOD1, UBXD1 and PLAA to drive clearance of ruptured lysosomes by autophagy.. *EMBO Journal*, 36(2), pp. 135-150.
- Pardanani, A. et al., 2006. MPL515 mutations in myeloproliferative and other myeloid disorders: a study of 1182 patients.. *Blood*, 108(10), pp. 3472-3476.
- Parker, W. et al., 1988. Interaction of 2-halogenated dATP analogs (F, Cl, and Br) with human DNA polymerases, DNA primase, and ribonucleotide reductase.. *Molecular pharmacology*, 34(4), pp. 485-491.
- Parker, W. & Cheng, Y., 1987. Inhibition of DNA primase by nucleoside triphosphates and their arabinofuranosyl analogs.. *Molecular pharmacology*, 31(2), pp. 146-151.

- Passamonti, F. et al., 2011. Molecular and clinical features of the myeloproliferative neoplasm associated with JAK2 exon 12 mutations.. *Blood*, 117(10), pp. 2813-2116.
- Passamonti, F. et al., 2017. Ruxolitinib for the treatment of inadequately controlled polycythaemia vera without splenomegaly (RESPONSE-2): a randomised, open-label, phase 3b study.. *Lancet Oncology*, 18(1), pp. 88-99.
- Passamonti, F. et al., 2005. Leukemic transformation of polycythemia vera: a single center study of 23 patients.. *Cancer*, 104(5), pp. 1032-1036.
- Paul, F., Pellegrini, S. & Uzé, G., 2015. IFNA2: The prototypic human alpha interferon.. *Gene*, 567(2), pp. 132-137.
- Pearl, L., Prodromou, C. & Workman, P., 2008. The Hsp90 molecular chaperone: an open and shut case for treatment.. *The Biochemical Journal*, 410(3), pp. 439-453.
- Pellagatti, A. et al., 2010. Deregulated gene expression pathways in myelodysplastic syndrome hematopoietic stem cells.. *Leukemia*, 24(4), pp. 756-764.
- Periasamy, A., 2013. *Methods in Cellular Imaging*. New York: Springer.
- Pesu, M. et al., 2008. Therapeutic targeting of Janus kinases.. *Immunological Reviews*, Volume 223, pp. 132-142.
- Pietra, D. et al., 2008. Somatic mutations of JAK2 exon 12 in patients with JAK2 (V617F)-negative myeloproliferative disorders.. *Blood*, 111(3), pp. 1686-1689.
- Plunkett, W., Chubb, S., Alexander, L. & Montgomery, J., 1980. Comparison of the toxicity and metabolism of 9-beta-D-arabinofuranosyl-2-fluoroadenine and 9-beta-D-arabinofuranosyladenine in human lymphoblastoid cells.. *Cancer Research*, 40(7), pp. 2349-2955.
- Plunkett, W. et al., 1993. Fludarabine: pharmacokinetics, mechanisms of action, and rationales for combination therapies. *Seminars in oncology*, 20(5 Suppl 7), pp. 2-12.
- Pradhan, A., Lambert, Q. & Reuther, G., 2007. Transformation of hematopoietic cells and activation of JAK2-V617F by IL-27R, a component of a heterodimeric type I cytokine receptor.. *Proceedings of the National Academy of Sciences of the United States of America*, 104(47), pp. 18502-18507.
- Quentmeier, H., MacLeod, R., Zaborski, M. & Drexler, H., 2006. JAK2 V617F tyrosine kinase mutation in cell lines derived from myeloproliferative disorders.. *Leukemia*, 20(3), pp. 471-476.
- Quintás-Cardama, A. et al., 2013. Molecular analysis of patients with polycythemia vera or essential thrombocythemia receiving pegylated interferon α -2a. *Blood*, 122(6), pp. 893-901.
- Quintás-Cardama, A. et al., 2009. Pegylated interferon alfa-2a yields high rates of hematologic and molecular response in patients with advanced essential thrombocythemia and polycythemia vera.. *Journal of Clinical Oncology*, 27(32), pp. 5418-5424.
- Quintás-Cardama, A. et al., 2010. Preclinical characterization of the selective JAK1/2 inhibitor INCB018424: therapeutic implications for the treatment of myeloproliferative neoplasms.. *Blood*, 115(15), pp. 3109-3117.

- Rai, K. & Hollweg, A., 2011. Fludarabine versus chlorambucil: is the debate over?. *Clinical lymphoma, myeloma & leukemia*, 11(S1), pp. S7-9.
- Rajan, A. et al., 2011. A Phase 1 study of PF-04929113 (SNX-5422), an orally bioavailable heat shock protein 90 inhibitor in patients with refractory solid tumor malignancies and lymphomas. *Clinical Cancer Research*, 17(21), pp. 6831-6839.
- Randi, M. et al., 2014. Pregnancy complications predict thrombotic events in young women with essential thrombocythemia.. *American Journal of Hematology*, 89(3), pp. 306-309.
- Ray, S. et al., 2004. Genomic mechanisms of p210BCR-ABL signaling: induction of heat shock protein 70 through the GATA response element confers resistance to paclitaxel-induced apoptosis.. *Journal of Biological Chemistry*, 279(34), pp. 35604-35615.
- Reed, J., 1999. Mechanisms of apoptosis avoidance in cancer.. *Current Opinion in Oncology*, 11(1), pp. 68-75.
- Ren, Y. et al., 2014. Downregulation of expression of transporters associated with antigen processing 1 and 2 and human leukocyte antigen I and its effect on immunity in nasopharyngeal carcinoma patients.. *Molecular and Clinical Oncology*, 2(1), pp. 51-58.
- Ribeil, J. et al., 2007. Hsp70 regulates erythropoiesis by preventing caspase-3-mediated cleavage of GATA-1. *Nature*, 445(7123), pp. 102-105.
- Riley, C. et al., 2011. Increase in circulating CD4⁺CD25⁺Foxp3⁺ T cells in patients with Philadelphia-negative chronic myeloproliferative neoplasms during treatment with IFN- α .. *Blood*, 118(8), pp. 2170-2173.
- Rimsza, L. et al., 2004. Loss of MHC class II gene and protein expression in diffuse large B-cell lymphoma is related to decreased tumor immunosurveillance and poor patient survival regardless of other prognostic factors: a follow-up study from the Leukemia and Lymphoma Molecular. *Blood*, 103(11), pp. 4251-4258.
- Riss, T. et al., 2013. Cell Viability Assays. In: G. Sittampalam, et al. eds. *Assay Guidance Manual*. eBook: Bethesda (MD). Eli Lilly & Company and the National Centre for Advancing Translational Sciences.
- Röder, S., Steimle, C., Meinhardt, G. & Pahl, H., 2001. STAT3 is constitutively active in some patients with Polycythemia rubra vera.. *Experimental Hematology*, 29(6), pp. 694-702.
- Rojnuckarin, P. et al., 1999. Thrombopoietin-induced activation of the mitogen-activated protein kinase (MAPK) pathway in normal megakaryocytes: role in endomitosis.. *Blood*, 94(4), pp. 1273-1282.
- Ross, S., McTavish, D. & Faulds, D., 1993. Fludarabine. A review of its pharmacological properties and therapeutic potential in malignancy. *Drugs*, 45(5), pp. 737-759.
- Rotunno, G. et al., 2014. Impact of calreticulin mutations on clinical and hematological phenotype and outcome in essential thrombocythemia.. *Blood*, 123(10), pp. 1552-1555.
- Royer, Y. et al., 2005. Janus kinases affect thrombopoietin receptor cell surface localization and stability.. *The Journal of Biological Chemistry*, 280(29), pp. 27251-27261.

- Rumi, E. et al., 2014. JAK2 or CALR mutation status defines subtypes of essential thrombocythemia with substantially different clinical course and outcomes. *Blood*, 123(10), pp. 1544-1551.
- Rumi, E. et al., 2013. Acquired copy-neutral loss of heterozygosity of chromosome 1p as a molecular event associated with marrow fibrosis in MPL-mutated myeloproliferative neoplasms.. *Blood*, 121(12), pp. 4388-4395.
- Sahasrabudde, A. et al., 2015. Oncogenic Y641 mutations in EZH2 prevent Jak2/ β -TrCP-mediated degradation.. *Oncogene*, 34(4), pp. 445-454.
- Sajic, T. et al., 2018. Similarities and Differences of Blood N-Glycoproteins in Five Solid Carcinomas at Localized Clinical Stage Analyzed by SWATH-MS.. *Cell Reports*, 23(9), pp. 2819-2831.
- Sallah, S. W. J., 2001. Inhibitors against factor VIII associated with the use of interferon-alpha and fludarabine.. *Thrombosis and haemostasis*, 86(4), pp. 1119-1121.
- Samuelsson, J. et al., 2006. A phase II trial of pegylated interferon alpha-2b therapy for polycythemia vera and essential thrombocythemia: feasibility, clinical and biologic effects, and impact on quality of life.. *Cancer*, 106(11), pp. 2397-2405.
- Sasaki, A. et al., 2000. CIS3/SOCS-3 suppresses erythropoietin (EPO) signaling by binding the EPO receptor and JAK2.. *The Journal of Biological Chemistry*, 275(38), pp. 29338-29347.
- Satler, R. & Creswell, P., 1986. Impaired assembly and transport of HLA-A and -B antigens in a mutant TxB cell hybrid. *The EMBO Journal*, 5(5), pp. 943-949.
- Sattler, M. et al., 1995. The thrombopoietin receptor c-MPL activates JAK2 and TYK2 tyrosine kinases.. *Experimental Haematology*, 23(9), pp. 1040-1048.
- Schmitt, A. et al., 2000. Pathologic interaction between megakaryocytes and polymorphonuclear leukocytes in myelofibrosis.. *Blood*, 96(4), pp. 1342-1347.
- Schoenwaelder, S. et al., 2010. Phosphoinositide 3-kinase p110 beta regulates integrin alpha IIb beta 3 avidity and the cellular transmission of contractile forces.. *The Journal of Biological Chemistry*, 285(4), pp. 2886-2896.
- Schönberg, K. et al., 2015. JAK Inhibition Impairs NK Cell Function in Myeloproliferative Neoplasms.. *Cancer Research*, 75(11), pp. 2187-2199.
- Scott, D. et al., 2016. Two Distinct Types of E3 Ligases Work in Unison to Regulate Substrate Ubiquitylation.. *Cell*, 116(5), pp. 1198-1214.
- Scott, L. et al., 2007. JAK2 exon 12 mutations in polycythemia vera and idiopathic erythrocytosis.. *New England Journal of Medicine*, 356(5), pp. 459-468.
- Seliger, B., 2012. Novel insights into the molecular mechanisms of HLA class I abnormalities.. *Cancer Immunology, Immunotherapy*, 61(2), pp. 249-254.
- Seliger, B., Cabrera, T., Garrido, F. & Ferrone, S., 2002. HLA class I antigen abnormalities and immune escape by malignant cells.. *Seminars in Cancer Biology*, 12(1), pp. 3-13.

- Senyuk, V. et al., 2009. Consistent up-regulation of Stat3 Independently of Jak2 mutations in a new murine model of essential thrombocythemia.. *Cancer Research*, 69(1), pp. 262-271.
- Shan, N., Zhou, W., Zhang, S. & Zhang, Y., 2016. Identification of HSPA8 as a candidate biomarker for endometrial carcinoma by using iTRAQ-based proteomic analysis.. *OncoTargets and Therapy*, Volume 9, pp. 2169-2179.
- Shen, N. et al., 2015. A phosphorylation-related variant ADD1-rs4963 modifies the risk of colorectal cancer.. *PLoS One*, 10(3).
- Shi, J., Yuan, B., Hu, W. & Lodish, H., 2016. JAK2 V617F stimulates proliferation of erythropoietin-dependent erythroid progenitors and delays their differentiation by activating Stat1 and other nonerythroid signaling pathways.. *Experimental Hematology*, 44(11), pp. 1044-1058.
- Shilling, A. et al., 2010. Metabolism, excretion, and pharmacokinetics of [14C]INC018424, a selective Janus tyrosine kinase 1/2 inhibitor, in humans.. *Drug Metabolism and Disposition*, 38(11), pp. 2023-2031.
- Sigmond, J. & Peters, G., 2005. Pyrimidine and purine analogues, effects on cell cycle regulation and the role of cell cycle inhibitors to enhance their cytotoxicity.. *Nucleosides, nucleotides & nucleic acids*, 24(10-12), pp. 1997-2022.
- Silva, C., 2004. Role of STATs as downstream signal transducers in Src family kinase-mediated tumorigenesis.. *Oncogene*, 23(48), pp. 8017-8023.
- Skov, V. et al., 2011. Whole-blood transcriptional profiling of interferon-inducible genes identifies highly upregulated IFI27 in primary myelofibrosis.. *European Journal of Hematology*, 87(1), pp. 54-60.
- Skov, V. et al., 2012. Molecular profiling of peripheral blood cells from patients with polycythemia vera and related neoplasms: identification of deregulated genes of significance for inflammation and immune surveillance.. *Leukemia Research*, 36(11), pp. 1387-1392.
- Skov, V. et al., 2013. Whole blood transcriptional profiling reveals significant down-regulation of human leukocyte antigen class I and II genes in essential thrombocythemia, polycythemia vera and myelofibrosis.. *Leukemia & Lymphoma*, 54(10), pp. 2269-2273.
- Skov, V. et al., 2012. Gene expression profiling with principal component analysis depicts the biological continuum from essential thrombocythemia over polycythemia vera to myelofibrosis.. *Experimental Hematology*, 40(9), pp. 771-780.
- Slot, S. et al., 2015. Effect of conditioning regimens on graft failure in myelofibrosis: a retrospective analysis.. *Bone Marrow Transplantation*, 50(11), pp. 1424-1431.
- Stark, G. & Darnell, J. J., 2012. The JAK-STAT pathway at twenty. *Immunity*, 36(4), pp. 503-14.
- Stauffer Larsen, T. et al., 2013. Long term molecular responses in a cohort of Danish patients with essential thrombocythemia, polycythemia vera and myelofibrosis treated with recombinant interferon alpha.. *Leukemia research*, 37(9), pp. 1041-1045.
- Steensma, D. & Tefferi, A., 2008. JAK2 V617F and ringed sideroblasts: not necessarily RARS-T.. *Blood*, 111(3), p. 1748.

- Stein, B. & Tiu, R., 2013. Biological rationale and clinical use of interferon in the classical BCR-ABL-negative myeloproliferative neoplasms.. *Journal of Interferon & Cytokine Research*, 33(4), pp. 145-153.
- Sur, S. & Agrawal, D., 2016. Phosphatases and kinases regulating CDC25 activity in the cell cycle: clinical implications of CDC25 overexpression and potential treatment strategies.. *Molecular and Cellular Biochemistry*, 416(1), pp. 33-46.
- Szelag, M. et al., 2013. In silico simulations of STAT1 and STAT3 inhibitors predict SH2 domain cross-binding specificity.. *European Journal of Pharmacology*, 720(1-3), pp. 38-48.
- Szymańska, J. et al., 2015. Pro-Apoptotic Activity of Ruxolitinib Alone and in Combination with Hydroxyurea, Busulphan, and PI3K/mTOR Inhibitors in JAK2-Positive Human Cell Lines.. *Advances in clinical and experimental medicine: official organ Wroclaw Medical University*, 24(2), pp. 195-202.
- Talpaz, M., Mercer, J. & Hehlmann, R., 2015. The interferon-alpha revival in CML.. *Annals of Hematology*, 94(S2), pp. S195-207..
- Tarafdar, A. et al., 2017. CML cells actively evade host immune surveillance through cytokine-mediated downregulation of MHC-II expression.. *Blood*, 129(2), pp. 199-208.
- Tefferi, A., 2000. Myelofibrosis with myeloid metaplasia.. *New England Journal of Medicine*, 342(17), pp. 1255-1265.
- Tefferi, A. et al., 2006. The clinical phenotype of wild-type, heterozygous, and homozygous JAK2V617F in polycythemia vera.. *Cancer*, 106(3), pp. 631-635.
- Tefferi, A., Vannucchi, A. & Barbui, T., 2018. Essential thrombocythemia treatment algorithm 2018. *Blood Cancer Journal*, 8(2).
- Tefferi, A., Vannucchi, A. & Barbui, T., 2018. Polycythemia vera treatment algorithm 2018. *Blood Cancer Journal*, 8(3).
- Tefferi, A. & Vardiman, J., 2008. Classification and diagnosis of myeloproliferative neoplasms: the 2008 World Health Organization criteria and point-of-care diagnostic algorithms. *Leukaemia*, 22(1), pp. 14-22.
- Them, N. et al., 2015. Molecular responses and chromosomal aberrations in patients with polycythemia vera treated with peg-proline-interferon alpha-2b.. *American Journal of Hematology*, 90(4), pp. 288-294.
- Thompson, P. et al., 2016. Fludarabine, cyclophosphamide, and rituximab treatment achieves long-term disease-free survival in IGHV-mutated chronic lymphocytic leukemia.. *Blood*, 127(3), pp. 303-309.
- Tobelaim, W. et al., 2015. Tumour-promoting role of SOCS1 in colorectal cancer cells.. *Scientific Reports*, 14301(5).
- Tono, C. et al., 2005. JAK2 Val617Phe activating tyrosine kinase mutation in juvenile myelomonocytic leukemia.. *Leukemia*, 19(10), pp. 1843-1844.
- Townsend, A. et al., 1989. Association of class I major histocompatibility heavy and light chains induced by viral peptides.. *Nature*, 340(6233), pp. 443-448.

- Townsend, P. et al., 2004. STAT-1 interacts with p53 to enhance DNA damage-induced apoptosis.. *Journal of Biological Chemistry*, 279(7), pp. 5811-5820.
- Tran, S., Puhar, A., Ngo-Camus, M. & Ramarao, N., 2011. Trypan blue dye enters viable cells incubated with the pore-forming toxin HlyII of *Bacillus cereus*. *PLoS One*, 6(9), p. e22876.
- Tsuchihara, K. et al., 2005. Ckap2 regulates aneuploidy, cell cycling, and cell death in a p53-dependent manner.. *Cancer Research*, 65(15), pp. 6685-6691.
- Ungureanu, D. et al., 2002. Regulation of Jak2 through the ubiquitin-proteasome pathway involves phosphorylation of Jak2 on Y1007 and interaction with SOCS-1.. *Molecular and Cellular Biology*, 22(10), pp. 3316-3326.
- Uozumi, K. et al., 2000. Establishment and characterization of a new human megakaryoblastic cell line (SET-2) that spontaneously matures to megakaryocytes and produces platelet-like particles.. *Leukemia*, 14(1), pp. 142-152.
- Vainchenker, W., Dusa, A. & Constantinescu, S., 2008. JAKs in pathology: role of Janus kinases in hematopoietic malignancies and immunodeficiencies.. *Seminars in Cell & Developmental Biology*, 19(4), pp. 385-393.
- Vambutas, A., Bonagura, V. & Steinberg, B., 2000. Altered expression of TAP-1 and major histocompatibility complex class I in laryngeal papillomatosis: correlation of TAP-1 with disease.. *Clinical and Diagnostic Laboratory Immunology*, 7(1), pp. 79-85.
- van de Weerd, B. & Medema, R., 2006. Polo-like kinases: a team in control of the division.. *Cell Cycle*, 5(8), pp. 853-864.
- Vannucchi, A., 2014. How I treat polycythemia vera.. *Blood*, 124(22), pp. 3212-3220.
- Vannucchi, A. et al., 2007. Clinical profile of homozygous JAK2 617V>F mutation in patients with polycythemia vera or essential thrombocythemia.. *Blood*, 110(3), pp. 840-846.
- Vannucchi, A. et al., 2015. Philadelphia chromosome-negative chronic myeloproliferative neoplasms: ESMO Clinical Practice Guidelines for diagnosis, treatment and follow-up.. *Annals of Oncology*, 26(Suppl. 5), pp. 85-99.
- Vannucchi, A. H. C., 2017. Emerging treatments for classical myeloproliferative neoplasms.. *Blood*, 129(6), pp. 693-703.
- Vannucchi, A. et al., 2015. Ruxolitinib versus standard therapy for the treatment of polycythemia vera.. *New England Journal of Medicine*, 372(5), pp. 426-435.
- Vannucchi, A. et al., 2013. Mutations and prognosis in primary myelofibrosis.. *Leukemia*, 27(9), pp. 1861-1869.
- Vannucchi, A. et al., 2009. Increased risk of lymphoid neoplasms in patients with Philadelphia chromosome-negative myeloproliferative neoplasms. *Cancer Epidemiology, Biomarkers & Prevention*, 18(7), pp. 2068-73.

Vantroyen, B. & Vanstraelen, D., 2002. Management of essential thrombocythemia during pregnancy with aspirin, interferon alpha-2a and no treatment. A comparative analysis of the literature.. *Acta haematologica*, 107(3), pp. 158-169.

Vardiman, J. et al., 2009. The 2008 revision of the World Health Organization (WHO) classification of myeloid neoplasms and acute leukemia: rationale and important changes.. *Blood*, 114(5), pp. 937-951.

Verger, E. et al., 2018. Ropoginterferon alpha-2b targets JAK2V617F-positive polycythemia vera cells in vitro and in vivo.. *Blood Cancer Journal*, 8(10), p. 94.

Verstovsek, S. et al., 2012. A Double-Blind Placebo-Controlled Trial of Ruxolitinib for Myelofibrosis. *New England Journal of Medicine*, 366(9), pp. 799-807.

Verstovsek, S. et al., 2014. A phase 2 study of ruxolitinib, an oral JAK1 and JAK2 Inhibitor, in patients with advanced polycythemia vera who are refractory or intolerant to hydroxyurea.. *Cancer*, 120(4), pp. 513-520.

Verstovsek, S. et al., 2014. Long-Term Results from a Phase II Open-Label Study of Ruxolitinib in Patients with Essential Thrombocythemia Refractory to or Intolerant of Hydroxyurea. *Blood*, 124(1847).

Verstovsek, S. et al., 2017. Ruxolitinib for essential thrombocythemia refractory to or intolerant of hydroxyurea: long-term phase 2 study results.. *Blood*, 130(15), pp. 1768-1771.

Verstovsek, S. et al., 2016. Ruxolitinib versus best available therapy in patients with polycythemia vera: 80-week follow-up from the RESPONSE trial. *Haematologica*, 101(7), pp. 821-829.

Waibel, M. et al., 2013. Combined targeting of JAK2 and Bcl-2/Bcl-xL to cure mutant JAK2-driven malignancies and overcome acquired resistance to JAK2 inhibitors.. *Cell Reports*, 5(4), pp. 1047-1059.

Walther, T. & Mann, M., 2010. Mass spectrometry-based proteomics in cell biology. *Journal of Cell Biology*, 190(4), pp. 491-500.

Walz, C. et al., 2012. Essential role for Stat5a/b in myeloproliferative neoplasms induced by BCR-ABL1 and JAK2(V617F) in mice. *Blood*, 119(5), pp. 3550-3560.

Wang, J. et al., 2006. Quantitative analysis of growth factor production in the mechanism of fibrosis in agnogenic myeloid metaplasia.. *Experimental Hematology*, 34(12), pp. 1617-1623.

Wang, J., Lee, J., Liem, D. & Ping, P., 2017. HSPA5 Gene encoding Hsp70 chaperone BiP in the endoplasmic reticulum.. *Gene*, Volume 618, pp. 14-23.

Wang, L. et al., 2014. α -Adducin gene G614T polymorphisms in essential hypertension patients with high low density lipoprotein (LDL) levels.. *The Indian Journal of Medical Research*, 139(2), pp. 273-278.

Weber-Nordt, R. et al., 1996. Constitutive activation of STAT proteins in primary lymphoid and myeloid leukemia cells and in Epstein-Barr virus (EBV)-related lymphoma cell lines.. *Blood*, 88(3), pp. 809-816.

Welsh, R., Bahl, K., Marshall, H. & Urban, S., 2012. Type 1 Interferons and Antiviral CD8 T-Cell Responses. *PLoS Pathogens*, 8(1), p. e1002352.

- Weniger, M. et al., 2006. Mutations of the tumor suppressor gene SOCS-1 in classical Hodgkin lymphoma are frequent and associated with nuclear phospho-STAT5 accumulation.. *Oncogene*, 25(18), pp. 2679-2684.
- Wen, Q. et al., 2015. Targeting megakaryocytic-induced fibrosis in myeloproliferative neoplasms by AURKA inhibition.. *Nature Medicine*, 21(12), pp. 1473-1480.
- Wilks, A. et al., 1991. Two novel protein-tyrosine kinases, each with a second phosphotransferase-related catalytic domain, define a new class of protein kinase.. *Molecular and Cellular Biology*, 11(4), pp. 2057-2065.
- Willman, C. et al., 1993. Deletion of IRF-1, mapping to chromosome 5q31.1, in human leukemia and preleukemic myelodysplasia.. *Science*, 259(5097), pp. 968-971.
- Winston, L. & Hunter, T., 1995. JAK2, Ras, and Raf are required for activation of extracellular signal-regulated kinase/mitogen-activated protein kinase by growth hormone.. *The Journal of Biological Chemistry*, 270(52), pp. 30837-30840.
- World Health Organisation, W., 2015. WHO Model List of Essential Medicines. April. Volume 19th List.
- Xu, M. et al., 2005. Constitutive mobilization of CD34+ cells into the peripheral blood in idiopathic myelofibrosis may be due to the action of a number of proteases.. *Blood*, 105(11), pp. 4508-4515.
- Xu, Q. et al., 2016. The Effect of Ruxolitinib on the Expression of VEGF and HIF-1 α in Leukemia HEL Cells. *Journal of Sichuan University. Medical science edition*, 47(5), pp. 669-673.
- Yajnanarayana, S. et al., 2015. JAK1/2 inhibition impairs T cell function in vitro and in patients with myeloproliferative neoplasms.. *British Journal of Hematology*, 169(6), pp. 824-833.
- Yan, D., Hutchison, R. & Mohi, G., 2012. Critical requirement for Stat5 in a mouse model of polycythemia vera.. *Blood*, 119(15), pp. 3539-3549.
- Yin, H. et al., 2015. Antitumor potential of a synthetic interferon-alpha/PLGF-2 positive charge peptide hybrid molecule in pancreatic cancer cells. *Scientific Reports*, 16975(5).
- Yoo, L., Yoon, A., Yun, C. & Chung, K., 2018. Covalent ISG15 conjugation to CHIP promotes its ubiquitin E3 ligase activity and inhibits lung cancer cell growth in response to type I interferon.. *Cell Death & Disease*, 9(2), p. 97.
- Yoshida, N. & Kojima, S., 2018. Updated Guidelines for the Treatment of Acquired Aplastic Anemia in Children.. *Current oncology reports*, 20(9), p. 67.
- Zeidner, J. et al., 2014. A phase II trial of sequential ribonucleotide reductase inhibition in aggressive myeloproliferative neoplasms.. *Haematologica*, 99(4), pp. 672-678.
- Zhang, X. et al., 2017. Efficacy and safety evaluation of fludarabine-based chemotherapy regimen for patients with non-Hodgkin lymphoma: A meta-analysis.. *Medicine*, 96(33), p. 7781.
- Zinzani, P. et al., 2015. Fludarabine-Mitoxantrone-Rituximab regimen in untreated indolent non-follicular non-Hodgkin's lymphoma: experience on 143 patients.. *Haematological Oncology*, 33(3), pp. 141-146.

